UNIVERSITY OF HELSINKI
Faculty of Agriculture and Forestry
Department of Food and Nutrition

Dissertationes Universitatis Helsingiensis 275/2024

Decoding the interfacial structure of emulsions stabilized by birch glucuronoxylans

Felix Abik

ACADEMIC DISSERTATION

To be presented, with the permission of the Faculty of Agriculture and Forestry of the University of Helsinki, for public examination in room 1041, Biocenter 2, Viikinkaari 5, on 8 November 2024 at 13.00.

Helsinki 2024

Custos and main supervisor	Professor Kirsi S. Mikkonen Department of Food and Nutrition University of Helsinki, Finland
Co-supervisor	Docent Thao Minh Ho Department of Food and Nutrition University of Helsinki, Finland
Pre-examiners	Professor Henrikki Liimatainen Fiber and Particle Engineering Research Unit University of Oulu, Finland
	Dr. Kevin Roger Laboratoire de Génie Chimique à Toulouse CNRS, France
Opponent	Professor Tommy Nylander Department of Chemistry Lund University, Sweden

Study completed under the Doctoral Program in Food Chain and Health at the Department of Food and Nutrition, Faculty of Agriculture and Forestry, University of Helsinki

Front cover illustration by Anindya Nitya Samardhya

Publisher : Helsingin yliopisto
Series : Dissertationes Universitatis Helsingiensis 275/2024

ISBN 978-952-84-0336-4 (print)
ISBN 978-952-84-0335-7 (online)
ISSN 2954-2898 (print)
ISSN 2954-2952 (online)

Printed by PunaMusta
Joensuu 2024

O divine Master, grant that I may not so much seek
to be consoled as to console,
to be understood as to understand,
to be loved as to love.

For it is in giving that we receive,
it is in pardoning that we are pardoned,
and it is in dying that we are born to eternal life.

- - -

Ya Tuhan, semoga aku lebih ingin
menghibur daripada dihibur,
memahami daripada dipahami,
mencintai daripada dicintai.

Sebab dengan memberi aku menerima,
dengan mengampuni aku diampuni,
dengan mati suci aku bangkit lagi,
untuk hidup selama-lamanya.

Final part of the Prayer of St. Francis

Abstract

Lignocellulosic materials from various plant biomass are increasingly sought after to satisfy the growing need for sustainable and environmentally-compatible resources. Among the different lignocellulosic materials, hemicelluloses have received little attention despite constituting between 25-35% of the plant biomass. While they can be extracted through various methods, pressurized hot water extraction (PHWE) stood out for using no harsh solvents, making it suitable to produce food-grade hemicelluloses. However, this method co-extracts a significant amount of residual lignin, which exists in the extract as insoluble particles as well as covalently-bound to the hemicelluloses. The residual lignin has been proven to be functionally beneficial when the hemicelluloses were used as emulsifiers; it enhanced the physical stability of the emulsions and protected them against oil oxidation. On the other hand, it endowed a strong brown color and woody flavor, which may not be desirable in many food-based applications. Nevertheless, partial removal of the residual lignin reduced the physical and chemical stabilization capability, prompting the need to understand the mechanism upon which the polysaccharide and lignin stabilize the emulsions. A complete understanding of the stabilization mechanism would rationalize the biorefining strategy for PHWE hemicelluloses, potentially allowing their physicochemical properties to be tailored based on the desired end-products.

Therefore, this doctoral thesis aimed to establish the roles of the polysaccharide and lignin components of PHWE hemicelluloses in stabilizing emulsions, both individually and in conjunction with each other. For this purpose, glucuronoxylans (GX) from birch were used as a model hemicellulose and analyzed not only as crude extracts, but also fractionated and chemically-derivatized, comparing them with relevant established emulsifiers. First, investigation of the adsorption behavior of GX at the oil-water interface revealed that the residual lignin acted to enable the diffusion of the hemicelluloses to the interface, which in turn constructed the bulk structure of the interfacial layer. The adsorbed layer, which had similar thickness regardless of the chemical environment and type of GX, appeared to show an orientation of the different chemical moieties, where the polysaccharide fraction faced towards the aqueous phase and the lignin fraction towards the oil phase. Next, *in-vitro* digestion experiments of GX-stabilized emulsions containing vitamin D3 showed that the orientation of the polysaccharide and lignin fractions also existed in emulsions made by high-pressure homogenization, where the insoluble lignin particles were well-covered by the polysaccharide-rich interfacial layer. Simultaneously, the *in-vitro* digestion experiments demonstrated the viability of GX-stabilized emulsions as oral-based delivery systems of hydrophobic compounds. Finally, a comprehensive emulsion stability study in different pH and ionic strength revealed that GX-stabilized emulsions rely heavily on electrostatic repulsion to maintain a stable dispersion of the oil droplets. An excess of insoluble lignin was shown to destabilize the emulsions as it promoted droplet flocculation, suggesting an optimal polysaccharide-to-lignin ratio for maximum stability. Overall, the results of this doctoral thesis showcased the tunability of PHWE hemicelluloses, which can potentially be used as a scientific rationale to accelerate the adaptation of hemicelluloses from lignocellulosic biomass in commercial emulsion-based products.

Tiivistelmä

Eri kasvijakeista saatavaa lignoselluloosaa tutkitaan yhä enemmän vastaamaan kestävien ja ympäristöystävällisten materiaalien kasvavaan kysyntään. Lignoselluloosan tärkeimmistä yhdisteistä hemiselluloosia ei ole tutkittu yhtä kattavasti kuin selluloosaa ja ligniiniä, vaikka se muodostaa lignoselluloosasta suuren osan, 25-35%. Hemiselluloosia voidaan kerätä talteen uuttamalla lignoselluloosaa paineistetulla kuumavesiuutolla (pressurized hot water extraction, PHWE) ilman haitallisten liuottimien käyttöä, jolloin lopputuotteeseen ei päädy prosessikemikaaleja. Uute sisältää kuitenkin vaihtelevia määriä ligniiniä, jota vapautuu lignoselluloosasta samaan aikaan hemiselluloosien kanssa. Tämä jäännösligniini esiintyy uutteessa sekä liukenemattomina partikkeleina että kovalenttisesti hiilihydraatteihin sitoutuneina tähteinä. Hemiselluloosauutteiden sisältämä ligniini on osoittautunut hyödylliseksi apuyhdisteeksi emulsiosovelluksissa, koska se parantaa öljypisaroiden fysikaalista pysyvyyttä ja suojaa öljyä hapettumiselta. Aiemmissa tutkimuksissa on havaittu, että uutteen kyky stabiloida emulsioita heikentyy, kun jäännösligniinin määrä vähenee. Jäännösligniini kuitenkin aiheuttaa hemiselluloosauutteelle ruskeaa väriä ja puumaista sivumakua, mikä saattaa heikentää sen käytettävyyttä elintarvikesovelluksissa. PHWE-uutteen elintarvikekäyttöä suunniteltaessa tarvitaan kokonaisvaltainen näkemys hemiselluloosien ja ligniinin vuorovaikutuksesta.

Tämä väitöskirja tutkii PHWE-hemiselluloosauutteen sisältämien polysakkaridien ja ligniinin rooleja emulgointiaineissa. Malliyhdisteenä käytettiin koivun glukuronoksylaania (GX). Muokkaamatonta GX-uutetta verrattiin osittain puhdistettuun ja kemiallisesti muokattuun uutteeseen sekä yleisesti käytettyyn emulgointiaineeseen. GX hakeutui öljy-vesi-rajapinnalle jäännösligniinin ansiosta, vaikka rajapinnalle kiinnittyneen GX:n rakenne muodostui pääsääntöisesti polysakkarideista. Rajapinnan paksuus oli samankaltainen GX-uutetyypistä riippumatta. Rajapinnalla ligniiniosa kiinnittyi öljyyn ja polysakkaridiosa veteen. *In-vitro* ruoansulatuskokeet, joissa käytettiin D3-vitamiinia sisältäviä, GX-stabiloituja emulsioita, osoittivat samankaltaisen rajapinnan rakenteen myös kun emulsio valmistettiin korkeapainehomogenoinnilla. Ruoansulatuskokeet osoittivat, että GX-stabiloidut emulsiot voisivat soveltua suun kautta otettavien hydrofobisten yhdisteiden annostelujärjestelmiksi. Kattava emulsioiden säilytyskoe eri pH:n ja ionivahvuuden tasoilla osoitti, että GX-stabiloitujen emulsioiden merkittävin stabilointimekanismi oli elektrostaattinen hylkimisvoima. Kun GX-uutteessa oli runsaasti liukenematonta ligniiniä, emulsiopisarat aggregoituivat. Tämä osoitti, että on olemassa optimaalinen polysakkaridi–ligniinisuhde, jolla saavutettiin korkea emulsion pysyvyys. Kaikkiaan väitöskirjan tulokset osoittavat, että PHWE-uutteiden koostumusta voidaan säädellä käyttökohteen mukaan. Tutkimustulosten avulla voidaan nopeuttaa hemiselluloosien kaupallisten sovellusten kehitystä.

Abstrak

Bahan baku berbasis lignoselulosa dari biomassa hayati semakin terkemuka dalam beberapa tahun terakhir untuk memenuhi kebutuhan material fungsional berkelanjutan dan ramah lingkungan. Dari berbagai komponen penyusun lignoselulosa, fraksi hemiselulosa cenderung terabaikan meskipun mencakup 25-35% dari total biomassa tumbuhan. Metode ekstraksi hemiselulosa berbasis air panas bertekanan tinggi (bahasa Inggris: *pressurized hot-water extraction*, PHWE) berpotensi untuk diterapkan dalam produksi hemiselulosa bermutu pangan karena metode tersebut tidak menggunakan pelarut organik berbahaya. Namun, metode ini turut mengekstrak lignin secara signifikan dalam wujud partikel taklarut dan yang terikat secara kovalen pada rantai hemiselulosa. Kandungan pencemar lignin ini justru terbukti menjadikan ekstrak hemiselulosa PHWE sebagai pengemulsi yang baik dari segi kestabilan fisik maupun kestabilan terhadap oksidasi asam lemak. Akan tetapi, kandungan lignin ini memberikan warna cokelat dan aroma kayu yang umumnya tidak diinginkan dalam produk makanan. Di sisi lain, pengurangan kadar lignin menurunkan kinerja stabilisasi emulsi ekstrak hemiselulosa PHWE. Untuk itu, pemahaman mendalam terkait kontribusi fraksi hemiselulosa dan lignin terhadap mekanisme stabilisasi emulsi ekstrak hemiselulosa PHWE diperlukan agar pengolahan biomassa lignoselulosa dapat dikembangkan secara efektif dan tepat sasaran untuk memproduksi ekstrak hemiselulosa yang optimal sebagai pengemulsi.

Atas dasar itu, disertasi doktoral ini bertujuan untuk memahami peran fraksi polisakarida dan lignin dalam mekanisme stabilisasi emulsi oleh ekstrak hemiselulosa PHWE, baik secara individual maupun dalam sinergi dengan satu sama lain. Dalam studi ini, glukuronoxilan (GX) dari pohon burja (bahasa Inggris: *birch*) digunakan sebagai model hemiselulosa dan dianalisis tidak hanya sebagai ekstrak mentah GX saja, tetapi juga sebagai ekstrak terfraksionasi dan terderivatisasi. Perilaku stabilitas emulsi ekstrak-ekstrak GX tersebut dibandingkan dengan pengemulsi lain yang mekanisme stabilisasinya telah diketahui. Studi adsorpsi GX pada batas antarfasa minyak dan air menunjukkan peran komponen lignin sebagai jangkar untuk GX berdifusi ke batas antarfasa. Lapisan antarfasa tersebut memiliki struktur utama berbasis polisakarida yang ketebalannya tidak dipengaruhi jenis GX maupun lingkungan kimiawinya. Di lapisan antarfasa tersebut, fraksi polisakarida GX menghadap ke fasa air, sementara fraksi lignin ke arah fasa minyak. Analisis daya cerna emulsi terstabilkan-GX secara *in-vitro* membuktikan potensinya sebagai metode penghantaran senyawa nutrasetikal hidrofobik secara oral. Di saat yang sama, uji tersebut juga membuktikan bahwa orientasi fraksi penyusun GX juga ditemukan pada emulsi yang difabrikasi menggunakan sistem homogenisasi bertekanan tinggi, dengan partikel lignin taklarut dalam ekstrak GX terpendam di bawah lapisan antarfasa. Studi stabilitas emulsi terstabilkan-GX dalam variasi pH dan kadar garam menunjukkan peran tolakan elektrostatis dalam mekanisme stabilisasi emulsi oleh GX. Kadar lignin yang terlalu tinggi, terutama dalam rupa partikel taklarut, dapat menginduksi flokulasi butiran minyak, terutama dalam kondisi asam dan dengan kehadiran garam. Hal ini menunjukkan adanya rasio optimal antara kadar polisakarida dan lignin. Hasil dari studi doktoral ini telah menunjukkan bahwa sifat pengemulsi hemiselulosa PHWE dapat diatur sesuai dengan kebutuhan dan dapat diterapkan dalam desain pengolahan biomassa hayati yang tepat guna.

Preface

This doctoral study was conducted primarily in the Food Materials Science (FoMSci) research group, Department of Food and Nutrition, University of Helsinki, Finland. A short-term research visit was conducted at the Quadram Institute, Norwich, United Kingdom, in 2023. Smaller parts of the experiments were also conducted in the Department of Chemistry, University of Helsinki, Finland; Department of Bioproducts and Biosystems, Aalto University, Finland; and ISIS Pulsed Neutron and Muon Sources, Rutherford Appleton Laboratory, Didcot, United Kingdom. The study was firstly funded by the Research Council of Finland (formerly Academy of Finland) as part of the ENVISION project (project nr. 322514) during 2019-2023 granted to Prof. Kirsi S. Mikkonen. Continuation towards the completion of this thesis was funded by the Finnish Cultural Foundation (grant nr. 00230186) under the auspices of Alma and Jussi Jalkanen Funds.

I would like to thank Kirsi, as my main supervisor, for trusting me to be part of the ENVISION project. I especially am grateful for the tremendous freedom and independence that Kirsi entrusted in me to conduct and shape this doctoral thesis to in its current shape, and for guiding me in becoming a better scientist. I also thank Dr. Thao Minh Ho for his patience in co-supervising me and conducting experiments in the ENVISION project with me. Special thanks to my thesis committee members Prof. Orlando Rojas, Dr. Marianna Kemell, and Dr. Laura Flander for their counselling and advices during my studies. I would also like to express my gratitude for the critical assessments and constructive inputs of Prof. Henrikki Liimatainen and Dr. Kevin Roger as the pre-examiners, and Prof. Tommy Nylander for the fruitful discussions and evaluation as the opponent for the thesis defense.

I am grateful for the contributions of my collaborators: Dr. Sami Hietala and Dr. Sami-Pekka Hirvonen for numerous help in the interfacial tension, NMR, SEC, and other measurements in the Department of Chemistry, University of Helsinki; Dr. Katariina Solin for her guidance in the use of QCM-D at Aalto University; Dr. Mari Lehtonen and Dr. Anna-Maija Lampi, for helping me develop the vitamin D measurement protocol; Prof. Pete Wilde and Dr. Giusy Cockram for hosting me in Quadram Institute, as well as Mr. Mark Philo, Dr. Catherine Booth, and other Quadram personnel who welcomed me during my stay; Dr. Mario Campana, with whom I planned and conducted the NR experiments, as well as helped process my results; and finally, to other collaborators in other countries, with whom we have had fruitful works. Special thanks to Mr. Kimmo Peltola and my master's thesis student Ms. Zhongying Feng, who helped with running several experiments, and also to Mr. Troy Faithfull who has provided numerous proofreading and valuable discussions. Additionally, thank you to all the technicians: Taru, Jutta, Miikka, Mikko, Outi, and Tuulia, who have helped me in using all the equipment in the lab safely and helped during any issues, as well as all the other FAN staff and FoMSci members for our interactions and discussions. Kiitos Jarkolle tiivistelmän oikoluvusta.

Doing a PhD has always been a part of my lifetime goal since I was in grade school, and thus, I feel absolutely glad and proud to be able to make it this far. Nevertheless, I know for sure that I would not have finished this PhD if it weren't for the support from all the people

around me, which went beyond technical and scientific support. I would like to first thank my LDR Buddies Ike and Anin, who have acted as a tremendous support system for me despite all three of us living in different countries; you guys know my misery sometimes more than I do. Then I'd like to thank the Christmas Dinner folks, particularly Fabio, Patrícia, Tiago, Christos, Afsane, Priscille, Kateřina, Lin, Manel, and Angel; thank you for the hang outs, the nights outs, the dinners (obviously), and all the fun we have been having together, keeping me sane all the way through. A special shoutout to Emilie: for all of our heart-to-heart conversations, be it at midnight, in Eira and in Saukonpaadenranta, at your place, and wherever, I will be forever grateful for them. To my Indonesian friends in Helsinki, thank you for all the laughs and all the relatabilities that would simply not work in English; special shoutout to Mba Tita for the makan-makan dan bincang-bincang dan gosip-gosipnya! For all my friends in Finland, Denmark, the Netherlands, Indonesia, and everywhere else. I've recently realized that I have been blessed to be able to call so many amazing people around the world as my friends, all of whom have truly supported me in my PhD journey in one way or another. With prayers. With words of encouragement. With scientific discussions. By listening to my rants and complaints. As much as I would have liked to mention everyone here, there is obviously no space, but please do know that I am truly grateful for your companionship and support throughout my studies even if I don't mention your names here. You guys are the reason I am able to finish this degree, in more ways than one.

I dedicate this PhD thesis to my family, especially to Mama and Papa. I will forever be grateful for all you have done and sacrificed for me, and for all the trust and freedom you have given me to choose my own path. I know I will never be able to repay you for everything, so I hope this thesis will serve as a token of appreciation, that everything you gave me has not been in vain.

Finally, this thesis is also for You, my eternal place of refuge, who has loved me from before I was even born, who called me to You as I am and for who I am, for only by Your grace, guidance, and blessing I could get this far. *Fiat voluntas Tua, ad maiorem Dei gloriam.*

Helsinki, 2024
Felix Abik

List of original publications

This thesis is based on the following publications and additional unpublished data. The full versions of the publications are attached at the end of this thesis.

I Abik, F.; Solin, K.; Hietala, S.; Rojas, O. J.; Ho, T. M.; Mikkonen, K. S., Adsorption study on the formation of interfacial layers based on birch glucuronoxylans. *Carbohydrate Polymers* **2024,** 339, 122242.

II Abik, F.; Ho, T. M.; Lehtonen, M.; Philo, M.; Booth, C.; Mandalari, G.; Wilde, P. J.; Mikkonen, K. S., The two-faced functionality of birch glucuronoxylan in an emulsion-based carrier of vitamin D3. *Food Hydrocolloids* **2024,** 157, 110442.

III Abik, F.; Ho, T. M.; Campana, M.; Mikkonen, K. S., Birch glucuronoxylans as emulsifiers: the roles of polysaccharide and residual lignin in emulsion stabilization. *Journal of Colloid and Interface Science*. Submitted.

 The publications are referred to in the text by their roman numerals.

Contribution of author to articles I-III

Felix Abik planned the studies together with the other authors of the respective publications, conducted most of the experiments, was primarily responsible for the data analyses, interpretation, and drafted the initial manuscript of all Publications, all for which he is the corresponding author. Thao Minh Ho performed the emulsion droplet size measurements in all Publications; the results were then processed and interpreted by Felix Abik. Mario Campana processed the neutron reflectometry data to obtain the interfacial layer thickness, subsequently interpreted by Felix Abik in Publication III.

Supporting publications

A. Ho, T. M.; Abik, F.; Hietala, S.; Isaza Ferro, E.; Pitkänen, L.; Juhl, D. W.; Vosegaard, T.; Kilpeläinen, P. O.; Mikkonen, K. S., Wood lignocellulosic stabilizers: effect of their characteristics on stability and rheological properties of emulsions. *Cellulose* **2023**, 30, 753-773.

B. Abik, F.; Palasingh, C.; Bhattarai, M.; Leivers, S.; Ström, A.; Westereng, B.; Mikkonen, K. S.; Nypelö, T., Potential of Wood Hemicelluloses and Their Derivates as Food Ingredients. *Journal of Agricultural and Food Chemistry* **2023**, 71(6), 2667-2683.

C. Halahlah, A.; Abik, F.; Lahtinen, M. H.; Kemppinen, A.; Kaipanen, K.; Kilpeläinen, P. O.; Granato, D.; Ho, T. M.; Mikkonen, K. S., Effects of pH and temperature of ultrafiltration on the composition and physicochemical properties of hot-water-extracted softwood galactoglucomannans. *Industrial Crops and Products* **2023**, 198, 116656.

Abbreviations

AFM	: Atomic Force Microscopy
AG	: arabinogalactan
AGP	: arabinogalactan-protein complex
ANOVA	: analysis of variance
BE	: benzyl ether
C10:0	: capric acid, decanoic acid (denoting its saturation)
C8	: caprylic acid, octanoic acid
C8:0	: caprylic acid, octanoic acid (denoting its saturation)
Cas	: casein
CMC	: carboxymethylcellulose
CMGX	: carboxymethylglucuronoxylans
CNC	: cellulose nanocrystals
DIC	: Differential Interference Contrast
DIFT	: dynamic interfacial tension
Dis	: dispersion
DLS	: dynamic light scattering
DMSO	: dimethylsulfoxide
Em	: emulsion
epGX	: ethanol-precipitated glucuronoxylans
esGX	: ethanol-soluble glucuronoxylans
FA	: fatty acids
FID	: flame ionization detector
G	: guaiacyl
GC	: gas chromatography
GE	: γ-ester
GGM	: galactoglucomannans
GP	: glycoprotein
GX	: glucuronoxylans
H	: *p*-hydroxyphenyl
HPMC	: hydroxypropylmethylcellulose
HT	: high temperature storage (40 °C)
IMC	: Integrated Modulation Contrast
LCC	: lignin-carbohydrate complexes

LCMS/MS	: liquid chromatography tandem mass spectrometry
MC	: methylcellulose
MCT	: medium-chain triglycerides
MG	: monoglycerides
NMR	: nuclear magnetic resonance spectroscopy
NR	: neutron reflectometry
PG	: phenylglycosides
PHWE	: pressurized hot wate extraction
QCM-D	: quartz crystal microgravimetry with dissipation monitoring
RT	: room temperature (±22 ^{o}C)
S	: syringyl
S/G ratio	: syringyl-guaiacyl ration
SANS	: small-angle neutron scattering
SAXS	: small-angle X-ray scattering
SDS	: sodium dodecyl sulfate
SEC	: size-exclusion chromatography
sGX	: spray-dried glucuronoxylans
TG	: triglycerides
TSI	: Turbiscan Stability Index
UV	: ultraviolet
v/v	: volume-by-volume ratio
w/v	: weight-by-volume ratio
w/w	: weight-by-weight ratio

Symbols

D[4,3]	: volume-averaged diameter
D[3,2]	: surface-averaged diameter
λ	: wavelength
γ	: interfacial tension
Δf	: frequency change
ΔD	: dissipation change
Q	: scattering vector
k	: destabilization rate constant
TSI	: Turbiscan Stability Index
TSI_{max}	: maximum TSI value at infinite storage time
-	: absence of salt
+	: presence of salt
log P	: water-octanol partition coefficient

Table of contents

1 Introduction

The ongoing climate crisis, combined with the exponential growth of human population, has necessitated a need to shift from the current linear way of consumption to a more circular and sustainable economy[1]. The concept of circular economy aims to maximize the use of resources through minimalization of waste and recirculation of materials, which means that all the components of an extracted raw material should be processed as high-value products suitable for human utilization, and that products that have completed their life cycles must be repurposed or recycled[1, 2]. Additionally, there is an urge to replace materials derived from the exhaustible fossil fuels. Hence, there is a growing interest in valorizing materials that had previously been overlooked, especially from by-products of existing industries, in order to secure a sustainable future for humankind[3-5].

A source of renewable materials that is currently receiving a lot of attention is the lignocellulosic biomass, especially those from the by-products of the agriculture and forestry industry. Lignocellulosic biomass itself is not a completely new material; one of its main uses is in the production of paper, where the cellulose component is separated and refined while the rest are processed to become fuel[6, 7]. Over the past few decades, however, the interest in valorizing the hemicellulose and lignin fractions has increased significantly. While both have been subjected to numerous research exploring their breakdown into simpler chemicals (which are subsequently used as feedstock for the synthesis of other materials)[8, 9], lignin has been subject to more investigation towards their direct development into functional materials[10] compared to hemicellulose[9, 11]. One possible explanation for this imbalance could be that hemicelluloses have a large structural diversity, as different plants contain different types of hemicelluloses; even extraction methods also determine the properties of the extracted hemicellulose[12]. While the source and extraction method also determine the structure of lignin, industrial-scale extraction of lignin is more common [13], and thus it has been much more accessible compared to hemicelluloses. Nevertheless, multiple efforts have been made to create hemicellulose-based functional materials for various applications[14-17].

Of the different ways to extract hemicelluloses from lignocellulosic biomass, pressurized hot water extraction (PHWE) is a particularly interesting method that presents a unique opportunity for the valorization of hemicelluloses. Firstly, it has

been proven to be industrially viable to use wood sawdust as its feedstock, which means that it can contribute to a more complete utilization of wood biomass from the sawmill industry[18, 19]. The extraction process also uses only water[18-21]; making it an environmentally compatible process that can potentially produce hemicelluloses suitable for human consumption[22]. Moreover, the properties of the extracted hemicelluloses can be tailored by adjusting the extraction parameters[23] or subjecting the extract to a filtration process[24, 25], allowing the usage of the same extraction method to produce hemicelluloses for a wide range of applications. Furthermore, the remaining cellulose mass, while having experienced changes in their crystalline structure[26, 27], remains viable for further processing as dissolving pulp[27], which by itself is a high-value cellulose product[28]. Nevertheless, the PHWE method is also known to produce hemicellulose with the most amount of co-extracted lignin[29]. This presence of lignin is not necessarily a setback; multiple evidence points to the central role of the residual lignin towards the functionality of the hemicelluloses, particularly in emulsions[12, 30-33]. Furthermore, they have also been shown to contribute positively towards relevant health biomarkers, enhancing the functionality of the hemicelluloses as dietary fibers[34-37]. However, the residual lignin may impart a woody flavor and brown color that are perceivable at a high concentration, which may present as a barrier towards consumer acceptance of the product when such flavor or color is not desirable expected in the product[38].

Emulsions are macroscopically homogenous but microscopically heterogenous dispersions of oil and water. Food emulsions are ubiquitous; they exist either as stand-alone products, such as milk, butter, mayonnaise, and salad dressings, or incorporated into other food matrices, such as in flavored beverages[39]. Physically, mixtures of oil and water are unstable and will separate into two different phases; thus, an emulsion stabilizer is needed to prevent the separation. Several of the current emulsion stabilizers approved for foods are derived from petroleum-derived or other non-renewable materials in their industrial productions, such as polysorbates and polypropylene glycol esters[40]. Therefore, as the food consumption pattern shifts towards a more sustainable practice, the demand for environmentally-compatible emulsifiers also increases, in particular those that are derived from plant-based materials[41, 42]. PHWE hemicelluloses can potentially fill this gap. They have been proven to produce emulsions at submicron droplet sizes with comparable stability to commercial polysaccharide-based emulsifiers[30, 31, 43], despite still being inferior compared to petroleum-derived small-molecule surfactants like Tween 20[44]. Additionally, those emulsions have a low viscosity[43, 45] and are protected from oil oxidation by virtue of the residual lignin[31, 32]. This gives them the potential to be used as a nutrient fortification agent in emulsion-based food and beverages, as it can stabilize the oil phase physically and chemically, and can be added without imparting large textural changes[46].

However, the unique combination of polysaccharide and lignin in PHWE hemicelluloses extracts also endows a major hurdle to their widespread application as emulsifiers. The hemicelluloses extracts are complex mixtures that are composed of polysaccharides, insoluble lignin nano- and macroparticles, and covalently-bound complexes between polysaccharide and lignin (lignin carbohydrate complexes, LCC). While it is clear that these components contribute to the stabilization of the oil droplets[32, 33, 47], there is a lack of mechanistic understanding in the way by which those components interact with each other to stabilize the emulsions. For example, both the lignin-rich and polysaccharide-rich extracts (made by ethanol precipitation) produced less-stable emulsions compared to the crude hemicellulose extract[45, 47]. While the PHWE process is tailorable[23, 24], the chemical composition of the wood feedstock may vary[48-50], which may lead to inconsistent products when the extraction is performed without any understanding of the effect of lignin-polysaccharide proportions towards emulsion stability. Considering their future applications as food products, it became crucial to figure out their interfacial properties, as food emulsions may contain multiple components that may interact with the emulsion droplets and affect their stability. Additionally, different food products may require different emulsifying properties based on their expected characteristics and shelf life, requiring the hemicelluloses to be tailored accordingly[41]. The effect of the complexity on the digestibility of the encapsulated oil phase must also be taken into account, especially when the emulsion is intended as a carrier of bioactive and nutritionally beneficial compounds[51]. Thus, it is important to thoroughly understand the contribution of polysaccharide and lignin towards the emulsion stabilization to realize the hemicelluloses' full potential as versatile emulsifiers.

This thesis aimed to investigate the contributions of the polysaccharide and lignin fractions in PHWE birch glucuronoxylans (GX) extracts. GX from birch was chosen for this study, as birch is one of the most prominent wood species in the Finnish forest industry and is the main hardwood species in Northern Europe[52, 53]. The studies were divided into three parts: 1) understanding the formation of interfacial layers at the oil-water interface by GX (Publication I), 2) understanding the behavior of GX emulsions as a carrier of nutrients under *in-vitro* digestion (Publication II), and 3) understanding the effects of the chemical environment of the emulsion's aqueous phase towards the emulsification properties of GX (Publication III). These three approaches gave different perspectives towards the emulsion stabilization mechanism of GX in relation to their complex composition. The results of this thesis provide a more detailed relationship between polysaccharide and lignin in the emulsion stabilization mechanism of PHWE hemicelluloses. In turn, this would allow the development of a rational design of extraction and post-extraction treatments to achieve end-products that suit their respective applications, enabling a more complete utilization of wood biomass and offers a sustainable alternative of emulsifiers to the food industry.

2 Literature review

2.1 Wood polymers

From the perspective of material sciences, wood is an excellent source of biopolymers. Wood is primarily constructed out of an intricate configuration of biopolymers, arranged in different hierarchical levels of the cell wall structure. These biopolymers can be extracted using different methods, which can either preserve their native structure or create new structural features. In this section, the role of the different cell wall components as well as their industrial functionalities will be reviewed, putting an emphasis on hemicelluloses and lignin.

2.1.1 Structure of cell wall polymers

Cellulose is the most abundant polymer in plant cell walls[54]. Most of the glucan chains are arranged in crystalline units, which are subsequently connected to each other by an amorphous domain. Those cellulose units are bundled together by hemicelluloses, which forms an interface both between the cellulose bundles and the lignin, as depicted in Figure 1. Such hierarchical arrangement of these polymers builds the structure of the cell walls and imparts important macroscopic physical properties to the wood, such as strength and flexibility[55, 56]. As such, while the general structural hierarchy of these polymers are considered similar between hardwood and softwood species[57], there are differences in the molecular level that impacts the properties of the wood[58]. With regards to cellulose, the different sources are characterized by having different proportions of the crystalline and amorphous component[54]; on the other hand, the hemicelluloses and lignin components are more markedly different, especially in terms of composition, between hardwood and softwood[59].

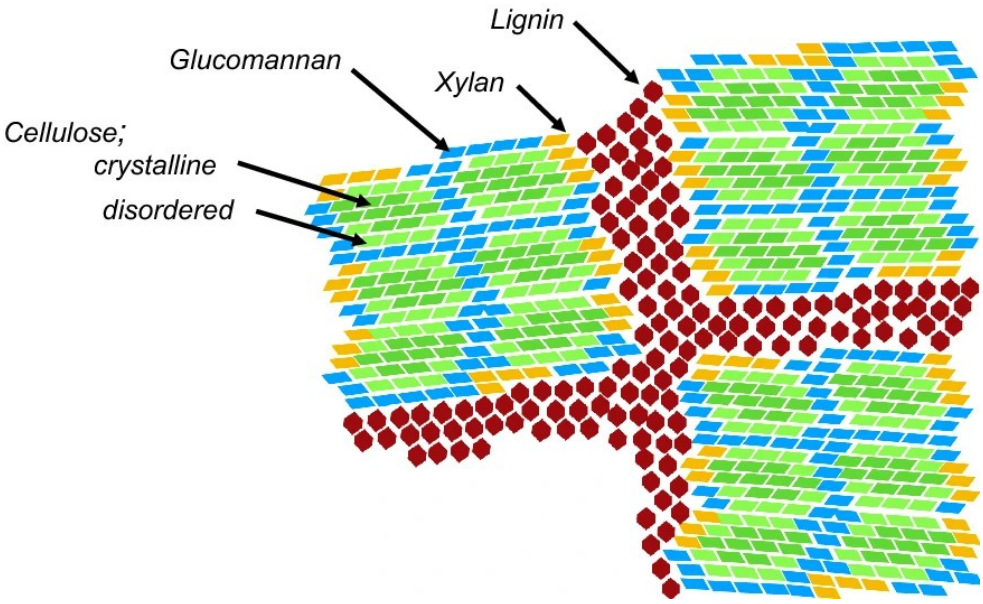

Figure 1. A simplified illustration of the molecular architecture of the secondary cell wall in softwood. Reproduced without modification from Salmén (2022)[55] under CC BY 4.0 license.

The hemicellulose component of wood is usually not composed of a single type of hemicellulose, and similar hemicelluloses can be found in both softwood and hardwood species[54, 59]. However, the predominant hemicellulose component differs between the two. In hardwood species, such as birch, beech, and poplar, the principal hemicellulose is glucuronoxylans (GX), which comprises around 15-30% of the dry biomass, whereas softwood species, such as spruce and pine, have galactoglucomannans (GGM) as the main component, making up to 20% of the dry mass. GX is composed of a linear backbone of (1→4)-β-D-xylan with residues of 4-*O*-methylglucuronic acid residues connected by (1→2) glycosidic bonds; while the exact ratio may differ depending on the extraction method, there is an average ratio of 10:1 xylose:methylglucuronic acid[60]. Meanwhile, GGM is composed of β-D-glucopyranose and β-D-mannopyranose backbone connected by (1→4) glycosidic bonds, with galactose residues bound to the backbone by (1→6) glycosidic bonds. Similar to GX, the ratio of galactose:glucose:mannose in GGM varies depending on the extraction method, which can yield either a low-galactose (at 0.1:1:4) or high-galactose (at 1:1:3) variants[54, 60]. In both softwood and hardwood, these hemicelluloses are acetylated at positions C-2 and C-3 of the backbone; on average, the degree of acetylation is at around 0.35 for hardwood GX and 0.13 for softwood GGM (corresponding to approximately seven and three acetyl groups for every ten hexose units, respectively)[54]. Their molar mass, on the other hand, are harder to measure accurately, since different extraction methods tend to yield different lengths of hemicelluloses even from the same source; nevertheless, molar mass

values of between 5-85 kDa for GX and 4-67 kDa for GGM have been previously reported[12]. The partial chemical structure of GX is given in Figure 2.

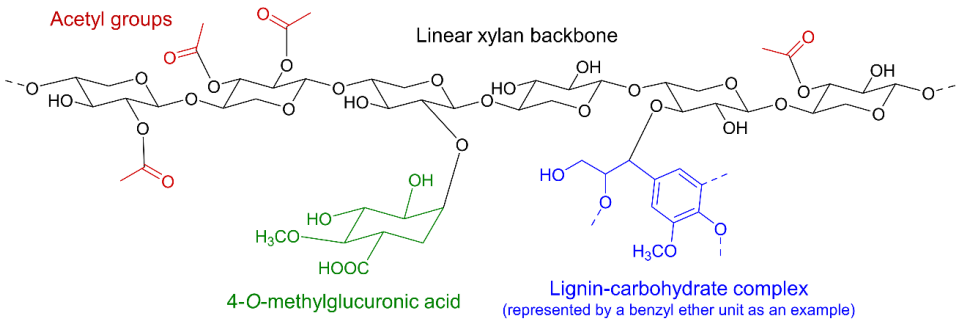

Figure 2. Partial structure of GX, showing the acetylation (red), 4-*O*-methylglucuronic acid residues (green), and lignin-carbohydrate complex (LCC, blue). The LCC structure given is of a benzyl ether bond as an example.

Lignin, on the other hand, is composed of polyphenolic polymers formed by radical polymerization of phenylpropanoid units. It is typically characterized by the proportions of its three most common constituent units, the structures of which are given in Figure 3: *p*-hydroxyphenyl (H), guaiacyl (G), and syringyl (S) units, which are linked together by numerous different linkages into a complex network of aromatic rings[13, 61, 62]. While normally lignin from any biomass would contain all three units, lignin from wood biomass is primarily composed of S and G units, and therefore the S/G ratio is often used to characterize lignin. Softwood lignin is almost exclusively composed of G-units (with S/G value as low as 0.05), while hardwood lignin has a higher proportion of S-units, with reported S/G values ranging from 1.5-3; however, the actual S/G ratio values may vary even within the same species of wood[61-63]. Meanwhile, monocots such as grass and straws produce lignin with a higher proportion of H-units than either soft- or hardwood[59, 62]. Lignin molar mass, on the other hand, is more challenging to determine compared to hemicelluloses due to its highly branched nature and the fluorescence effect from the aromatic rings[64]. Nevertheless, similarly to hemicelluloses, the molar mass of lignin depends on the extraction method, where softwood lignin has been reported to be around 12-14 kDa obtained by alkali extraction[65] and 36-61 kDa from sulfite process[66]; for hardwood, the value is around 5.7-13 kDa for both extraction methods[65, 66]. It has been found that lignin may form covalent bonding with carbohydrate moieties in the cell wall, termed lignin-carbohydrate complexes (LCC)[67]. More details about LCC will be covered in Section 2.3.2.

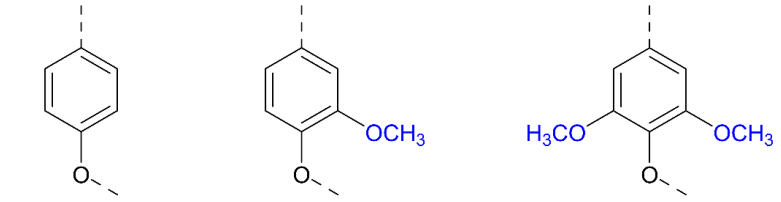

p-Hydroxyphenyl (H) | Guaiacyl (G) | Syringyl (S)

Figure 3. Structure of the most common lignin units.

2.1.2 Extraction and functionalities of hemicelluloses and lignin

While plant materials are often used as they are without extensive treatments, extraction of the different polymeric constituents of plants allows for a wider range of applications. Interestingly, the choice of extraction method is the first step in defining the end product's functionalities, as the treatments involved during the extraction may induce structural changes to the target polymers regardless of whether physical or chemical treatments were employed. Additionally, care must be taken to ensure that the cellulose component of the plant biomass remain technologically (and ultimately economically) viable, considering that the extraction process may induce changes to the remaining cellulose, such as a change in crystallinity[27, 68], shortening of the cellulose chains[68, 69], or a conversion from one cellulose allomorph to the other[70, 71]. The removal of hemicellulose and lignin may also alter the packing of the cellulose strands[72, 73], which may change the physical properties of the remaining fibers. Ultimately, as this thesis is focused more on hemicelluloses and lignin, this section will be focused on the extraction of those biopolymers.

The extraction of hemicelluloses from biomass is normally performed prior to or as part of the liberation of cellulose. One of the simplest methods is to treat the biomass with water (which can either be neutral, acidified, or alkaline) at an elevated temperature; the extraction can also be facilitated by high pressure, ultrasound, or microwave[74]. This kind of treatment is sometimes termed the autohydrolysis (if only water is used) or prehydrolysis (if acidified water is used), as the process involves the hydrolysis of the acetyl side chains and the glycosidic bonds of the hemicelluloses[75, 76]. The polymeric integrity of the hemicelluloses' chains depends on the different extraction parameters (e.g., extraction temperature, duration of exposure, and pressure level). As a rule of thumb, the more severe the treatment (i.e., higher temperature at a longer duration), shorter chains will be obtained[77, 78]; in some cases, the process could be designed to yield mono- and oligosaccharides as well as furfural derivatives[79, 80]. Meanwhile, the alkali extraction method is commonly used to obtain polymeric grade hemicelluloses, as

an alkaline environment is less damaging to glycosidic bonds and increases the solubility of polysaccharides in water[81, 82]. However, the alkali conditions also deacetylates the hemicelluloses more completely, resulting in products that are less soluble in neutral water[83, 84]. Non-aqueous and enzyme-assisted extraction methods have also been developed; the former uses various types of solvents which include, but not limited to, organic solvents, ionic liquid, and deep eutectic solvents[74]. Commercially-extracted hemicelluloses for laboratory-scale usage have been in the market for a while, for example those provided by Megazyme[85]. On the other hand, to the author's knowledge, there are only very few companies that provide large amounts of hemicelluloses; in Finland, only CH-Bioforce[86] and Boreal Bioproducts[87] are commercially providing extracted hemicelluloses in large quantities.

The GX used in this thesis were extracted from birch sawdust by PHWE. Principally, the wood biomass was exposed to high-temperature water at a high pressure, which would then extract the hemicelluloses into the water to be collected at the end of the extraction process[18, 19]. PHWE hemicelluloses are quite interesting for the lignocellulose industry, as they are extracted without using hazardous chemicals, which makes it suitable for human-related uses, such as in food or pharmaceutics. Additionally, the extraction process has been optimized to use wood sawdust, a byproduct of the sawmill industry that is often discarded. As such, it contributes to a more complete and environmentally conscious utilization of wood biomass. PHWE hemicelluloses are characterized as having the highest proportion of lignin[29] and a relatively lower molar mass compared to the other extraction methods (generally less than 10 kDa)[12, 45, 88]. Spray-dried crude extract powders of PHWE hemicelluloses could contain up to 25% (w/w) lignin, which can be reduced significantly by antisolvent precipitation using ethanol[45, 47, 89]. In these hemicellulose extracts, lignin exists as both insoluble particles and covalently bound to the hemicelluloses as LCCs, in addition to hemicellulose chains not associated to lignin. Ethanol precipitation primarily removes the insoluble lignin particles in addition to some soluble polysaccharide and lignin fractions; however, it is also possible to remove these insoluble particles by centrifugal fractionation[31, 33]. Interestingly, both centrifugation and ethanol precipitation correspond to a molar mass-based fractionation; fractions that are more soluble in water and insoluble in ethanol appeared to be of a higher molar mass compared to the fraction insoluble in water. Therefore, it has been concluded that the larger lignin moieties are associated with low-molar mass polysaccharide species[33, 89]. However, it must be noted that these results were based on size-exclusion chromatography (SEC) results using dimethylsulfoxide (DMSO)-based solvents. The limitation in SEC instrumentations required the samples to be filtered prior to analysis, which means that larger particles that do not pass through the filtration membrane may have not been analyzed during the measurement[90]. Additionally, determination the molar mass of lignin and lignin-containing molecules is complicated by their

fluorescent nature, which interferes with light scattering detectors commonly used in SEC and other chromatography-based methods[64].

After the extraction process, the hemicelluloses are utilized in various different forms. They can be broken down chemically or microbially to produce smaller molecules such as monosaccharides[91], furfurals[79, 80], and alcohols[92, 93], which can be used as precursors for synthetic compounds. While some applications are well-known and have been produced commercially, many other usages of hemicelluloses are still at a laboratory-scale, proof-of-concept stage. For example, xylose extracted from hardwood and monocots can be converted into xylitol, which can be used as an artificial sweetener[94, 95] with various health benefits, the most famous being its role in dental health[96]. It is now produced worldwide, with Finland remaining in the forefront of the world's xylitol production; the first commercial xylitol factory was established in Kotka, Finland in the 1970s[97], and in 2022 the Fazer Group, one of the most prominent confectioners in Finland, started the operation of the first xylitol factory that uses oat hulls as its raw material[98]. The hemicelluloses can also be extracted as oligosaccharides, which are known to be probiotics that are beneficial for human health[99-101]; however, only xylooligosaccharides are produced commercially from lignocellulosic biomass, while other prebiotic oligosaccharides are produced from monosaccharides or enzymatic transglycosylation[102, 103]. While polymeric hemicelluloses can be broken down post-extraction, they can also be utilized as-is. Many extracted hemicelluloses have the ability to increase the viscosity of solutions and even form gels, leading to their use as texture modifiers[104, 105], depending on their extraction methods.

Lignin, on the other hand, was initially taken as a side-product from the pulping process. As such, the earlier types of extracted lignin were named after their corresponding pulping process: kraft, sulfite, and soda lignin[13, 106, 107]. Parallel to the progress in lignin valorization, other extraction methods more dedicated to extract lignin were developed. Among those, one of the most popular is the organosolv method, which used organic solvents to solubilize lignin from the biomass matrix[106, 107]. Additionally, many of the hydrothermal treatments that are used to extract hemicelluloses also liberate lignin. As such, both polymers are often present in the extracted product to varying proportions depending on the extraction method[19, 108]. Many major companies, especially those traditionally associated with the pulp and paper industry, has diversified their product portfolio by including lignin extracted by different methods, such as Stora Enso (Finland), Domtar (United States), and Klabin (Brazil), which utilize the LignoBoost® process[109]. However, there are also smaller start-up companies around the world aiming to produce lignin of different qualities using a variety of different extraction methods[110].

In the pulp and paper industry lignin has traditionally been used to generate energy for the pulping mill by direct burning in the recovery boiler (which also recovers the pulping chemicals)[111]. However, lignin has generated more attention in its valorization, and as such more efforts have been made to commercialize lignin-derived materials. For example, it has been proven that higher quality fuel and feedstock for chemical synthesis can be produced from black liquor by gasification and pyrolysis[112, 113], which has led to the creation of at least one start-up company, RenFuel, which is based in Sweden[114]. There has also been an increased interest in valorizing lignin into higher-value materials, as lignin is a natural source of aromatic compounds[8]. In many such cases, lignin is combined with other chemical feedstocks or materials. One such example is the development of phenolic resins using lignin in combination with formaldehyde, which can be applied as adhesives[115]; another is to combine them with natural and synthetic polymers to create strong films that can be used as functional materials[116-119], which were commercialized by Prisma Composites based in the United States[120]. Lignin can also be converted into other colloidal forms, such as hydrogels[121, 122] and nanoparticles[123-125], which can then be used as-is or in other composite systems. Lignovations, a company established in Austria in 2016, claimed to be the first to produce colloidal lignin particle at a large scale[126].

2.2 Emulsions and the oil-water interface

An emerging application of hemicelluloses is in stabilizing colloidal systems such as emulsions. The stabilization may occur by virtue of viscosity modification or interfacial activity, depending on the physicochemical properties of the hemicelluloses, which may involve the presence of residual lignin in the hemicellulose extracts. This section will describe the stability of emulsion systems and the different ways an emulsion can be stabilized, with an emphasis on the role of the adsorbed layer at the oil-water interface towards stabilizing the emulsions. It will focus primarily on oil-in-water emulsions, with mentions of other emulsion systems as necessary; hence, unless mentioned otherwise, the term “emulsion” refers to oil-in-water emulsions.

2.2.1 Emulsifiers and emulsion stabilizers

The dispersion of hydrophobic compounds such as oil in water is thermodynamically unfavorable because the interaction between oil and water is weaker compared to that between water molecules. Consequently, the oil molecules would try to minimize the contact area with water in order to reach the lowest energy level. Thus, there is an energy barrier that needs to be overcome in order to increase this contact area, which is proportional to the interfacial tension between oil and water, which can be defined as the force needed to create new areas of

interface between two materials [39]. The interfacial tension can be lowered by inserting an amphiphilic material, which contains two faces: one face that interacts favorably with oil, and the other that interacts favorably with water molecules, effectively acting as a bridge. Subsequently, this lowers the energy barrier of dispersion, facilitating the emulsification process[39, 127]. Such an amphiphilic material is called an emulsifier, which can take various forms: small molecule surfactants, with a hydrophobic tail and a hydrophilic head; macromolecules containing hydrophobic and hydrophilic domains, which may unfold themselves at the interface; or solid particles, containing hydrophobic and hydrophilic faces (commonly referred to as Pickering emulsifiers)[39]. Figure 4 summarizes the different types of emulsifiers based on the physical state they are adsorbed as.

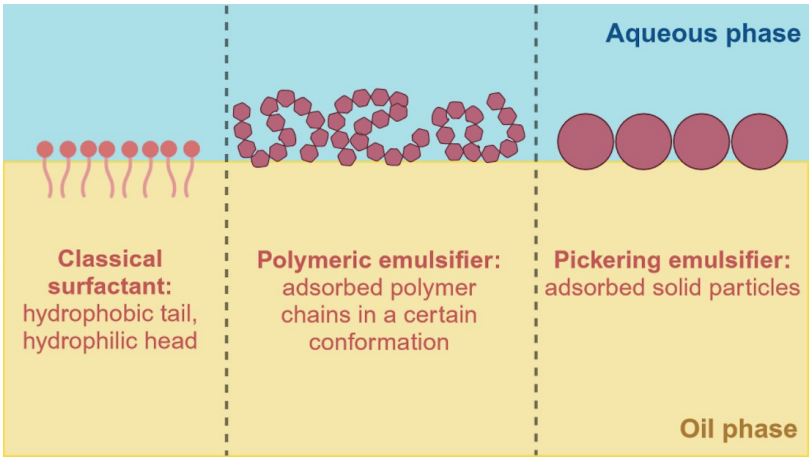

Figure 4. Illustration of the different types of emulsifiers based on their physical forms. Created using BioRender.com.

However, part of the emulsification process is the formation of new interfaces between oil and water. These fresh interfaces do not contain any emulsifier, as the adsorption of the emulsifier to the oil-water interface does not occur instantly. Therefore, the newly-formed oil droplets are prone to coalescence, leading to enlarged droplets. Consequently, in order to prevent their association, the dispersed oil molecules must be prevented from getting into contact with each other (i.e., kinetic stabilization)[39, 128]. This kinetic stabilization can be prevented by having the emulsifiers adsorb rapidly enough to the fresh interfaces before coalescence occurs (which then prevent coalescence through Gibbs-Marangoni mechanism)[128-130] or by modifying the viscosity of the continuous phase to physically slow down the droplets from colliding with each other[39, 131]. Herein the concept of emulsion stabilizer is introduced. All emulsifiers are considered as stabilizers, while not all stabilizers are emulsifiers, as some stabilizers may not have the interfacial activity to be adsorbed at the oil-water interface. Many macromolecular emulsifiers, however, may stabilize emulsions both by being

adsorbed and by modifying the viscosity of the continuous phase[131]. Table 1 shows a non-exhaustive list of commercially-used emulsifiers and emulsion stabilizers.

Table 1. Examples of emulsifiers and emulsion stabilizers used commercially. E-numbers were extracted from the European Commission database[132].

Name	E-number	Type	Source
Polysorbate/Tween	E 432-436	Small-molecule surfactant	Ethoxylation of sorbate esters of fatty acids [133]
Mono- and diglycerides of fatty acids	E 471	Small-molecule surfactant	Glycerolysis of triglycerides[134]
Gum arabic	E 414	Polysaccharide emulsifier	Extracted from acacia tree[135]
Hydroxypropyl methyl cellulose	E 464	Polysaccharide emulsifier	Derivatized from cellulose[135]
Locust bean gum	E 410	Viscosity modifier	Extracted from carob seeds[135]
Xanthan gum	E 415	Viscosity modifier	Bacterial fermentation[135]
Carboxymethyl cellulose	E 466	Viscosity modifier	Derivatized from cellulose[135]

2.2.2 Stability of emulsions during storage

After the emulsification process is completed, an emulsion will continue to be destabilized over time. Destabilization may occur in many forms. The easiest destabilization to observe is the occurrence of creaming and oiling-off, where many of the oil droplets are no longer suspended homogenously in the aqueous phase, but instead formed a separate layer; in the case of oiling-off, the integrity of the droplets has been compromised, resulting in a pooling of the oil phase on top of the emulsion[39]. In most cases regarding emulsion-based food or pharmaceutical products, such destabilization is undesirable, particularly during storage. However, there are cases where conditional destabilization (i.e., destabilization triggered by changing the environment of the emulsion) is desirable, such as in targeted oral drug delivery[136-138] or in enhanced recovery of petroleum[139-141].

On a microscopic level, destabilization takes place as an increase in droplet size, which may be the result of Ostwald ripening, droplet aggregation, or both processes

simultaneously[39]. Ostwald ripening refers to the increase of droplet size at the expense of smaller droplets, due to the diffusion of oil molecules from the smaller droplets to the larger ones across the aqueous phase. Hence, it is one of the main destabilization mechanisms for emulsions made using hydrophilic oils, such as aroma and essential oils[142, 143]. It is also considered as one of the primary destabilization mechanisms for nanoemulsions due to their small droplet sizes[144, 145]. Aggregation, on the other hand, requires the droplet to come into contact with each other. If the interfacial layer surrounding the droplets are compromised during the collision, coalescence will occur as the droplets fuse with each other. On the other hand, if the interfacial layer remains intact, but the attractive force between the droplets was strong enough to resist detachment, flocculation occurs instead[39, 130]. In all three cases, the buoyant force experienced by the droplets will increase as their size grows (following the Stokes' Law), subsequently accelerating the creaming process[130]. The different forms of emulsion destabilization are illustrated in Figure 5.

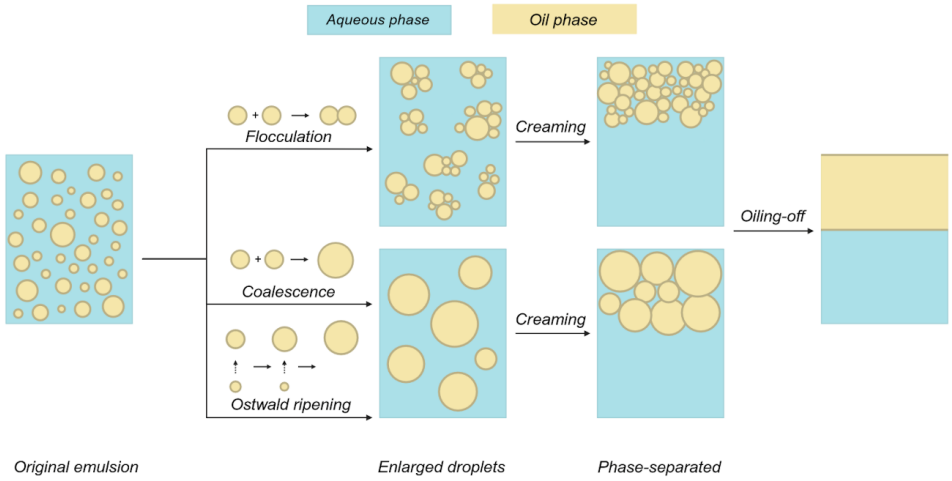

Figure 5. An overview of the different mechanisms of emulsion destabilization. Created using BioRender.com.

The interfacial layer plays an important role in keeping the emulsion droplets stable in several ways. Firstly, the interfacial layer may hamper Ostwald ripening by acting as a physical barrier, which prevents the migration of oil molecules to another droplet[146, 147]. Secondly, it may impart repulsive surface forces to the oil droplets to prevent them from getting into contact with each other, for example through electrostatic repulsion or steric hindrance[130]. Lastly, if contact occurs nonetheless, a strong and elastic interfacial layer may be able to resist coalescence[148, 149]. However, it is also possible that the material involved in forming the interfacial layer promotes destabilization instead, such as through depletion[150, 151] and bridging[152-154] flocculation. It is therefore important to

remember that while a good interfacial layer promotes a stable emulsion, there are multiple other factors that can also support the stabilization.

2.3 Polysaccharides and their conjugates as emulsion stabilizers

Polysaccharides have long been utilized as emulsion stabilizers, which can be obtained from multiple sources. Such polysaccharides can be extracted from plants (e.g., gum arabic and locust bean gum), produced through microbial fermentation (e.g., xanthan gum), or synthesized by chemically derivatizing other polysaccharides (e.g., methylcellulose and carboxymethylcellulose). This section discusses the mechanisms through which different polysaccharides stabilize emulsions, particularly for polysaccharides that are conjugated with other chemical moieties.

2.3.1 Role of polysaccharides in the stability of emulsions

The role of polysaccharides in stabilizing emulsions depends on whether the polysaccharide adsorbs at the oil-water interface. Polysaccharide stabilizers without interfacial activity normally stabilize emulsion by modifying the viscosity of the continuous phase[155]. This is achieved by the formation of three-dimensional networks formed by the polysaccharides themselves[155-157] or through an interaction with the oil droplets and the adsorbed emulsifier[158-160]. Examples of non-adsorbing polysaccharide stabilizers include xanthan gum[161], purified locust bean gum[160, 162], and carboxymethyl cellulose (CMC)[163]. As they do not form an interfacial layer, they are often used in addition to the main, adsorbing emulsifiers.

Adsorbing polysaccharide emulsifiers, on the other hand, can form an interfacial layer that further stabilizes the emulsion by similar mechanisms to small-molecule emulsifiers[155, 164], and the physical forms they adsorb as may vary depending on the type of the molecule, as illustrated in Figure 6. They may add electrostatic repulsion, steric hindrance[164], or trigger depletion attraction and bridging[159, 165]; the risk for the latter to occur is even higher compared to small-molecule emulsifiers, as the polysaccharide chains of one droplet may interact with those on another droplets, forming a bridge[166]. Their adsorption, however, is not as straightforward compared to small-molecule emulsifiers. In its solution, these polysaccharides behave similarly to polyelectrolytes and amphiphilic polymers, existing in such a conformation that reduces the contact between water and its hydrophobic moieties. As they adsorb at the interface, they undergo unfolding of the chain prior to attachment to the interface, forming an interfacial layer network . Therefore, any supramolecular assembly that exists in the solution state may not

be retained at the interface[167, 168]. Examples of polysaccharide emulsifiers are cellulose ethers, such as methylcellulose (MC)[169, 170] and hydroxypropyl methylcellulose (HPMC)[171]. It is worth noting that both MC and HPMC increase the viscosity of their respective aqueous phase; the degree of which depends on their concentration in the emulsion and their molar mass[172], and as such may stabilize emulsions by both viscosity modification and adsorption.

In addition to soluble polysaccharides, insoluble polysaccharides, such as cellulose nanocrystals (CNC), chitin nanocrystals, and starch, can also act as emulsifiers by forming Pickering emulsions[173-176]. Pickering emulsions are stabilized by insoluble particles that are adsorbed irreversibly at the oil-water interface[175]. Polysaccharide-based insoluble particles may appear counterintuitive as emulsifiers; it is their strong network of hydrophilic hydrogen bonds, after all, that rendered them insoluble. However, the surfaces of these particles are often partially hydrophobic. For example, native starch granules from different plant sources have different wettability, which was attributed to the presence of surface-associated lipid and protein impurities[173, 177]. CNC, on the other hand, are known to be both hydrophilic and lipophilic at the same time by virtue of the level of exposed crystalline plane on the surface of the crystal particles[178]. Interestingly, the surface activity of CNC can also be adjusted by tailoring its surface charge[179]. The insoluble polysaccharide particles can also by hydrophobically modified by the addition of hydrophobic moieties to improve their adsorption[180-182].

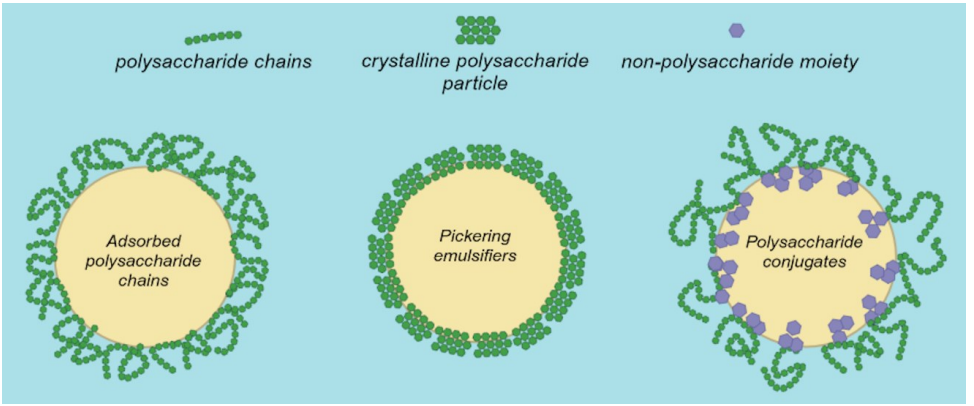

Figure 6. Illustrated overview of the possible forms of polysaccharide-based adsorbed emulsifiers. Created using BioRender.com.

2.3.2 Emulsifying properties of polysaccharide conjugates

Many natural polysaccharide emulsifiers obtain their interfacial activity by virtue of having other hydrophobic molecules attached to their polysaccharide backbones. For some cases, this attachment is simply due to reversible intermolecular

attractions; such is the case for unpurified locust bean gum[162] and corn fiber gum[183], where fatty acids molecules that were co-extracted during the extraction process of the gums became associated with the polysaccharide chains. This association gives an apparent interfacial activity to these emulsifiers, which is removed upon purification of the polysaccharides. It is also possible, however, to have the hydrophobic molecules covalently bound to the polysaccharide chains, creating "hybrid" molecules that are termed "polysaccharide conjugate"[184, 185]. These polysaccharide conjugates may act in a similar manner as small-molecule surfactants with the hydrophilic and hydrophobic ends, but also retain their macromolecular characters.

One type of polysaccharide conjugate is the protein-polysaccharide conjugate, where a protein chain is covalently bound to a polysaccharide chain. This type of conjugate occurs frequently in nature in various biological systems, such as in glycosylated antibodies[186]. As emulsifiers, however, the most famous example is gum arabic, extracted from the sap of acacia trees. Its primary constituent is the polysaccharide arabinogalactan (71-84% by mass)[135], containing residues of glucuronic acid and 4-*O*-methylglucuronic acid, while the rest is composed mainly of protein; its apparent molar mass has been measured to range from 250-2000 kDa[187]. Gum arabic can be fractionated into three main species: the arabinogalactan (AG) fraction (88.4% of total gum mass, of which 0.35% protein), the arabinogalactan-protein (AGP) complex fraction (10.4% of total gum mass, of which 11.8% protein), and the glycoprotein (GP) fraction (1-2% of total gum mass, of which 47.3% protein)[187-190]. The AGP fraction has been found to be the main fraction responsible for gum arabic's emulsifying property[187, 191]; the adsorption was driven by the reorientation of the protein moieties to expose its hydrophobic residues to the oil, followed by the subsequent formation of interfacial network by the interlinking of both protein and polysaccharide. The formation of this strong interfacial network is attributed to enhancing the stability of gum arabic-stabilized emulsions[168, 191]. In addition to naturally occurring gums, polysaccharide-protein conjugates can also be synthesized; often through a Maillard reaction between the reducing end of a polysaccharide chain and the amine end of a protein chain, although enzyme-catalyzed reactions can also be utilized[192]. For example, tea-bovine serum albumin[193] and gelatin-pectin[194] conjugates have separately been synthesized and proven to be efficient emulsifiers.

Another type of polysaccharide conjugate is the combination between polyphenols and polysaccharides. The presence of polyphenols endows antioxidant activities to the polysaccharides, which has potential health benefits when applied in foods[185, 192], and it may also protect an emulsion's oil phase from oxidation[192, 195]. These polysaccharide-polyphenol conjugates have been extracted from various plants, including tea[196], chamomile[197], and other medicinal plants[185, 192, 198]. Additionally, there are several methods to synthesize them *in-vitro*, either by

free-radical grafting, carbodiimide-assisted coupling, or enzymatically[185, 199]. Those extracted from plants, however, have rarely been exploited as emulsifiers; most research regarding the functionalities of polysaccharide-polyphenol conjugates as emulsifiers have been on synthetic conjugates[192, 199]. One interesting example is chitosan grafted by epigallocatechin gallate that was able to stabilize beta-carotene loaded emulsion both chemically and physically[200]. On the other hand, naturally-occurring conjugates have primarily been investigated for their antioxidant properties[195-197].

In lignocellulosic materials, polysaccharide-polyphenol conjugates can be found as a lignin-carbohydrate complex (LCC), where lignin is covalently bound to polysaccharides, most often to the hemicelluloses. They have been detected in both wood and pulp through various methods[67, 201, 202], although nuclear magnetic resonance spectroscopy (NMR) has been particularly useful in identifying them[203, 204]. There are three main types of LCC bonds: phenylglycosides (PG), formed between a phenolic hydroxyl group to the reducing end of the polysaccharide chain; benzylether (BE), formed by the α-carbon of the lignin's phenylpropane unit to one of the polysaccharide's hydroxyl groups; and γ-ester (GE), formed by the carboxyl group of the phenylpropane unit to the polysaccharide's hydroxyl group, or, when uronic acid residues are present, by the carboxyl groups of the uronic acid to the hydroxyl group at the γ-carbon of the phenylpropane unit[47, 67]. These different LCCs are depicted in Figure 7. The presence of LCC in hemicelluloses extracted from wood has been proven to play an integral role in their functionality as emulsifiers, where they have been proven to be adsorbed at the oil-water interface; by utilizing fractionation methods to analyzed adsorbed and unadsorbed fractions of wood hemicelluloses, it was revealed that the different LCCs are not adsorbed equally at the oil-water interface[47].

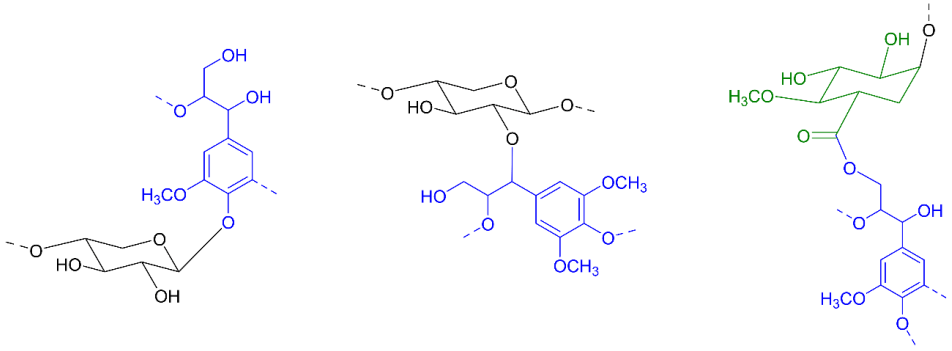

Figure 7. Types of LCC found in hardwood hemicelluloses. Blue indicates the lignin units, black indicates the xylan backbone, and green indicates the 4-*O*-methylglucuronic acid residues.

2.3.3 Current knowledge on hemicelluloses from wood as emulsifiers

While there have been plenty of research to exploit hemicelluloses as a more holistic approach to utilize lignocellulosic biomass, most valorization efforts have focused on their applications as non-polymeric materials, for example as a source of oligosaccharides[84, 101], as fermentation feed for ethanol production[92, 205], or as degraded monosaccharides for chemical feedstocks[14, 79, 80]. Nevertheless, valorization efforts towards polymeric hemicelluloses have also been performed, focused on their application as either packaging materials[16, 206], hydrogels[14, 207], or as emulsifiers[12, 83]. This section will briefly review the state-of-the-art of the latter.

The emulsifying properties of hemicelluloses from lignocellulosic biomass have been explored using different types, sources, and physical form of hemicelluloses, for example from sorghum[15], sugarcane bagasse[208], bamboo[209], and wood[12, 83, 210]. While most of the aforementioned examples have focused on solubilized hemicelluloses, crystalline xylan obtained by alkali extraction has also been investigated as Pickering emulsifiers[211, 212]. For those extracted from wood, there are several extraction methods that have been tested as emulsifiers, mainly those extracted from thermomechanical pulp (TMP) wastewater[213, 214] or directly extracted from wood chips via the patented BLN (a trade name, not an abbreviation) process or pressurized hot water extraction (PHWE)[29]. Most work on the emulsifying properties of hemicelluloses from wood, however, has focused on chemically modifying the hemicelluloses to lower their hydrophilicity and/or to improve their solubility. One proven method was through the etherification of the hemicellulose chains. Studies introducing dodecyl[215], hydroxypropyl and butoxypropyl[216], and carboxymethyl[217] groups on alkali-extracted wood hemicelluloses respectively produced water-soluble hemicelluloses derivatives that exhibited enhanced interfacial activities. Esterification, where carboxylic acids were grafted to the hemicellulose chains, has also been successfully applied with similar results to etherification, using fatty acids[218] and alkenyl succinic acid[219].

As previously mentioned in Section 2.1.2, hemicelluloses and lignin are often co-extracted during the extraction of one or the other to varying proportions, and therefore the possible participation of lignin in the emulsifying mechanism of a given hemicellulose should not be completely overlooked. Unfortunately, there has been a lack of research about how the combination of hemicellulose and lignin, especially as LCCs, contribute to emulsion stabilization. This is likely due to the highly-disperse nature of the extracts in terms of molar mass and particle size, making it challenging to deduce the stabilization mechanism. Nonetheless, one of the main hypotheses of the stabilization mechanism is that the emulsions are primarily stabilized by the LCCs present in the extract, with the phenolic moieties

pointed towards the oil phase and the polysaccharide fraction pointed towards the aqueous phase. This hypothesis was first developed in emulsions stabilized by TMP GGM through partitioning of the adsorbed and non-adsorbed emulsifiers[214] as well as by deducing the mechanism through which TMP GGM inhibited oil oxidation in the emulsions[32, 220]. Subsequently, it was also observed in PHWE GGM- and GX-stabilized emulsions[31, 47]. LCCs extracted using the Björkman method (i.e., using non-aqueous solvents) have also recently been proven to stabilize high-internal-phase emulsions[221]. Further studies investigating the mechanism of emulsion stabilization by LCC structures found that the BE LCC was preferentially adsorbed at the oil-water interface, while PG and GE were found both in the continuous phase and at the interface[47]. These LCCs are not only partitioned at the oil-water interface; BE and PG LCCs were enriched in the ethanol-soluble fraction of crude PHWE GX and GGM[47, 89], which indicates that these LCCs are associated with the more hydrophobic fraction of the hemicelluloses. However, while it is possible to fractionate the hemicelluloses by their molar mass[89], it has not been possible to isolate the pure LCCs. Nevertheless, it showed that BE and PG might play an integral role in the emulsion stabilizing mechanism. In addition to the LCCs, the insoluble lignin particles may also participate in the emulsion stabilization as Pickering emulsifiers. This was first identified in emulsions stabilized by PHWE GGM extracts fractionated by ultracentrifugation, which managed to isolate lignin macro- and nanoparticles from the crude GGM extract. These particles were found to be surface active and were able to stabilize the emulsions with a comparable stability to the crude extract[33]. This Pickering emulsifier feature was also evident in the flow behavior of PHWE GGM and GX emulsions, which had similarities to Pickering emulsions stabilized by cellulose nanocrystals[45]. However, considering that both the insoluble particles and the LCCs are present simultaneously in the hemicellulose extracts, it is currently unclear whether there are any interplay or synergistic effect between the two components, or even whether there are any contributions from other, non-adsorbed components of the hemicelluloses towards the stabilization mechanism.

Emulsions stabilized by wood hemicelluloses have two main features that would make them particularly attractive for industrial applications. The first one is the low viscosity of these emulsions, close to the viscosity of water[43, 45]. This feature may act as an advantage, which allows the fabrication of emulsions made with sticky resins[29], which are normally difficult to disperse in water, or they can stabilize emulsions intended to fortify another liquid product, especially when a high viscosity is undesirable, such as in beverages[38, 222]. However, considering that viscosity of the continuous phase is one of the ways to control emulsion stability[39], it may also act as a double-edged sword. The second feature is that the presence of phenolic compounds (primarily lignin) in wood hemicelluloses can act as antioxidants that deter oil oxidation[31, 32, 220]. This protection feature is especially beneficial in many edible applications, as most edible oils are composed

of mono- and polyunsaturated fatty acids that are prone to oxidation[223]. Having protection against oil oxidation will prevent the emulsion from becoming rancid, at which point it becomes no longer fit for consumption[224]. The antioxidative protection of the wood hemicelluloses is directly correlated to the lignin content of the hemicellulose extract[31, 32, 220]. However, the amount of lignin in crude wood hemicellulose extracts imparts a perceivable brown color and woody flavor, which can be off-putting for products where such aspects are unexpected[38]. Therefore, such considerations and trade-offs must be taken into account when designing emulsion-based products using wood hemicelluloses.

2.4 Emulsions as digestible systems

Food emulsions are, in essence, lipid-containing foods, and therefore their digestion is fundamentally similar to the digestion of other lipid-containing foods. The digestion of lipids starts already in the mouth and stomach, facilitated by the lingual and gastric lipases, respectively[225-228]. The lingual and gastric lipolysis is, however, limited by the activity of these lipases, which can only cleave one of the three fatty acids in a molecule of triglyceride. Additionally, the cleaved fatty acid is amphiphilic enough to populate the oil-water interface, further limiting the access of these lipases to the undigested lipids[228]. Thus, most of the lipid is instead digested in the duodenum, where pancreatic lipases (in combination with colipases), assisted by the combination of bile salts, phospholipids, and other polar lipids, are able to adsorb to the oil-water interface and commence the hydrolysis of most of the triglycerides, turning them into absorbable forms, be it in the form of mixed micelles, lipoprotein, or simply free fatty acids[228, 229]. Figure 8 illustrates the interfacial processes involved in the digestion of lipids in the duodenum.

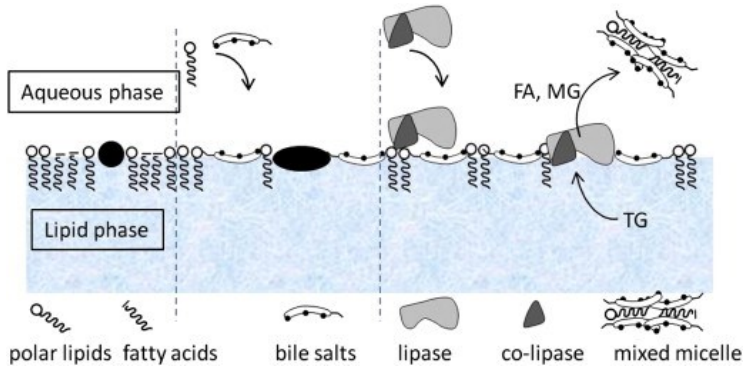

Figure 8. Schematic of the interfacial processes during the digestion of lipids in the duodenum. Reproduced from Wilde and Chu (2011)[228] with permission from Elsevier.

All biomolecules related to lipid digestion functions at the oil-water interface. Lipases, bile salts, and the phospholipids competitively adsorb to the oil-water interface, although their modes of action support each other. Lipids that come from non-emulsion foods are emulsified by bile salts and phospholipids, so that more surface areas are created for lipases to adsorb and hydrolyze the lipids. As the formed free fatty acids may inhibit the lipases, the bile salts and phospholipids subsequently form mixed micelles that take the free fatty acids away[228]. Emulsion foods, on the other hand, are already emulsified and therefore have a large surface area. However, the presence of an interfacial layer formed by the emulsifiers may influence the progression of lipid digestion, depending on the type of the emulsifiers and the properties of the interfacial layer. While some emulsifiers may be immediately displaced by bile salts due to their relatively lower interfacial activity, other emulsifiers are able to inhibit lipolysis by hindering the adsorption of lipase[228, 230]. For example, protein emulsifiers are known to form viscoelastic interfacial films that are more resistant to displacement by bile salts, especially those that underwent crosslinking by heating or chemical treatments. However, proteins are susceptible to proteolysis by the digestive proteases; once the proteins are digested, the lipid phase is then exposed for digestion by lipase[231]. Polysaccharides, in addition to forming a viscoelastic interfacial layer, may bind to the bile salts by electrostatic interactions and subsequently prevent the transport of lipolysis products, resulting in a further inhibition of lipolysis progression[231-233]. Some small-molecule emulsifiers may also prevent the adsorption of lipases by Gibbs-Marangoni mechanism[234]; however, in order to prevail in the competitive adsorption against bile salts, they must have high surface activity, be bulky enough to provide steric hindrance, and non-ionic to prevent attracting the bile salts by electrostatics[228].

The physical stability of a food emulsion during digestion is also an important parameter in its digestibility. A well-dispersed emulsion will be spread more homogenously across the bolus, while a destabilized, phase-separated emulsion, on the other hand, will instead float to the top of the mostly-aqueous gastric environment and be transferred later into the duodenum. Emulsions that remain stable during the gastric environment, however, have been shown to delay gastric emptying, and this is considered a method to prolong satiety[235, 236]. Additionally, smaller, non-aggregated emulsion droplets have a larger surface area than bigger and aggregated droplets, which means lipases may adsorb more effectively and hydrolyze more of the lipid droplets[230, 237]. However, the very nature of gastrointestinal digestion itself is not supportive in maintaining the stability of an emulsion, especially in relation to its interfacial layer. Firstly, the changes in chemical environment during digestion may compromise the interfacial interactions that keep the emulsion droplets dispersed. During digestion, an emulsion will pass through the different parts of the gastrointestinal tract with different chemical environments; one of the most profound changes is the

difference in the pH of the digestive fluids. When the emulsion is ingested at the mouth, it meets the salivary fluid, which has a pH value close to neutrality. As it is swallowed, it goes into the stomach and mixes with the gastric juice, which is substantially more acidic at a pH around 2-3. After gastric digestion, the emulsion is transferred to the duodenum, where it is mixed with the duodenal digestive fluid and neutralized back to around 7. These changes in pH, in addition to possible differences in ionic strength, may screen the electrical charges at the emulsion's interface, nullifying the electrostatic repulsion and triggering droplet aggregation[230, 238]. Additionally, the emulsifiers themselves may be digested, which leads to destabilization as the interfacial layer is chemically compromised; this is particularly the case with protein-stabilized emulsions[228]. Moreover, the presence of non-emulsifying components of the emulsion may also destabilize it, such as certain hydrocolloids that may promote bridging or depletion flocculation by adsorbing to the droplet interface[231, 239].

Overall, the digestion of emulsions as lipid-based foods can be tailored by controlling their interfacial layers, which can be achieved by either preventing the adsorption of lipases to the droplets' surface or triggering destabilization of the droplets as they are digested. Given the proper conditions, theoretically it is even possible to devise an emulsion system that passes through the gastrointestinal tract without being digested. These strategies can be particularly useful when the emulsion is used as a carrier for bioactive compounds or when designing foods that manipulate the level of satiety by regulating the digestion of lipids.

When an emulsion is used as an oral delivery system of lipophilic bioactive compounds, there are several aspects that must be taken into consideration. Firstly, the use of a lipid-based formulation, such as an emulsion, to deliver lipophilic compounds is primarily for the fact that such formulations can "solubilize" the cargo compounds; that is, to disperse them homogenously in an aqueous medium. This solubilization is important in two ways. First, in terms of the product itself, a homogenous product would allow the compound to be consumed more consistently, i.e., the same amount of cargo compound is ingested each time the same amount of the product is consumed. This homogenization is achieved by dissolving the compound in the oil phase, as such that the bioactive compound is dispersed together with the oil. Second, the solubilization assists the absorption of the cargo compound from the gastrointestinal tract to the rest of the body, as the aqueous nature of the digestive fluids may force the lipophilic compound to precipitate in the gastrointestinal tract instead of being absorbed[136-138, 240]. This solubilization is achieved in parallel to the digestion and absorption of the oil phase. As the oil phase of the emulsion is digested, mixed micelles of bile salt, phospholipids, and freshly-liberated free fatty acids are formed. The lipophilic compound, after being released from the oil matrix, may diffuse into these mixed micelles, which facilitate its absorption in the same way that the mixed micelles facilitate the absorption of fatty acids[137, 241]. Emulsifiers play a big role in this

solubilization, not only to facilitate the dispersion of the oil phase, but also in controlling the progression of lipid digestion, which in the end also controls the release of the loaded compound[241, 242]. At the end, these cargo compounds are diffused out of the mixed micelles and are absorbed together with the lipolysis products to enter the enterocytes that line the inner surface of the small intestine, subsequently transferred into the circulation system[240, 243].These consequent partitioning process is illustrated in Figure 9.

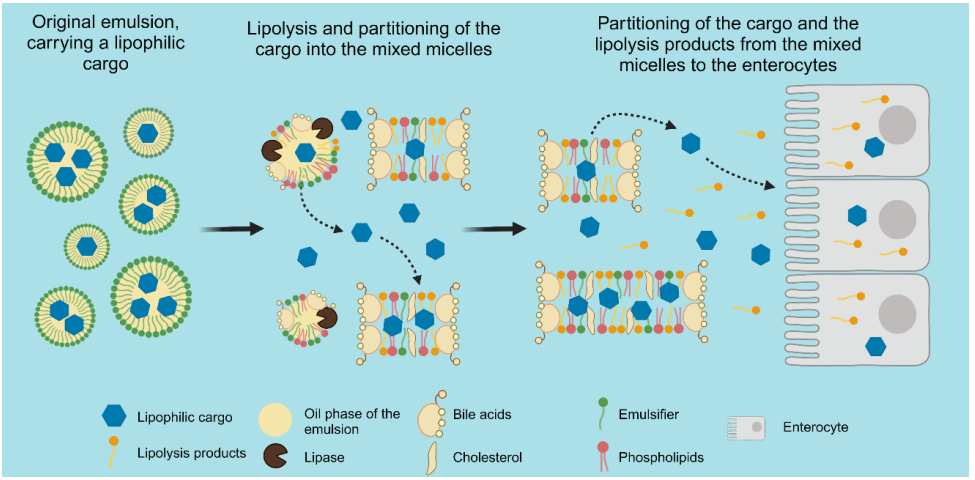

Figure 9. Illustration of the partitioning of lipophilic cargo compounds from an emulsion undergoing digestion to their absorption into the enterocytes[228, 240, 243]. Created using BioRender.com.

Another important aspect to consider is that the emulsion should also act as protection for the lipophilic compound. Such protection is needed in two manners. First, before the emulsion is consumed, it goes through different steps of production and supply chains, which would expose the lipophilic compound to various environmental hazards, such as light, oxidants, or thermal fluctuations[51]. Second, most lipophilic compounds are intended to be absorbed in the duodenum; however, to reach the duodenum, it must first pass the mouth and the stomach, where the fluctuating chemical environment and the extremely acidic stomach fluid may degrade the cargo compound[233]. Both forms of protection can be achieved by choosing the right emulsifier, which forms a protective layer on the surface of the oil droplets. Ideally, the emulsifier should maintain the integrity of the interfacial layer during the gastric phase, while subsequently it should allow the emulsion to be digested during the duodenal phase[46, 51, 192, 233].

In addition to the two aspects above, there are also other considerations that must be taken into consideration when designing an emulsion-based delivery system is

intended to be incorporated in foods, for example in fortification of foods with vitamins. The emulsion and its components should not negatively affect the physical properties of the food it is inserted into, such as the appearance, flavor, or texture. It should also involve ingredients that are known to be safe for consumption, so that it does not impart any adverse health impact to the consumers. Lastly, the ingredients should be economically viable so that its production can easily be scaled up without incurring too much cost[244-246].

Therefore, designing an emulsion system for the purpose of delivering a bioactive lipophilic compound is not straightforward. All components of the emulsion may influence the accessibility of the cargo compound, from the oil, emulsifier, additional stabilizers, to other smaller compounds that are added to the emulsions. Nevertheless, a good understanding of the interaction between the cargo compound, the emulsion components, and the gastrointestinal digestion system will allow the delivery system to be designed rationally and effectively.

3 Aims and hypothesis of the study

This doctoral thesis aimed to establish the roles of polysaccharide and lignin fractions in PHWE GX, both by themselves and in connection to each other, in their functionalities at the oil-water interface in an emulsion system, considering physical and chemical stability including during gastrointestinal digestion. The studies in this thesis were designed with the complex nature of PHWE GX in mind, taking into account the inability to separate the surface-active components of GX into their pure constituents. Thus, the interfacial properties of GX were primarily analyzed both by comparison to established emulsifiers and between the fractionated GX themselves. The primary hypotheses of this thesis are:

1. Residual lignin plays a central role in the interfacial activity of GX, supported by the polysaccharide fraction.
2. The superior emulsion stability exhibited by the crude GX extract is attributed to the presence of insoluble lignin particles in addition to a larger amount of polysaccharide.
3. The higher amount of lignin in the crude GX extract, which was correlated to a better protection against oil oxidation, also correlates to better protection of a hydrophobic cargo compound.
4. The nature of GX as indigestible fibers allows GX emulsions to carry a hydrophobic cargo compound safely to the duodenal phase during digestion.

To test the hypotheses, this thesis was divided into three studies addressing the following specific aims:

1. To understand the process of adsorption of GX onto the oil-water interface in forming an interfacial layer (Publication I and III)
2. To understand the roles of hemicellulose and residual lignin fractions in GX emulsions as an emulsion-based carriers of bioactive compounds in the gastrointestinal system (Publication II)
3. To understand the interplay between the hemicellulose and lignin fractions of GX and the chemical environment of the aqueous phase towards emulsion stabilization (Publication III)

The results of this thesis will provide additional information on the interplay between polysaccharide and lignin in PHWE GX, which can eventually be used to establish a sensible rationale in the fractionation of lignocellulosic biomass.

4 Experimental section

4.1 Materials

Spray-dried GX (sGX) from birch wood was kindly provided by Dr. Petri Kilpeläinen of the Natural Resources Institute of Finland (Luonnonvarakeskus, LUKE), which was produced by the PHWE method. Ethanol-precipitated (epGX) and ethanol-soluble (esGX) GX were prepared from sGX by antisolvent precipitation using ethanol as described for GGM[24]. Carboxymethylated GX (CMGX) was synthesized from epGX following an adapted procedure[217], as published in Supporting Publication A[45]. The complete characterization of the sGX, epGX, esGX, and CMGX are summarized in Section 4.1.1., and the results are displayed in Table 2.

Methylcellulose (MC, Methocel™ A15LV) and carboxymethylcellulose (CMC, Walocel™ CRT 30) were kindly provided by Dupont (Meyrin, Switzerland); their selected properties are listed in Publication I. Anionic cellulose nanocrystals (CNC) obtained by sulfuric acid hydrolysis of wood pulp was purchased from CelluloseLab (Fredericton, Canada); its zeta potential is -45 mV, with dimensions of 5-20 nm in width and 140-200 nm in length. Sodium caseinate was purchased from Sigma-Aldrich (St. Louis, MO, USA). Hexadecane (Sigma-Aldrich, St. Louis, MO, USA) was used as the oil phase for most of the studies in this dissertation (Publication I and III). Medium-chain triglyceride oil (MCT, Puhdistamo – Real Foods Oy, Lempäälä, Finland) was used for the vitamin D3-carrier studies (Publication II), where the fatty acid composition was determined to be 66 mol% caprylic acid (C8:0), 33 mol% capric acid (C10:0), and trace amount of longer-chain fatty acids (by fatty acid methyl ester analysis using gas chromatography). The procurement of other chemicals in the other sets of studies have otherwise been detailed in the Publications I-III. All chemicals were used without further purification or treatment unless otherwise indicated.

4.1.1 Physicochemical characterization of GX samples

Monosaccharide composition of the GXs were analyzed by performing acid methanolysis on the GXs, followed by silylation of the methanolysate and subsequent analysis by gas chromatography (GC) equipped with flame ionization

detector (FID); details of the experiments are given in Supporting Publication A[45].

Lignin content of the GXs were determined by acetobromination (for sGX and CMGX in all Publications; epGX in Publication I) or cysteine-sulfuric acid derivatization (for epGX in Publication II and III, esGX in Publication II), followed by UV spectrophotometry compared to a standard curve of lignin for both methods. Details of the measurement experiments were detailed in Supporting Publication A[45] (acetobromination) and C[24] (cysteine-sulfuric acid). Lignin content of CMGX was found to be overestimated due to the formation of hexenuronic acid during synthesis; this was addressed by UV-resonance Raman spectroscopy as elaborated in Supporting Publication A[45].

Acetyl content and degree of acetylation of sGX, epGX, and esGX in all Publications were determined by first hydrolyzing the bound acetyl groups using aqueous 0.1 M NaOH overnight, neutralizing the reaction mixture, then analyzing the released amount of acetyl group using acetic acid quantification kit (Megazyme, Bray, Ireland). Degree of carboxymethylation for CMGX was determined by quantitative solid-state NMR. Details of the measurements are detailed in Supporting Publication A[45].

Molar mass of the GXs were determined by size-exclusion chromatography (SEC), either in DMSO (containing 0.01 M LiBr) or water (containing 0.1 M $NaNO_3$). Details of the measurements were detailed in Supporting Publication A[45].

A summary of the physicochemical characteristics of the GXs is given in Table 2.

Table 2. Physicochemical characteristics of the GXs used in this thesis.

Parameters	sGX	epGX		esGX		CMGX
Publication	I, II, III	I	II, III	I[c]	III	I, III
Lignin content (g/100 g powder)	24.63 ± 3.82[a]	15.26 ± 0.07[a]	1.24 ± 0.62[b]	30.4 ± 1.3	27.46 ± 0.58[b]	18.67 ± 0.01[a]
Degree of acetylation	0.51	0.38	0.71	0.40	0.47	n.d.
Degree of carboxymethylation	n.d.	n.d.	n.d.	n.d.	n.d.	0.33
Molar mass (Da)/Dispersity						
in 0.01 M LiBr in DMSO	2800/4.8	3500/2.0	4500/2.4	1200/1.9	1100/2.3	n.d.
In 0.1 M $NaNO_3$ in H_2O	3600/2.5	3600/1.8	n.d.	n.d.	n.d.	7600/1.7
Monosaccharide content (g/100 g powder)						
Xylose	53.21 ± 0.71	55.36 ± 3.07	55.81 ± 3.75	63.8 ± 0.9	41.57 ± 1.87	35.02 ± 1.76
Glucose	1.92 ± 0.09	5.06 ± 0.25	2.37 ± 0.14	1.0 ± 0.4	1.04 ± 0.04	3.49 ± 0.20
Mannose	2.50 ± 0.11	3.63 ± 0.19	3.41 ± 0.18	1.9 ± 0.2	1.55 ± 0.10	2.40 ± 0.09
Galactose	1.56 ± 0.04	2.30 ± 0.19	1.99 ± 0.15	1.1 ± 0.1	0.82 ± 0.05	0.10 ± 0.01
Rhamnose	0.91 ± 0.04	0.8 ± 0.05	1.18 ± 0.09	1.5 ± 0.1	1.34 ± 0.05	0.67 ± 0.03
4-*O*-methylglucuronic acid	7.33 ± 0.22	7.11 ± 1.01	8.95 ± 1.48	n.d.	3.81 ± 0.74	7.08 ± 0.23
Galacturonic acid	1.98 ± 0.99	-	2.51 ± 0.19	-	-	-

Footnotes:

a. Determined by acetobromination method (Supporting Publication A)
b. Determined by cysteine-sulfuric acid method (Supporting Publication C)
c. Reproduced from Morais de Carvalho, et. al. (2021)[47] under CC BY ND 4.0 License

4.2 Preparation of GX dispersions and emulsions

All emulsifiers were dispersed in their respective buffers at pH 4.5 or 10 as indicated in the different publications (25 mM citrate, Publication I; 25 mM citrate with 0.05% w/v potassium sorbate, Publication II; 25 mM citrate-carbonate, Publication III) with the exception of casein, which was dissolved in 25 mM phosphate buffer pH 6.5 to avoid precipitation. Experiments involving salt in Publication I and III used 0.1 M NaCl and 0.1 M $NaNO_3$, respectively. GXs and casein were dissolved under stirring directly in their respective buffers at least overnight to ensure maximum dispersion; esGX was ultrasonicated (Branson 450 Digital Sonifier, Marshall Scientific, Hampton, NH, USA) at 50% amplitude for 30 s continuously in order to minimize aggregation. MC was dispersed using the hot-cold method as devised by the manufacturer: first, it was heated under stirring in approximately one-third of the total volume of buffer to near-boiling, followed by the addition of refrigerated buffer, stirring in an ice bath until the dispersion became transparent. The mixture was then topped off with the buffer to the required amount of total dispersion mass and left to stir overnight in an ice bath. CMC was dissolved under boiling in half of the required amount of buffer, followed by cooling the mixture down and topping off by the intended buffer, and finally left to stir overnight at room temperature. CNC was first dispersed overnight in the buffer, then ultrasonicated at 50% amplitude on a 10 s-on 10 s-off cycle for a total of 20 min (effectively 10 min exposure).

The emulsions used in the studies were prepared in two stages. All emulsions were composed of 1% emulsifier and 5% oil (w/w emulsion); for the vitamin D3 studies, the vitamin D3 was dissolved directly into the medium chain triglyceride (MCT) oil at approximately 1-2 mg/mL, kept at 5 ^{o}C in a dark bottle under nitrogen atmosphere prior to usage. The mixture was first pre-emulsified using a high-speed homogenizer (Ultra-Turrax T-18 basic, IKA, Staufen, Germany), followed by high-pressure homogenization (Microfluidizer, Microfluidics, Westwood, MA, USA); details of the homogenization processes are listed in the respective Publications I-III.

4.3 Characterization of the GX interfacial layer

4.3.1 Dynamic interfacial tension (DIFT)

The adsorption of GX and other emulsifiers at the liquid-liquid interface without external energy input was analyzed by evaluating the drop in interfacial tension value over time based on the reverse pendant drop method. Measurements were

done between a suspended drop of hexadecane against 0.03% (w/v) aqueous dispersion of the emulsifiers. Details of the experiments are found in Publication I.

4.3.2 Quartz crystal microgravimetry with dissipation (QCM-D)

QCM-D (E4 instrument, Q-Sense AB, Västrä Frölunda, Sweden) was performed to approximate the mass of the adsorbed layer formed by the emulsifiers at the oil-water interface. As there is currently no feasible method to directly measure the layer's mass at the liquid-liquid interface, a solid-liquid interface was utilized instead, where a layer of paraffin wax was used to simulate the hydrophobic interface between oil and water; the wax surface was then contacted by 0.03% (w/v) emulsifier dispersion. Details of the QCM-D experiments are found in Publication I.

4.3.3 Atomic force microscopy (AFM)

The attractive forces between GXs and paraffin wax was studied by force spectroscopy using an AFM (NanoWizard 4XP BioScience, Bruker Nano GmbH, Berlin, Germany). Details of the AFM force spectroscopy experiments are found in the supplementary materials of Publication I.

4.3.4 Neutron reflectometry (NR)

NR was performed to investigate the thickness of the adsorbed interfacial layer at the hexadecane-water interface, on an experimental setup using a thin layer of sapphire-matched hexadecane contacted against 0.3% (w/v) aqueous dispersions of the GXs. The reflectometry experiments were performed at the INTER time-of-flight reflectometer at ISIS Pulsed Neutron and Muon Source, United Kingdom. Details of the NR experiments are detailed in Publication III. Experimental data related to the NR experiments are available online at https://doi.org/10.5286/ISIS.E.RB2310039.

4.4 Characterization of GX emulsions as vitamin D3 carrier

4.4.1 *In-vitro* digestion

The digestibility of the vitamin D3-loaded emulsions was performed based on the static *in-vitro* digestion protocol INFOGEST 2.0. A sample of the emulsion (5 g) was incubated at 37 °C with constant agitation (60 rpm) for 2 min of oral phase, 2 h of gastric phase, and 2 h of duodenal phase. The digestion protocol was adapted to focus on the digestion of triglycerides on a starch-free system. As such, no amylase was used during the experiments, rabbit gastric lipase was used for the gastric phase, and the amount of pancreatin used for the intestinal phase was adjusted to its lipase activity instead of its protease activity. Details of the *in-vitro* digestion experiments are given in Publication II.

4.4.2 Measurement of the vitamin D3 content

Measurement of vitamin D3 content was performed on two instances in Publication II: A) from the emulsions before and after storage, to analyze the ability of the emulsifiers to stabilize the vitamin D3 contained in the emulsion during storage, and B) from the digesta of the *in-vitro* digestion to analyze the vitamin D3 release-over-time profile. In both cases, the vitamin D3 was first extracted from the sample matrices, and afterwards derivatized and analyzed by chromatographic methods. Extraction of the vitamin D3 was performed by room temperature alkali hydrolysis of the sample, followed by liquid-liquid extraction of the vitamin D3 into an organic phase. Vitamin D3 content in A was determined by GC-FID of silylated vitamin D3, with the results converted into the retention rate of vitamin D3 after five weeks of storage. In B, LCMS/MS was used to analyze the extracted vitamin D3 after derivatization, which afterwards was calculated into the recovery rate of vitamin D3 over digestion time. Details of the experiments and the calculations are given in Publication II.

4.4.3 Measurement of the released fatty acid

The release of a cargo compound from an emulsion-based delivery system is often related to the rate at which the oil phase is digested. Additionally, the emulsifier may block the lipolysis of the oil phase by blocking the lipase from adsorbing onto the surface of the oil droplets. The lipolysis of the studied emulsions during *in-vitro* digestion was monitored over time by measuring the amount of free fatty acid in the digesta over time, utilizing LCMS/MS. Details of the analysis are described in Publication II.

4.5 Characterization of GX dispersions and emulsions

4.5.1 Storage stability analyses

Two storage tests were performed on the emulsions: 1) analyzing the physical stability of GX-emulsions as vitamin D3 carrier, comparing the GXs to MC and casein (Publication II), and 2) analyzing the effect of pH and ionic strength towards stability (Publication III). The types of analyses and the timepoints on which the analyses were performed are detailed in Table 3.

Table 3. Overview of the emulsion storage stability experiments in their respective publications, along with the associated analyses.

Publication	Measured timepoints	Storage temperature	Tested GX	Analyses
II	Day 0, 7, 14, 21, 28, 35	Room temperature (±22 °C) and 40 °C	sGX, epGX	Droplet size, destabilization kinetics, optical microscopy, vitamin D3 retention
III	Hour 0, 6, 24, 48, 72, 96, 168	Room temperature (±22 °C)	sGX, epGX, esGX, CMGX	Droplet size (including SDS displacement), destabilization kinetics, optical microscopy, centrifugation, zeta potential, pH and salt effect

4.5.2 Optical microscopy analyses

Brightfield optical microscopy was used to analyze the effect of the chemical environments on the physical stability of the emulsion droplets, primarily to observe qualitatively the extent of flocculation and coalescence. Special contrast methods to visualize the three-dimensional nature of the emulsion droplets were employed, namely integrated modulation contrast (IMC) in Publication II and III, and differential interference contrast (DIC) in Publication II. Details of the microscopy experiments are given in Publications II and III.

4.5.3 Particle/droplet size measurements

Measurements of the size of GX particles in their dispersions were performed by dynamic light scattering (DLS, Zetasizer Nano ZS, Malvern Panalytical Ltd., Malvern, UK) at 25 °C after 30 s of equilibration, measuring the backscattering at 173°. The refractive indices for the dispersant (buffer) and the GX were set at 1.33 and 1.48, respectively; absorptivity of 0.38 was set to take into account the absorbance from the lignin moiety. The intensity-averaged particle diameter was obtained using Malvern's general-purpose algorithm embedded in the Zetasizer software.

Measurements of the size of emulsion droplets were performed by laser diffraction (Mastersizer Hydro 3000 SM equipped with Hydro EV accessory, Malvern Panalytical Ltd., Malvern, UK). The rotor speed of the dispersion module was set at 1500 rpm. 1.33 was used as the refractive index of the dispersant (water), whereas for the oil droplets 1.434 and 1.44 for hexadecane and MCT oil were used, respectively. Time points, for which the droplet size of the emulsions was measured, are detailed in the respective Publication. The results were presented as droplet size distribution, volume-averaged diameter (D[4,3]) and surface-averaged diameter (D[3,2]) calculated using the Mastersizer software v3.62 (Malvern Panalytical Ltd., Malvern, UK).

Flocculation and coalescence of the oil droplets in GX-stabilized emulsions were investigated by the addition of sodium dodecyl sulfate (SDS). As SDS is a surfactant with a high interfacial activity, it can displace the original emulsifiers without redispersing the oil droplets, and break flocs that are formed by bridging of the emulsifiers at the interface. The difference of droplet sizes obtained in the presence of SDS can therefore be taken as the droplet growth arisen solely from coalescence. The GX-stabilized emulsions were mixed with 10% (w/v) SDS in water at a 1:4 (v/v) emulsion:SDS ratio, mixed gently for a few seconds, then immediately subjected to droplet size measurements.

4.5.4 Measurement of zeta potential

Zeta potential, which is the electrical potential of the interfacial double layer of a given colloidal particle, reflects the electrical charge that is present at the surface of a colloidal particle, and as such in a rough estimate of the extent of electrostatic repulsion between colloidal particles. The zeta potential of the dispersions and emulsions were measured by electrophoretic light scattering (Zetasizer Nano ZS, Malvern Panalytical Ltd, Malvern, UK); the details of the experiments are described in Publications I and III.

4.5.5 Measurement of destabilization kinetics

Destabilization kinetics of the dispersions and emulsions were performed using Turbiscan Lab Expert analyzer (Formulaction, Toulouse, France), which involved the measurement of transmission and backscattering of a near-infrared light (λ=880 nm) over the entire height of the sample at the detector angles of 180° and 45°, respectively. The resulting transmission and backscattering profiles at the different measurement timepoints were then converted (Turbiscan software v. 1.2, Formulaction, Toulouse, France) into the Turbiscan Stability Index (TSI), which was calculated from the relative change in backscattering and transmission profile between two subsequent time points. The results were then analyzed based on both the curves of TSI progression over time and the fitted TSI_{max} and k values, which correspond to the maximum TSI reached at infinite time and the rate constant of the curve, respectively. Details of the Turbiscan destabilization experiments are described in more details in Publications I, II, and III.

4.6 Statistical analyses

The retention rates of vitamin D3 in the emulsions between RT and HT storage were compared within each of the emulsifiers using two-sample *t*-tests. The mean values of the emulsions' zeta potential, D[3,2], and D[4,3] were analyzed using two-way and three-way analysis of variance (ANOVA). Three-way ANOVA was performed to compare the means across the different emulsifier types, pH, and presence of salt using post-hoc Tukey's test, while two-way ANOVA was performed on individual emulsifiers to evaluate whether there were significant interactions between pH and salt content towards the respective responses. All analyses were conducted at 95% confidence interval using OriginPro software (version 2021b, OriginLab Corporation, MA, USA).

5 Results

In this chapter, all experimental results are presented without in-depth discussion. This chapter is divided into three sections, where first (Section 5.1) the experiments concerning the passive adsorption (i.e., adsorption without external energy input) of GX to the oil-water interface are presented. All GXs were tested in this part, with several comparisons with MC, CMC, and CNC. The second section (Section 5.2) covers the experiments related to the evaluation of GX as emulsifiers for emulsion-based carrier of vitamin D3, including the storage stability and *in-vitro* digestion experiments. Here, sGX and epGX were compared to MC and casein. Lastly, the third section (Section 5.3) presents the storage stability study of GX-stabilized emulsions at different pH and salt content, where the four types of GX were compared against each other.

5.1 Adsorption of GX to hydrophobic interfaces

5.1.1 Dynamic interfacial tension (DIFT)

DIFT results are generally shown as the change in the interfacial tension value over time; the pattern of which then describes the dynamic process of emulsifier adsorption at the interface. The evolution of interfacial tension over time between the GXs at 0.03% (w/v) against hexadecane, compared to those of other polysaccharide emulsifiers and emulsifier-free interface, are presented in Figure 10. Comparison between the GXs (Figure 10A) showed that each GX are adsorbed at a different rate, in the order of esGX > sGX > epGX > CMGX; this trend is in agreement to the amount of lignin contained in the GXs. The onset of the rapid fall phase also became shorter with increasing lignin content, which disappeared completely for esGX, having a similar dynamic compared to MC. Despite the difference in adsorption rate, all GXs exhibited adsorption, in contrast to CMC and CNC, both of which showed a similar interfacial tension dynamic to the bare interface, indicating minimal adsorption.

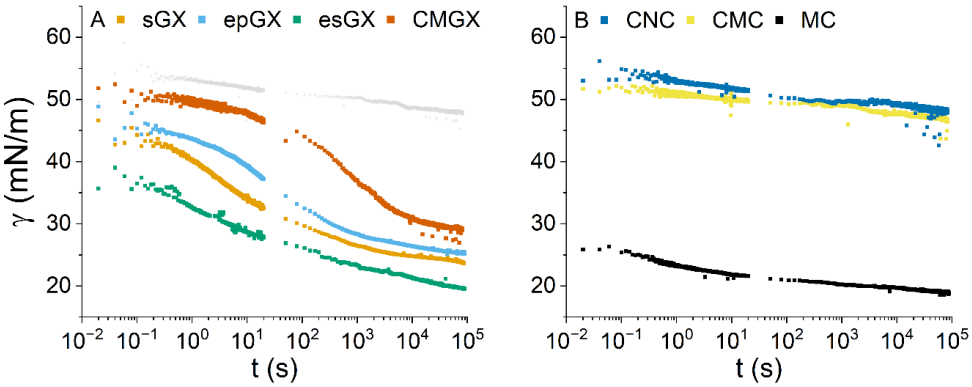

Figure 10. DIFT of the different GXs (A) and polysaccharide emulsifiers (B) at 0.03% (w/v) in citric acid buffer 25 mM pH 4.5 against hexadecane. Light grey in (A) indicates the DIFT profile of emulsifier-free citric acid buffer against hexadecane.

The DIFT profile of GXs appeared to be dependent on their concentration, as shown in Figure 11. The DIFT profiles of both sGX and esGX could not be measured above 0.15% and 0.1%, respectively, as both GXs contained insoluble particles that made the suspended drops invisible. Except for CMGX, the onset of the rapid fall phase disappeared at concentrations 0.1-0.3% onwards. The DIFT for epGX 1% was even so low, that the hexadecane drop could not be suspended for more than 5 minutes.

As elaborated in Section 2.3.3, there was evidence that the different LCCs were not distributed evenly during the fractionation of GX by ethanol precipitation. However, it is currently not possible to purify the individual LCCs from GX and characterize their interfacial activities. Therefore, by comparing the DIFT profiles of the GXs at 0.003% (w/v), the fraction containing the most active species can be identified, assuming that at a dilute enough concentration the adsorption profile will be dominated by the species that adsorbs the fastest. According to Figure 12, the DIFT profile of esGX and sGX at 0.003% overlapped, which signified that the fastest adsorbing species of GX was fractionated into the ethanol-soluble fraction.

The adsorption of the GXs at the hexadecane interface was also affected by the ionic strength of the GX dispersions. The presence of NaCl in the dispersions did not appear to shift the onset of the rapid fall phase, but instead it shifted the whole DIFT curve to lower interfacial tension values, as shown in Figure 13. The extent of the drop appeared to be correlated to the amount of hydrophilic polysaccharide fraction on the GX, where CMGX > epGX > sGX > esGX; the profile for esGX did not appear to be affected by the presence of salt. It is worth noting that in the presence of NaCl 100 mM (light red curve in Figure 12A) the buffer seemed to have a background interfacial activity, which can be attributed to the interfacial activity of citric acid, amplified by the presence of salt. However, the rapid fall phase occurred much later

than the interfacial activities of the GXs and therefore can be considered much less active than the GXs.

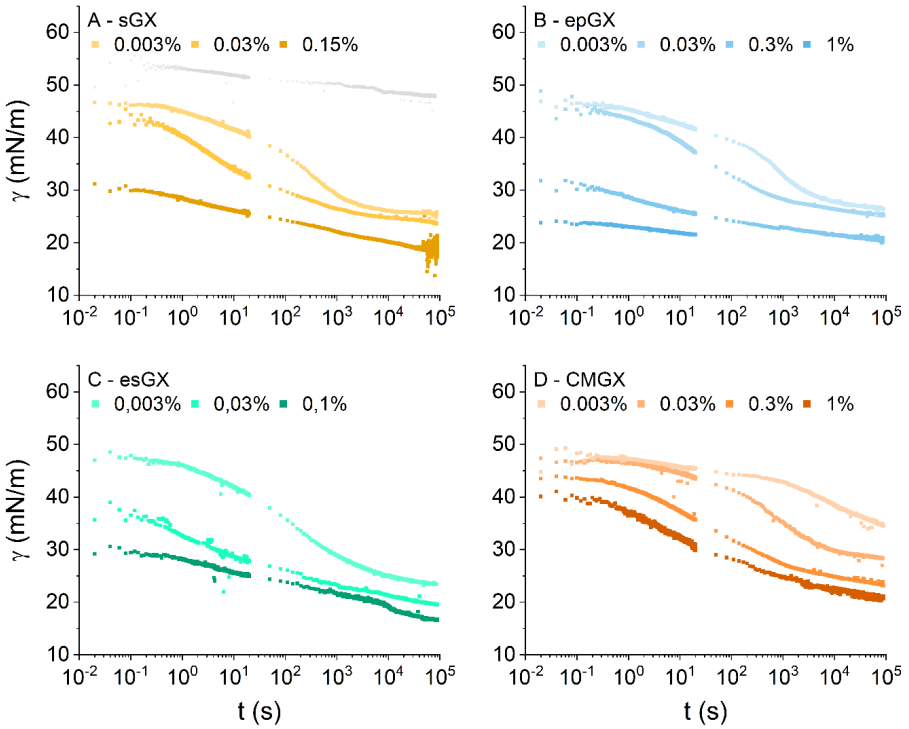

Figure 11. DIFT profiles of the GXs at different concentrations. Lighter colors indicate lower concentrations. The light grey curve in (A) is the DIFT profile of clean, emulsifier-free buffer.

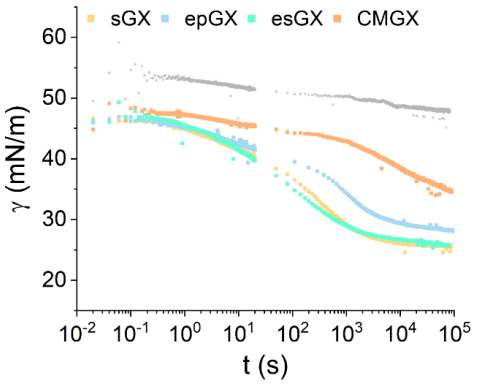

Figure 12. DIFT profiles of the GXs at 0.003% (w/v). Light gray DIFT profile indicates the DIFT of the bare buffer-hexadecane interface.

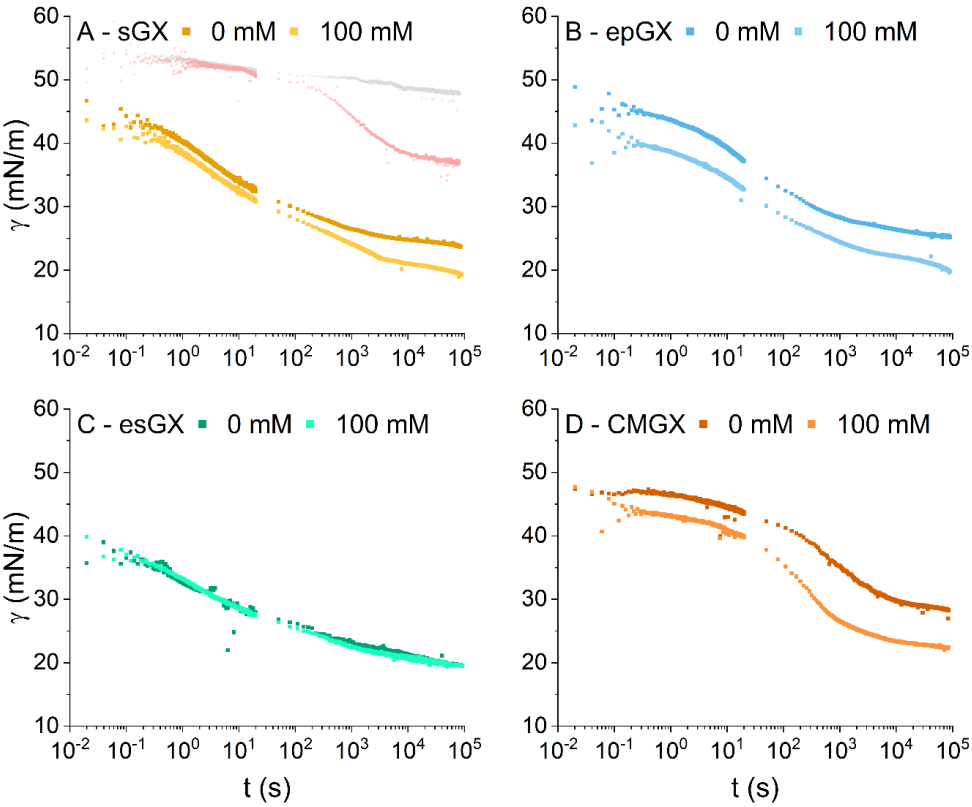

Figure 13. DIFT profiles of the GXs with (dark) and without (light) NaCl 100 mM. Light grey and light red DIFT profiles in A correspond to the DIFT profile of citric acid buffer 25 mM pH 4.5 without and with salt, respectively.

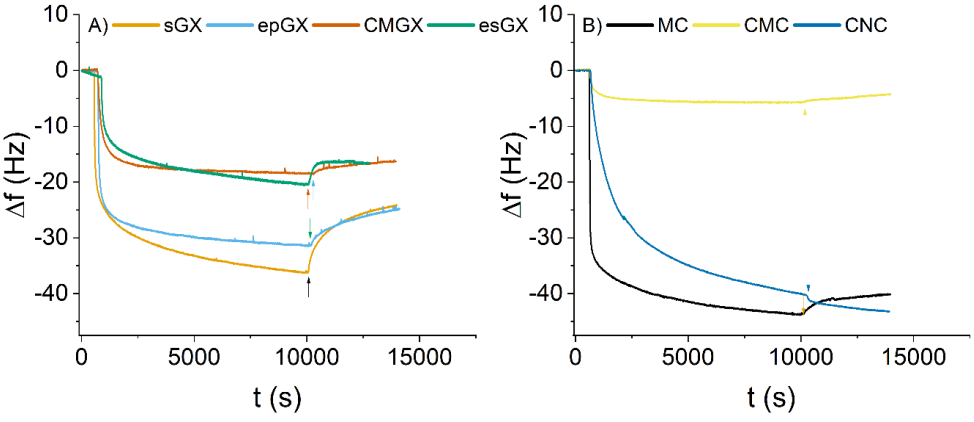

Figure 14. Changes in frequency at the 5th overtone over time between the GXs (A) and other polysaccharide emulsifiers (B). Arrows signify the point of rinsing step, when clean buffer was introduced.

5.1.2 Quartz crystal microgravimetry with dissipation monitoring (QCM-D)

One of the main measured parameters of QCM-D is the drop of the oscillating frequency overtime, which is correlated to the amount of adsorbed materials on the surface of the sensors; the more materials adsorbed, the heavier the sensor becomes, and therefore the oscillating frequency becomes lower. The frequency change-over-time profiles recorded by QCM-D at the 5^{th} overtone upon the adsorption of GX and other polysaccharide emulsifiers on paraffin wax are shown in Figure 14. All emulsifiers showed the characteristics of a viscoelastic adsorbed layer, where the dissipation and frequency change curves of the different overtones did not overlapped (data not shown); this suggested that the Sauerbrey equation could not be applied to estimate the mass of the adsorbed layer. However, upon fitting the results using the Kelvin-Voigt model, the data for esGX could not be fitted properly, and therefore the results can only be compared as they are. All emulsifiers exhibited adsorption, although to different extents. Initially, there seemed to be more sGX that was adsorbed compared to epGX; however, after clean buffer was introduced, the equilibrium level appeared to be similar between the two. CMGX was adsorbed the least among the GXs, which was in agreement with its DIFT result; however, esGX, which was adsorbed the fastest, lowered the frequency similarly to CMGX. The change of frequency profile for MC and CMC also appeared to be in agreement with their respective DIFT profile. CNC, however, showed a strong adsorption that increased slightly after the rinsing step. This can be attributed to the fact that the CNC particles were highly hydrated; QCM-D does not distinguish between hydrated and dry mass.

The D-f plots for sGX, epGX, and CMGX (Figures 15A, B, and D) appeared to show a similar trend, where the adsorbed layer started with a more viscoelastic property, which became more rigid as the layer becomes heavier. CMGX had a steeper curve compared to sGX and epGX, signifying a softer film. The curve for esGX (Figure 15C), on the other hand, showed a different trend, as the curve became steeper instead of levelling off as the adsorption continues, indicating that the layer started off as a rigid layer and matured to become more viscoelastic.

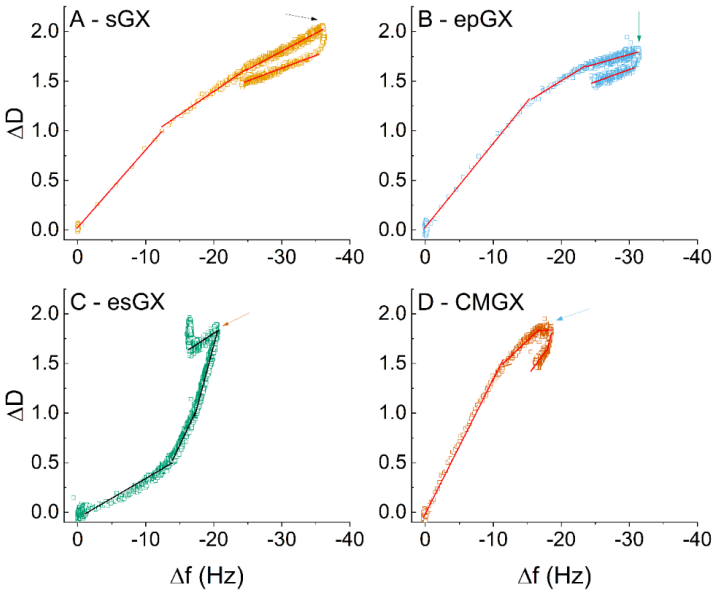

Figure 15. The change of dissipation (ΔD) against the change of frequency (Δf) for sGX (A), epGX (B), esGX (C), and CMGX (D), based on the measurements on the 5th overtone. Solid lines indicate the linear fitting of the different segments of the curve. Arrows indicate the point when rinsing started.

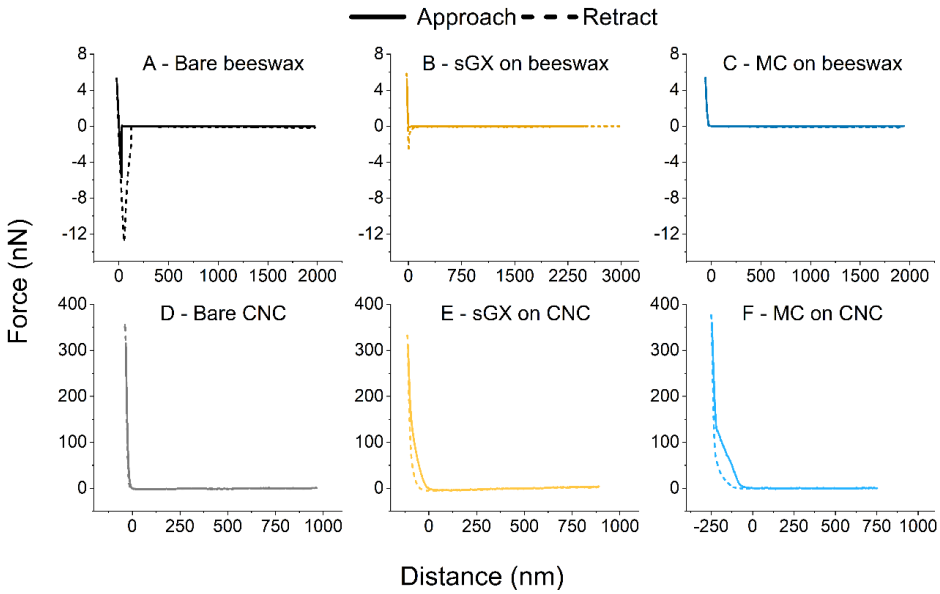

Figure 16. Force-distance curves of paraffin wax spheres against uncoated surface, sGX-coated, or MC-coated; A-C correspond to beeswax samples, while D-F correspond to CNC samples.

5.1.3 Force spectroscopy

Force spectroscopy in AFM measured the deflection of the cantilever as it approached, was in contact with, and separated from the tested surface, and presented as detected force against the separation distance (force-distance curve). Features shown in both the approach and retract curves describe the interaction forces that occurred between the tip of the cantilever and the tested surface, such as adhesion or a snap-in. The force-distance curves between paraffin wax colloidal probe and the different model surfaces are shown in Figure 16. From Figures 16A-C, where the hemicelluloses were adsorbed on beeswax layers, the strong adhesion recorded between the uncoated beeswax and the paraffin wax sphere was greatly reduced after coating with either sGX or MC. The sGX-coated wax still showed a small degree of adhesion, which was not observed for MC. No adhesion was recorded when CNC was used as the supporting material (Figure 16D-F); however, sGX and MC appeared to have formed a softer layer on top of the supporting CNC film, which manifested as the presence of two different slopes after the contact point on the approach curves. Please note that the colloidal probes used for the CNC-supported films were of a higher spring constant (TL-NCH, k ~42 N/m) than those used for the beeswax-supported films (NP-O10 A, k ~ 0.35 N/m).

5.1.4 Neutron reflectometry

The results obtained by the neutron reflectometry experiments is normally presented and fitted as the reflectivity as a function of scattering angle (Q), which can then be fitted to obtain various information about the physical properties of the measured thin film; in this study, the main fitted parameter was the total thickness of the interface. Background-subtracted neutron reflectivity profiles of the GXs adsorbed on hexadecane thin films are shown in Figure 17, including the model fit. Almost all emulsifiers were weakly reflecting, which made it difficult to align the neutron beams to the detector. Nevertheless, interfacial thickness data was still obtainable, which are presented in Figure 18, in comparison to the intensity-weighted average diameters of the GXs in aqueous dispersion; all the tested emulsifiers and environments could be fitted with a single-layer model, except for epGX at pH 4.5 with salt, which was better fitted using a two-layer model. Figure 18 showed that the adsorbed GXs formed an interfacial layer between 10-20 nm in thickness regardless of the emulsifier type and chemical environment, except for CMGX at pH 4.5 with salt which was around 4.8 nm. This was in contrast to the average particle size of the dispersions, which were considerably bigger than the layer thickness, despite having a high variability.

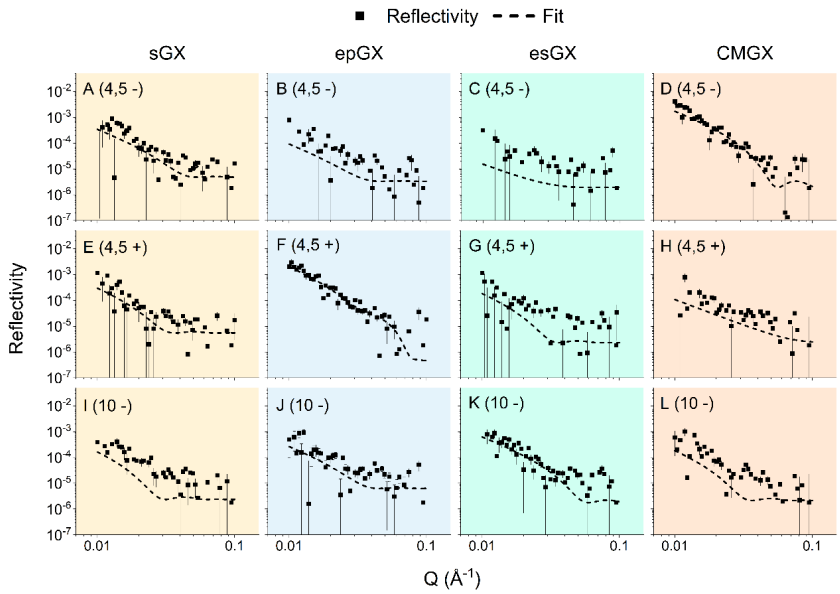

Figure 17. Reflectivity over Q profiles for the different GXs in different chemical environments. Plus (+) and minus (-) signs refer to the presence and absence of salt, respectively. Error bars represent the measurement uncertainties at each measurement point.

5.2 Performance of GX as a vitamin D3 carrier

5.2.1 Stability of vitamin D3 in GX-stabilized emulsions

The ability of sGX and epGX emulsions in stabilizing vitamin D3 is shown in Figure 19 as the vitamin D3 retention rate, defined as the remaining percentage of vitamin D3 in the emulsions after five weeks of storage compared to freshly-made emulsions. Both sGX and epGX retained over 80% of the vitamin D3 after storage, with no difference between the emulsions stored in room and elevated temperatures. This retention matched that of MC emulsions at both temperatures and casein emulsions at room temperature; the latter only retained above 50% of the vitamin D3 content at elevated temperature storage.

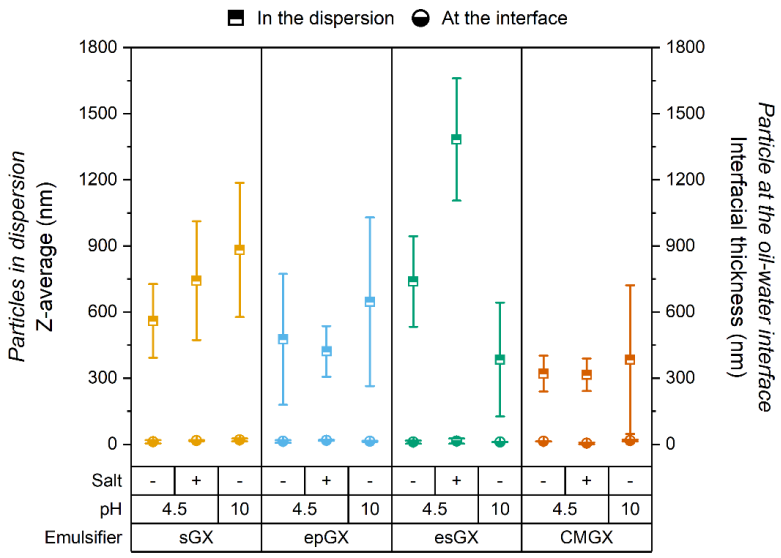

Figure 18. A comparison of measured intensity-averaged particle size of the different GXs in their aqueous dispersions of different chemical environments as measured by DLS (square icons) compared to their respective fitted interfacial thickness from the NR results (circle icons). Plus (+) and minus (-) signs refer to the presence and absence of salt, respectively. Error bars for the dispersion particle sizes indicate standard deviation and measurement uncertainty for the interfacial thickness.

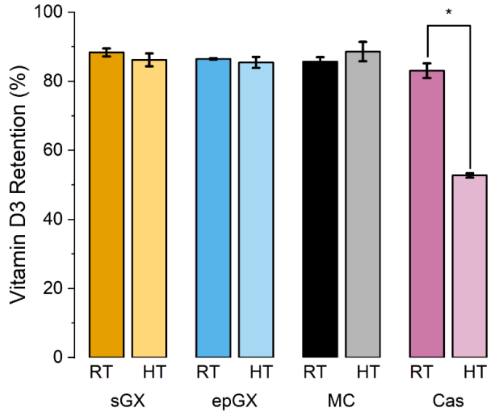

Figure 19. Retention rate of vitamin D3 in emulsions after five weeks of storage at room temperature (RT, ± 22 °C) and at elevated temperature (HT, 40 °C). Error bars signify standard deviation of the retention rates, calculated by propagation of the standard deviations of the vitamin D3 contents over triplicate measurements. The asterisk (*) indicates the pair with a significant difference between the vitamin D3 content at RT and HT.

5.2.2 Physical stability of GX-stabilized emulsions under *in-vitro* digestion

Changes in the emulsion droplet morphologies during *in-vitro* digestion are shown in Figure 20 as observed using an optical microscope. All of the tested emulsions were destabilized heavily during the gastric phase, as exhibited by the appearance of larger droplets compared to the original emulsions, indicating extensive coalescence. Additionally, emulsions stabilized by sGX and casein also exhibited heavy flocculation. The enzyme-free control showed similar destabilization, although more oil droplets were visible, particularly in the case of casein emulsion. Meanwhile, at the end of the intestinal phase most of the oil droplets were missing, leaving only a few remaining micro-sized droplets, which indicated that the lipolysis was not fully complete. The lipolytic activity of the pancreatic lipases were primarily responsible for the disappearance of the oil droplets, as the control experiments showed significantly more oil droplets compared to the enzymatic samples. The control intestinal phase also showed that the flocculation observed in the gastric phase of sGX and casein emulsions was reversed as the emulsions entered the intestinal phase.

5.2.3 Lipolysis of the oil phase of GX-stabilized emulsions

Figure 21A showed the progression of lipolysis over time for sGX and epGX emulsions compared to MC- and casein-stabilized emulsions, represented by the recovery percentage of caprylic acid over time, compared to that of the enzyme-free control experiments (Figure 21B). The progression is shown as the recovery rate over time; the recovery rate is defined as the percentage of detected amount of caprylic acid released compared to the theoretical amount if the entire oil content of the sample had been completely digested and released. The results showed that there is no significant difference in the lipolysis profile of all the polysaccharide-stabilized emulsions during both the gastric and intestinal phases. In contrast, casein-stabilized emulsions underwent more extensive lipolysis compared to the other emulsions. The control experiments showed negligible release of caprylic acid in both digestion phases.

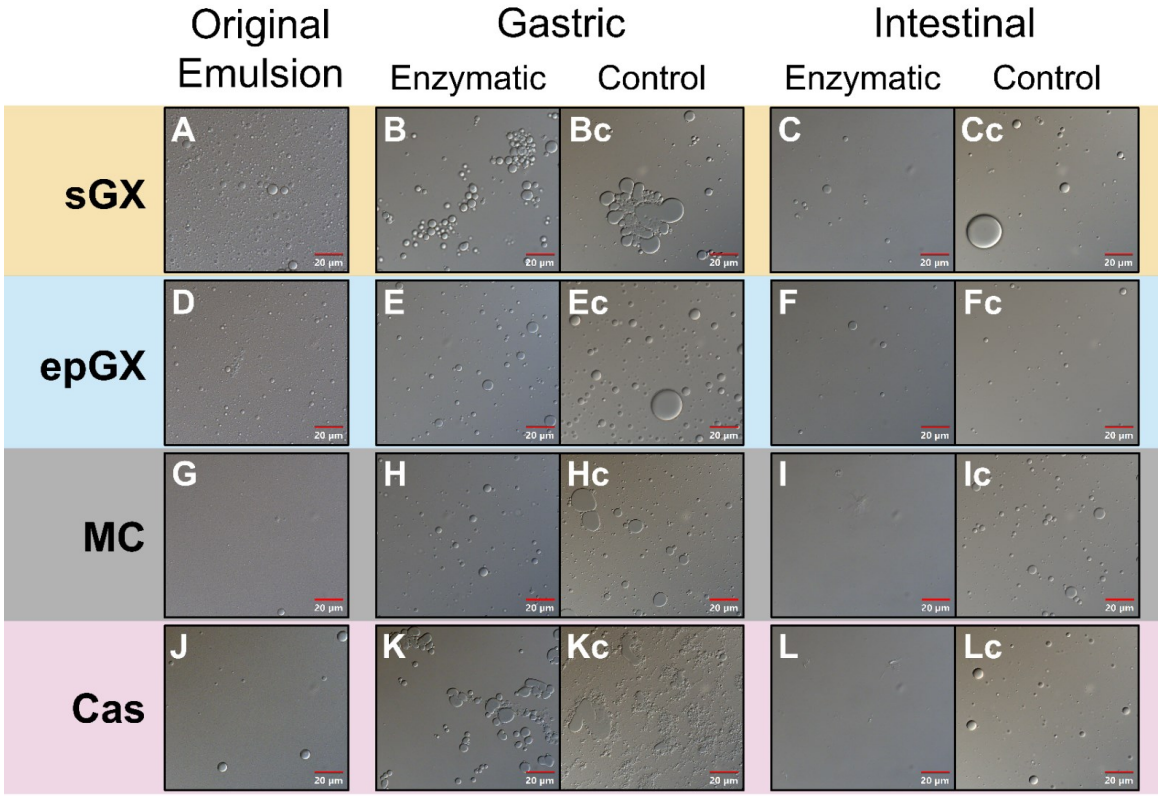

Figure 20. DIC micrographs of the different emulsions before (A, D, G, J) and during *in-vitro* digestion at the gastric (B, E, H, K) and intestinal (C, F, I, L) phases. Micrographs of the control run (digestion without enzymes) are presented next to the respective enzymatic digestion phases, denoted by lowercase 'c'.

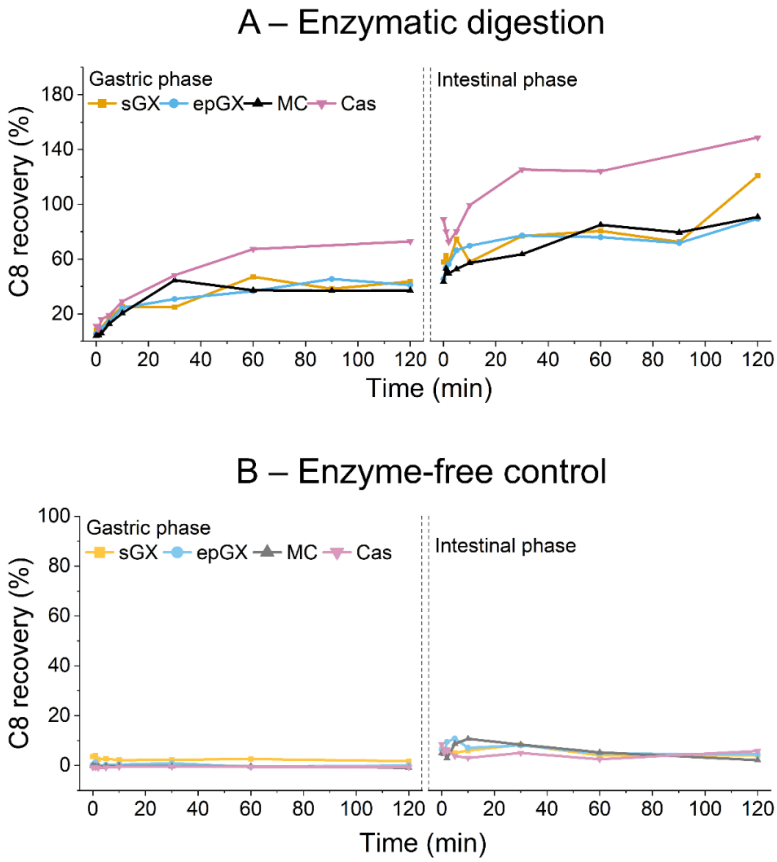

Figure 21. Progression of caprylic acid (C8) release over digestion time of the different emulsifiers, showing the enzymatic digestion (A, above) and the enzyme-free control experiments (B, below).

5.2.4 Release of vitamin D3 from the emulsions during *in-vitro* digestion

The release profile of vitamin D3 from the emulsions during the progression of the *in-vitro* digestion were shown in Figure 22A, also presented as the recovery rate of vitamin D3, calculated between the amount of detected amount of vitamin D3 in the sample compared to the theoretical amount of vitamin D3 should it be released completely. During the gastric phase, there did not seem to be any significant difference between the polysaccharide-stabilized emulsions, while the casein-stabilized emulsion released significantly higher amount of vitamin D3 compared to the others. During the intestinal phase, however, more vitamin D3 was released, with the different emulsifiers showing different release profiles. Emulsions made

using epGX and MC showed a small jump in the released amount of vitamin D3 during the first 10 minutes of the intestinal phase, which afterwards stabilized until the end of the experiment. Those made using sGX and casein, however, showed a more controlled release profile, starting with a similar level to the end of the gastric phase, then slowly increasing, stabilizing from around 30 minutes after the start of the intestinal phase. The enzyme-free control experiments (Figure 22B) interestingly showed a non-zero release of vitamin D3 despite the lack of lipolysis occurring, especially in the early minutes of the digestion. There was no difference in the release profiles of the different polysaccharide-based emulsions, both in the gastric and intestinal phases; the casein emulsions, however, released the highest amount of vitamin D3 despite the lack of enzymatic activity.

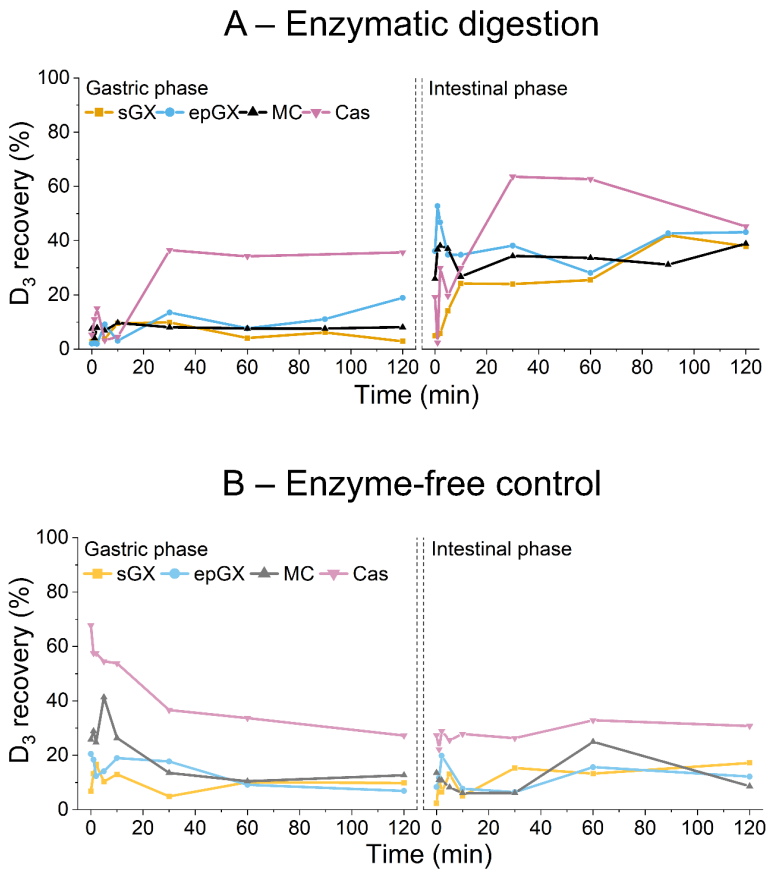

Figure 22. Progression of vitamin D3 release over digestion time of the different emulsifiers, showing the enzymatic digestion (A, above) and the enzyme-free control experiments (B, below).

5.3 Physical stability of GX emulsions

5.3.1 Macroscopic appearance of the emulsions

Visual appearances of the hexadecane emulsions stabilized by the GXs in different chemical environments before and after storage are shown in Figure 23. All emulsions had brown tints, with esGX and epGX having the most intense and lightest brown color respectively, corresponding to the polysaccharide-to-lignin composition. Emulsions made with esGX were especially unstable, forming coarse aggregates right after microfluidization, including at pH 10 without salt; this emulsion, however, appeared the most homogenous compared to other esGX emulsions. Comparing the appearance of all the emulsions before and after storage, all emulsions suffered from creaming. However, esGX emulsions at pH 4.5 showed some degree of precipitation. All esGX emulsions (except at pH 10, without salt) creamed heavily after one week, leaving the lower phase almost transparent.

Centrifugation of the emulsions and their corresponding dispersions showed differences in how the insoluble components of the GX were adsorbed to the oil droplets, as shown in Figure 24. Almost all GX dispersions showed precipitates after centrifugation, although to varying degrees. CMGX at pH 10 did not leave any precipitate regardless of the salt content. Dispersion of epGX at pH 10 without salt showed some white precipitate in contrast to other GXs, which produced brown precipitates. On the other hand, almost all emulsions produced no precipitate; only sGX pH 10 with salt, esGX pH 4.5 without salt, and epGX pH 10 without salt showed visible solid residues.

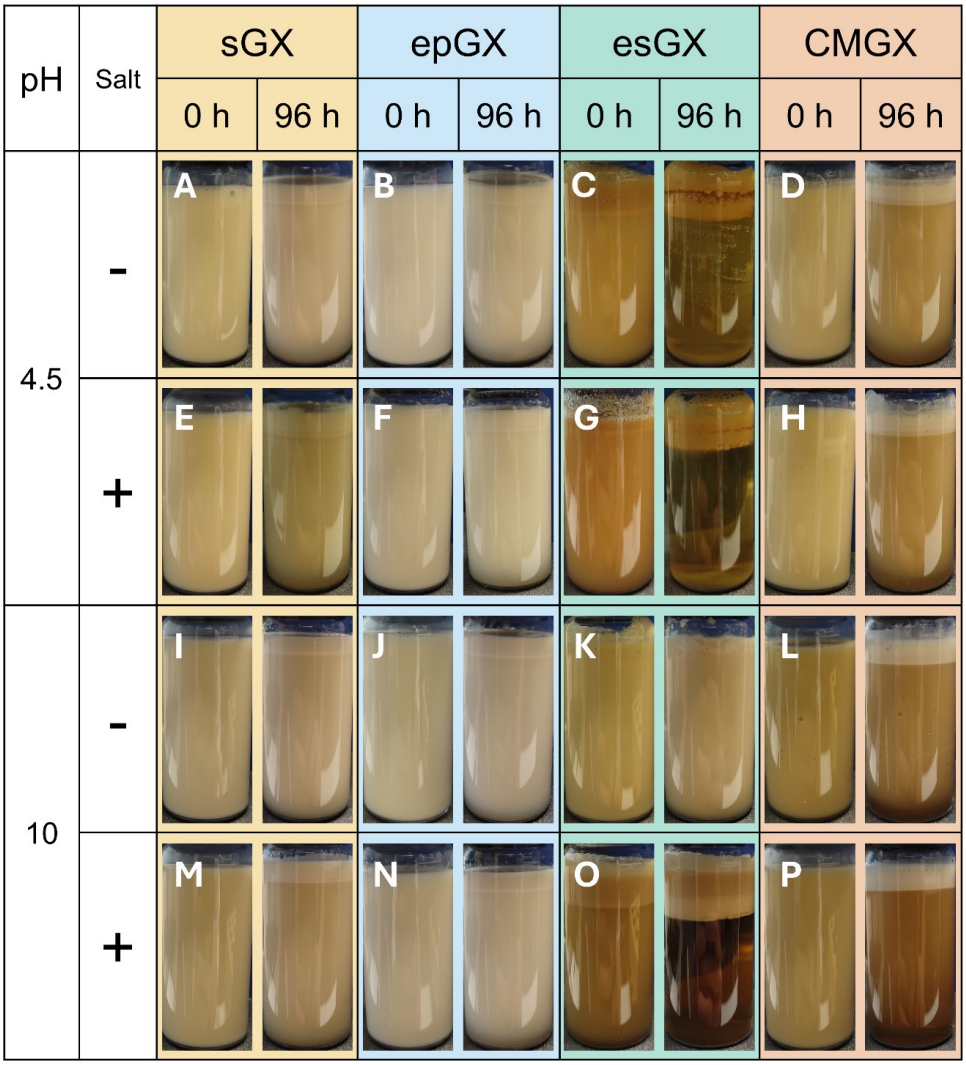

Figure 23. Visual appearance of the GX-stabilized emulsions in different chemical environments before (left) and after (right) 96-h storage. Plus (+) and minus (-) signs indicate the presence and absence of salt, respectively.

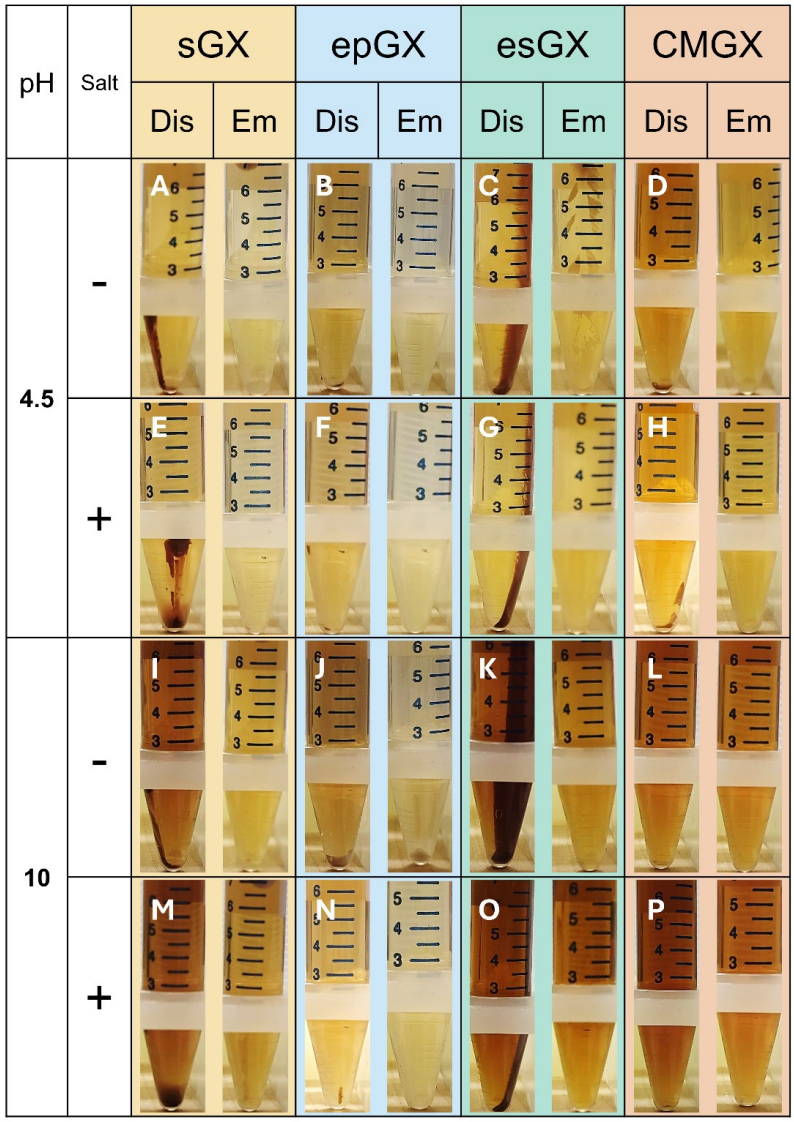

Figure 24. Bottom part of the centrifuge tube of the GX dispersions (Dis, left) and emulsions (Em, right) post-centrifugation. The images were corrected to increase brightness and contrast without any further modification. Plus (+) and minus (-) signs indicate the presence and absence of salt, respectively.

5.3.2 Morphology of the emulsion droplets after storage

Assessing the morphology of the emulsion droplets after storage could give an insight into the destabilization mechanism of the emulsions, in particular when flocculation occurred. IMC microscopic images of the GX emulsions after one week of storage are given in Figure 25. Emulsions made with sGX and epGX did not appear to show drastic differences between the different chemical environments. Generally, sGX, epGX, and CMGX emulsions showed two droplet populations: one droplet population that was so fine that they could not be focused on using a regular optical microscope, and another one which had micro-sized droplets. In CMGX emulsion at pH 10 with salt, a third population of droplets above 10 μm in diameter was also observed. There were flocs observed primarily for the larger droplet population across all emulsions.

Interestingly, the droplets of esGX emulsions showed different morphological profiles compared to the other GXs. The droplets in esGX emulsion pH 4.5 without salt showed extensive flocculation with almost no submicron droplet visible. At the same time, insoluble lignin particles were also visible, which were distributed on the surface of the oil droplets, with some concentration at the droplet-droplet junctions (Figure 26C). The presence of salt appeared to further localize the insoluble lignin particles to the droplet-droplet junction, as they no longer appeared to be distributed across the droplet surfaces. At pH 10, on the other hand, these insoluble lignin particles were not observed; the one without salt had a similar appearance to epGX emulsions, except for the occasional flocculates 5-10 μm in diameter. However, the presence of salt at pH 10 destabilized the emulsion and created larger flocs, although the floc size was smaller than those at pH 4.5, and there were no insoluble lignin particles observed. The addition of aqueous SDS 10% (w/v) to esGX emulsions appeared to remove the insoluble lignin particles seen in pH 4.5 emulsions, which led to the flocculates being broken (Figure 26B and D). Emulsions at pH 10 also showed a more extensive flocculation (Figure 26F and H); however, this was expected due to the high concentration of SDS used, which triggered depletion flocculation after the SDS molecules displaced the original emulsifiers.

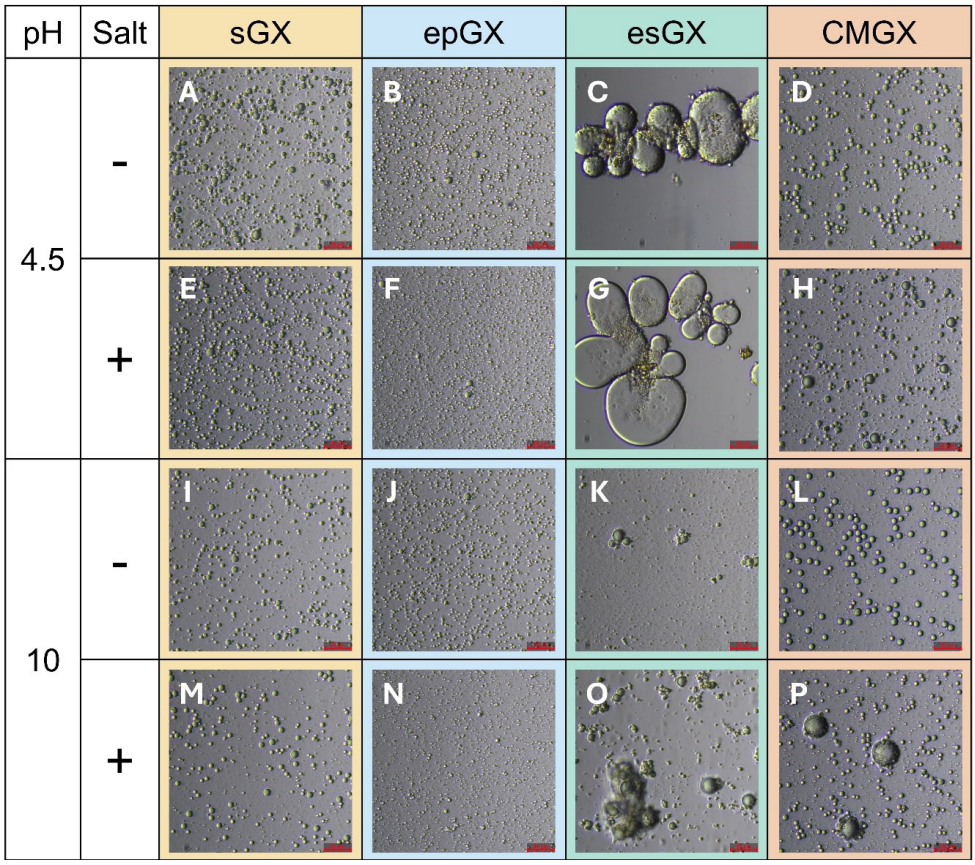

Figure 25. Micrograph of the different emulsions stabilized by GXs in different chemical environments after 7-day storage. The length of the scale bar is 20 μm. Plus (+) and minus (-) signs indicate the presence and absence of salt, respectively.

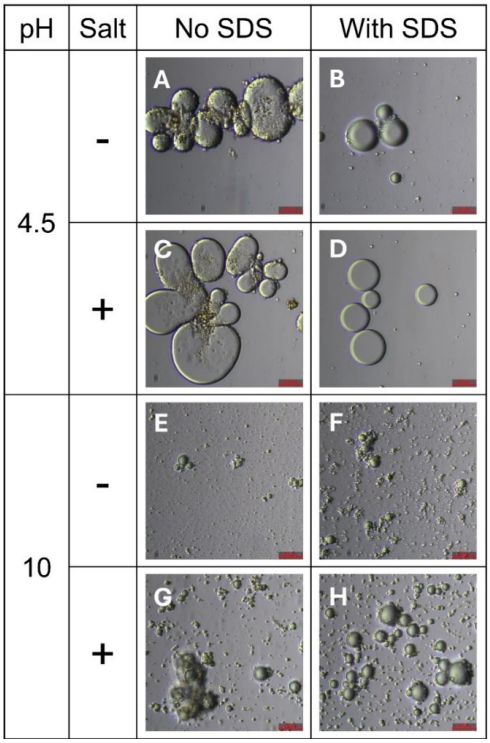

Figure 26. Changes in flocculate morphology of esGX emulsions at different chemical environments before and after the addition of SDS 10%. The length of the scale bar is 20 μm. Plus (+) and minus (-) signs indicate the presence and absence of salt, respectively.

5.3.3 Droplet size distribution and changes in droplet size

Given the importance of the droplet size of emulsions towards their stability, analyses of the size distribution and the changes in droplet size could give an insight into the stabilization mechanism of a given emulsifier. Volume-based droplet size distribution curves of the GX-stabilized emulsions are shown in Figure 27. All emulsions showed multimodal distributions, having droplets in both the nanometer and micrometer ranges in different proportions. Emulsions made with sGX and epGX seemed to have a higher proportion of submicron droplets relative to the micro-sized droplets, in contrast to esGX and CMGX emulsions; an exception being esGX at pH 10 without salt, which showed similar distribution peaks as sGX at pH 4.5 without salt. These droplet size distribution curves showed agreement to the observed microscope images of the emulsions. One week of storage appeared to impart changes primarily to the micro-sized droplets, while for most emulsions there were minimal changes to the submicron droplets. Interestingly, epGX emulsions did not show major changes to their droplet distribution regardless of the chemical environment.

A three-way ANOVA of the initial droplet diameter (i.e., the size of the droplets measured immediately after microfluidization) of the GX-stabilized emulsions (Table 4) showed that esGX generally produced larger droplets compared to the other GXs across all the chemical environments, with an exception at pH 10 without salt. The effect was particularly clear on the D[4,3] values, where all esGX emulsions had significantly larger diameters compared to most other emulsions (except at pH 10 without salt). The initial D[3,2] values were generally similar for all emulsions, with only esGX at pH 4.5 with salt and CMGX at pH 10 with salt having distinctively larger diameters. From the two-way ANOVA results, there were significant interactions between pH and salt towards the diameters within each emulsifier group ($p < 0.005$ for both D[4,3] and D[3,2]), although the differences were relatively minor when compared across emulsifiers (as indicated by the different groupings between the three-way and two-way ANOVA results).

Addition of 10% (w/v) SDS solution to the emulsions imparted some changes to the droplet distribution curves of the emulsions, as seen on Figure 28; only the distribution curves for emulsions at pH 4.5 without salt are shown, as the manner of change occurred similarly across the different chemical environments. The micro-sized droplets appeared to be affected the most, where the corresponding micro-sized distribution peaks for sGX and esGX became narrower and shifted to a smaller size; this corresponded to the presence of insoluble lignin in sGX and esGX. The size distribution of the epGX emulsions did not appear to be affected by the addition of SDS, showing identical size distribution with and without SDS. CMGX emulsions (Figure 28D), on the other hand, appeared to show a degree of enlargement of the submicron droplets, as evidenced by the reduction of the submicron droplet peak area in parallel to an increase in the micro-sized peak area.

While coalescence was not directly visible from the droplet size distribution curves, it was more evident when analyzing the degree of changes to the droplet size. Figure 29 shows the percentage of changes to the average droplet diameters for both D[4,3] (Figure 29A) and D[3,2] (Figure 29B) when measured in the presence of SDS. It was clear that while all emulsions experienced coalescence for both the smaller and larger droplet populations, esGX and CMGX suffered a much larger degree of coalescence than sGX and epGX. It was, however, difficult to determine whether the different chemical environments had any effect within the emulsifiers due to the large variability of the results. For example, the change of D[4,3] for sGX had large standard deviation values coinciding with the presence of salt, whereas esGX had a particularly large D[4,3] variation at pH 10 without salt, which, interestingly, was the most stable between the other esGX-stabilized emulsions.

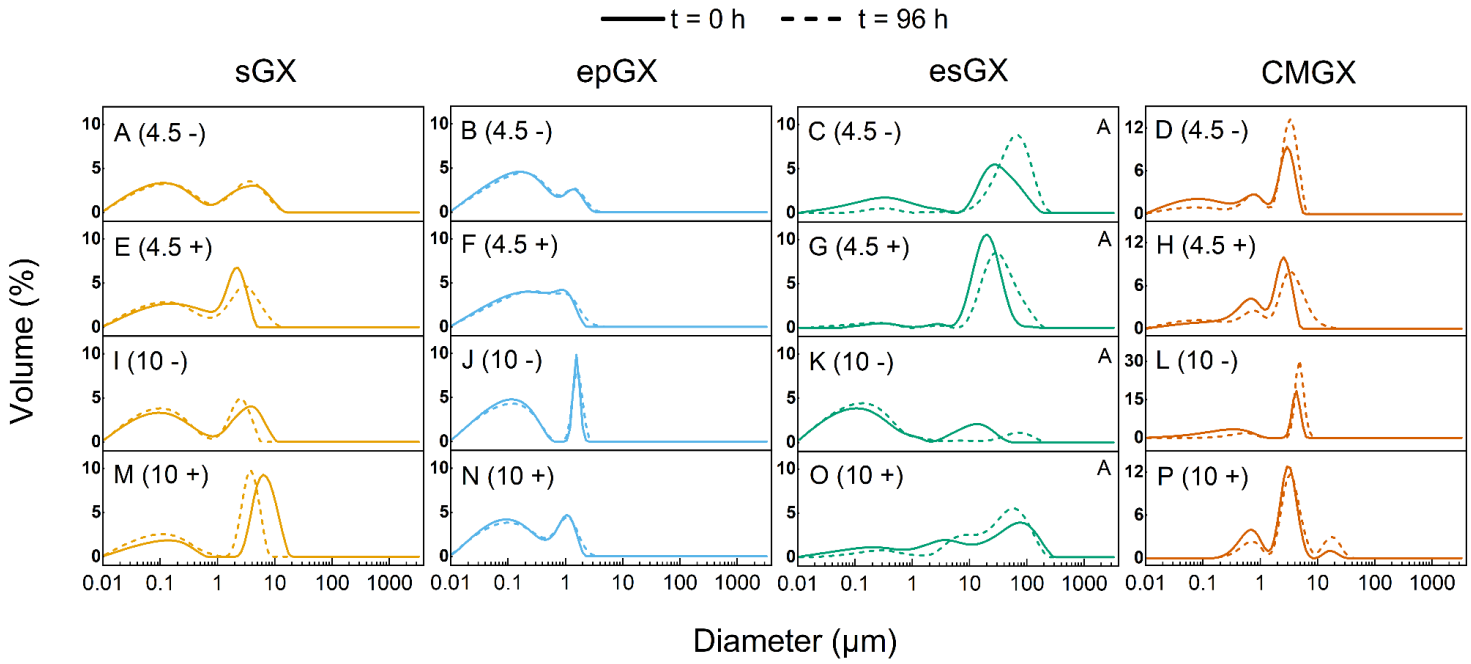

Figure 27. Droplet size distribution of the different GX-stabilized emulsions under different chemical environments right after production and after seven days of storage, measured without the addition of SDS. Plus (+) and minus (-) signs indicate the presence and absence of salt, respectively.

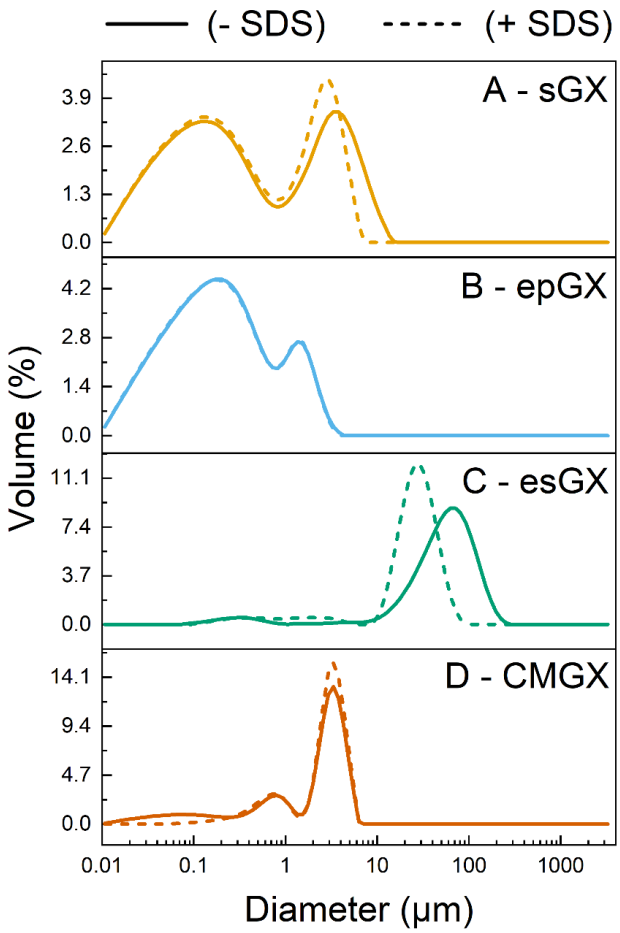

Figure 28. Difference of particle size distribution with and without SDS of the different GX-stabilized emulsions at pH 4.5 without salt after 96 h of storage.

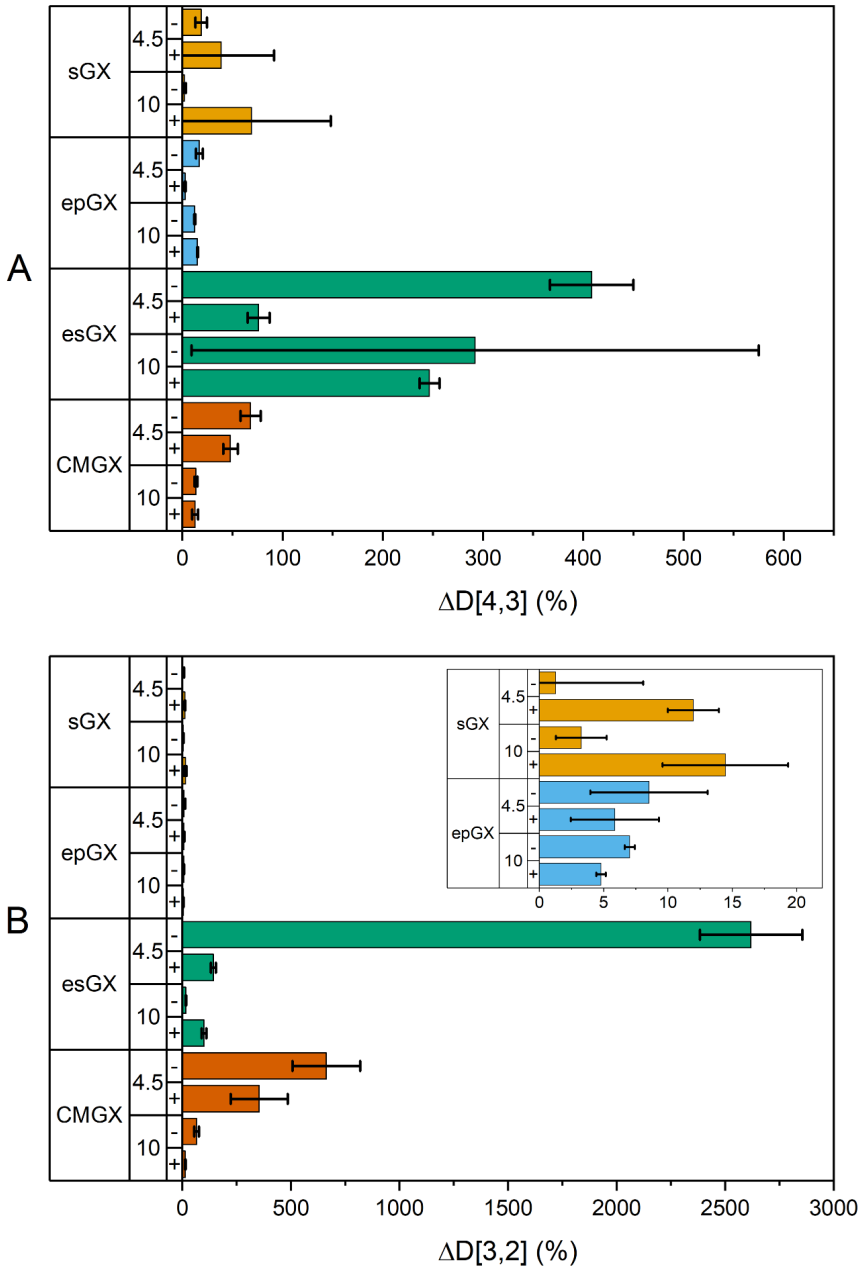

Figure 29. Percentage of change in D[4,3] (A) and D[3,2] (B) for of the GX-stabilized emulsions in the presence of SDS. Plus (+) and minus (-) signs indicate the presence and absence of salt, respectively. Error bars represent the propagated uncertainty calculated from the standard deviation values of the respective average diameters between the emulsion preparation and at the end of 96-h storage.

Table 4. Initial D[4,3] and D[3,2] values (in μm) of GX-stabilized emulsions at different chemical environments, measured without SDS. Plus (+) and minus (-) signs in the Salt column indicate the presence and absence of salt, respectively. Means with different letters indicate significant difference (upper case for the three-way ANOVA results *across* emulsifiers, lower case for the two-way ANOVA results *within* emulsifiers).

Emulsifier	pH	Salt	D[4,3]	D[3,2]
sGX	4.5	-	$1.50 \pm 1.40E\text{-}1^{A,a}$	$0.10 \pm 1.19E\text{-}3^{A,a}$
		+	$1.38 \pm 2.53E\text{-}1^{A,a}$	$0.15 \pm 1.78E\text{-}2^{A,b}$
	10	-	$1.44 \pm 6.55E\text{-}2^{A,a}$	$0.10 \pm 1.44E\text{-}3^{AB,a}$
		+	$4.88 \pm 6.96E\text{-}1^{AB,b}$	$0.18 \pm 1.14E\text{-}2^{AB,c}$
epGX	4.5	-	$0.38 \pm 2.99E\text{-}3^{A,a}$	$0.08 \pm 3.01E\text{-}4^{A,a}$
		+	$0.40 \pm 4.93E\text{-}3^{A,b}$	$0.10 \pm 1.36E\text{-}3^{AB,b}$
	10	-	$0.43 \pm 1.71E\text{-}3^{A,c}$	$0.07 \pm 5.00E\text{-}5^{A,c}$
		+	$0.40 \pm 8.42E\text{-}3^{A,b}$	$0.08 \pm 9.24E\text{-}5^{A,d}$
esGX	4.5	-	$28.76 \pm 23.49^{C,a}$	$0.70 \pm 7.28E\text{-}1^{B,a}$
		+	$19.87 \pm 2.49^{BC,ab}$	$4.27 \pm 7.33E\text{-}1^{C,b}$
	10	-	$3.20 \pm 4.52E\text{-}1^{A,b}$	$0.08 \pm 1.09E\text{-}3^{A,a}$
		+	$29.92 \pm 7.55^{C,a}$	$0.34 \pm 3.29E\text{-}2^{AB,a}$
CMGX	4.5	-	$1.61 \pm 6.57E\text{-}2^{A,a}$	$0.15 \pm 1.39E\text{-}2^{A,a}$
		+	$1.65 \pm 4.58E\text{-}2^{A,a}$	$0.34 \pm 2.95E\text{-}2^{AB,b}$
	10	-	$2.40 \pm 2.05E\text{-}1^{A,b}$	$0.29 \pm 6.47E\text{-}2^{AB,b}$
		+	$3.22 \pm 4.04E\text{-}1^{A,c}$	$1.41 \pm 5.44E\text{-}2^{D,c}$

5.3.4 Zeta potential of the emulsions

The zeta potential of an emulsion gives an overview of the magnitude of the electrical charge present on the surface of the droplets, which consequently contributes to the electrostatic repulsion that would stabilize the emulsion. The zeta potential values of the GX-stabilized emulsions are presented in Figure 30. All emulsions had negative zeta potential values, signifying a general negative charge surrounding the emulsion droplets. The presence of salt reduced the magnitude of the zeta potential (i.e., the value became less negative) across all emulsifiers ($p < 0.001$). Meanwhile, an alkali pH was associated to a higher magnitude of zeta potential (i.e., the value became more negative) compared to acidic pH ($p < 0.001$). There was a significant interaction between pH and salt towards the zeta potential values of each emulsifier ($p < 0.001$), although the magnitude of the effect was not analyzed within the scope of this study.

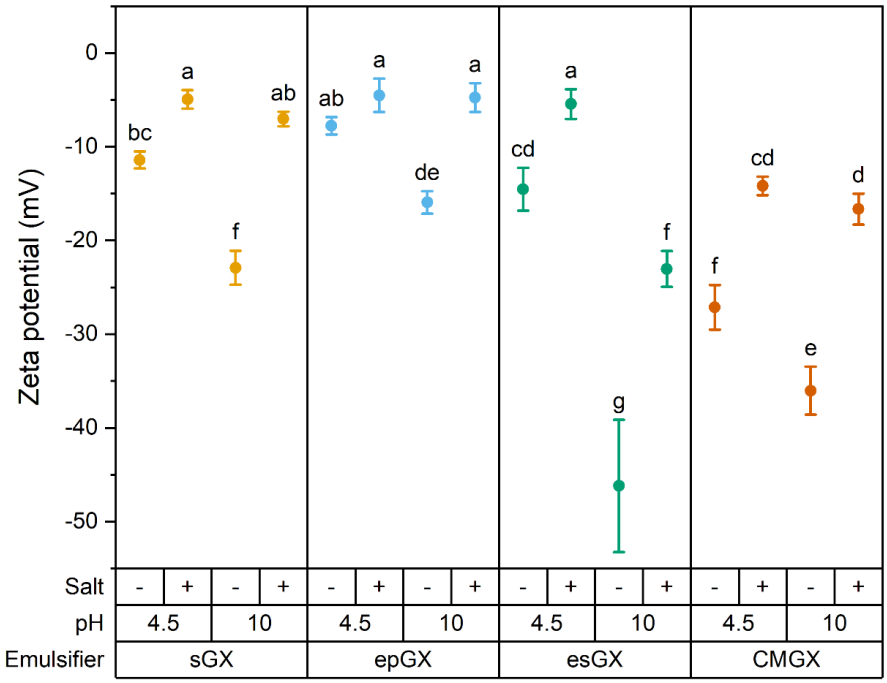

Figure 30. Zeta potential of the GX-stabilized emulsions in different chemical environments. Error bars signify standard deviations. Means with different letters are significantly different. Plus (+) and minus (-) signs in the Salt column indicate the presence and absence of salt, respectively.

5.3.5 Destabilization kinetics

The evolution of the global TSI values over time for the different GX-stabilized emulsions are shown in Figure 31, and the fitted values are shown in Table 5. Looking across the different emulsifiers, sGX and epGX emulsions showed better stability compared to esGX and CMGX, where the TSI values stabilized below 20 for all sGX and epGX emulsions (except for sGX at pH 4.5 with salt). Emulsions stabilized by esGX were generally the least stable, except at pH 10 without salt; this environment also produced the most stable emulsion for sGX and CMGX. Different pH and presence of salt did not appear to affect the stability of epGX emulsions greatly. Nevertheless, the presence of salt was shown to negatively affect the emulsion stability regardless of pH, exhibited by the higher TSI_{max} values compared to the salt-free counterparts.

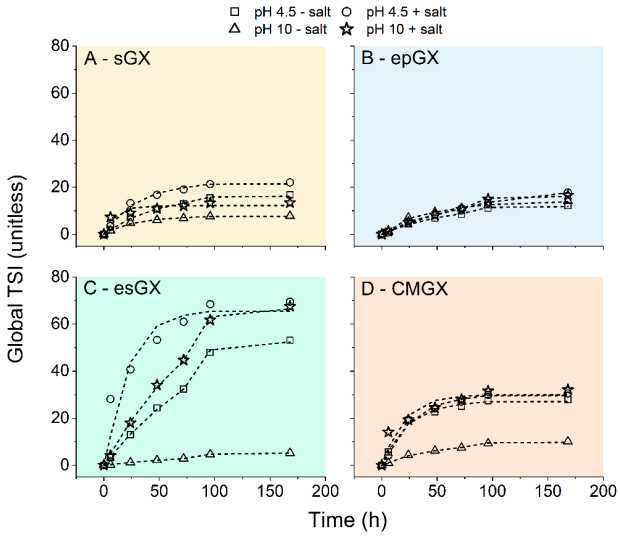

Figure 31. Global TSI value of the GX-stabilized emulsions over 96 h of storage. Dotted lines are the fitting of the curves. Plus (+) and minus (-) signs in the Salt column indicate the presence and absence of salt, respectively.

Table 5. Fitted TSI_{max} and k values of the different GX-stabilized emulsions in different pH and salt content over 96 h of storage.

Emulsifier	pH	Salt	TSI_{max}	k (h^{-1})
sGX	4.5	-	15.724 ± 1.242	0.020 ± 0.002
		+	21.112 ± 0.516	0.027 ± 0.010
	10	-	10.003 ± 3.418	0.044 ± 0.011
		+	13.654 ± 2.093	0.164 ± 0.094
epGX	4.5	-	15.270 ± 3.902	0.014 ± 0.005
		+	21.840 ± 0.019	0.013 ± 0.004
	10	-	14.058 ± 0.092	0.022 ± 0.0004
		+	16.983 ± 1.968	0.016 ± 0.005
esGX	4.5	-	58.245 ± 10.881	0.010 ± 0.0006
		+	63.934 ± 2.245	0.042 ± 0.008
	10	-	11.781 ± 5.181	0.005 ± 0.001
		+	71.589 ± 7.416	0.013 ± 0.003
CMGX	4.5	-	26.652 ± 0.560	0.042 ± 0.002
		+	28.356 ± 1.874	0.038 ± 0.002
	10	-	11.987 ± 2.585	0.032 ± 0.018
		+	30.317 ± 0.601	0.051 ± 0.004

5.3.6 Effect of oil type

In this section, the effect of substituting hexadecane for MCT oil was compared using sGX and epGX emulsions at pH 4.5 without salt. Both emulsions primarily suffered from creaming, but hexadecane-based emulsions destabilized faster as exhibited by the Turbiscan results (Figure 32, fitted results in Table 6). The multimodality of the droplet size distribution was maintained regardless of oil type (i.e., the submicron and micro-sized distribution peaks were present for hexadecane and MCT emulsions); however, the distribution peaks of MCT emulsions were slightly shifted to larger droplet sizes (Figure 33). This difference was evident in the average droplet diameters (Table 6) and the optical micrograph images of the emulsions (Figure 34), where larger droplet sizes were observed for MCT emulsions compared to hexadecane emulsions for both sGX and epGX.

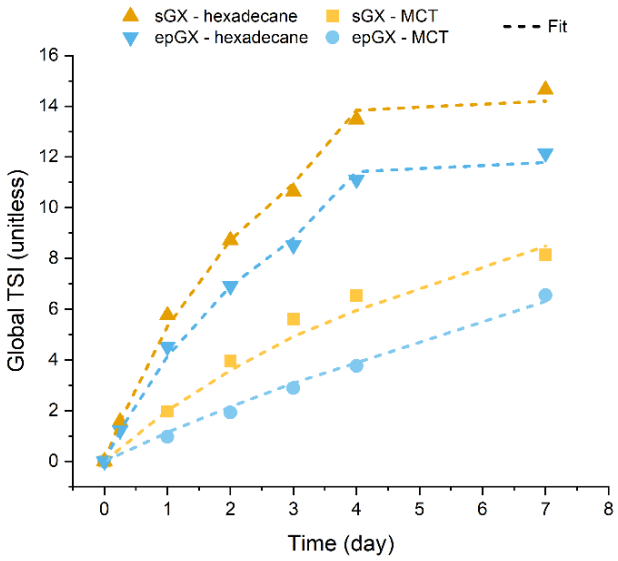

Figure 32. Comparison of the destabilization of sGX- and epGX-stabilized emulsions using hexadecane and MCT oil over 96 h storage.

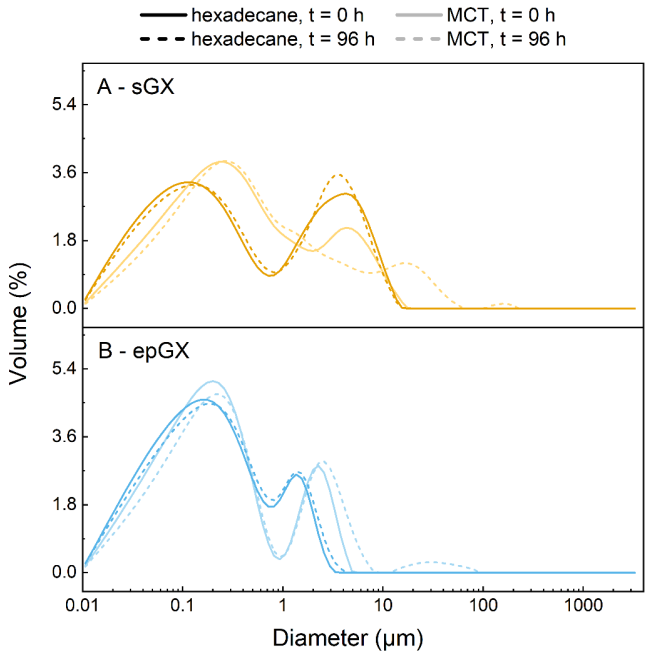

Figure 33. Droplet size distribution of sGX- and epGX-stabilized emulsions made using hexadecane and MCT oils, compared between before and after 96 h of storage.

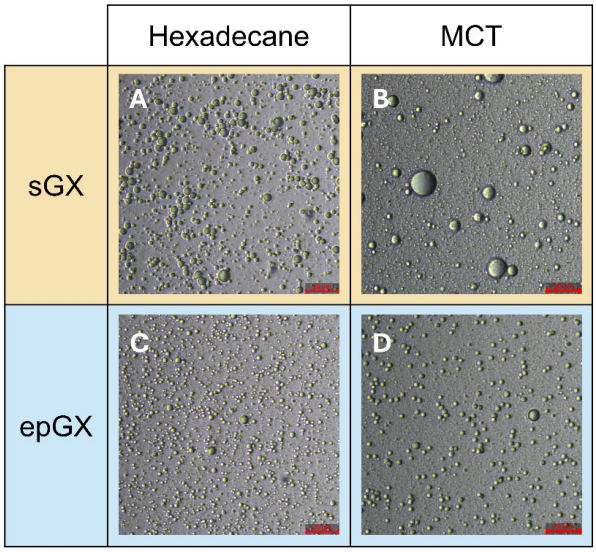

Figure 34. Micrographs of sGX and epGX emulsions made with hexadecane and MCT oils at the end of 96 h of storage. The length of the scale bar is 20 μm.

Table 6. Turbiscan fitted parameters (TSI_{max} and k) and surface- and volume-average droplet diameters (D[3,2] and D[4,3]) of sGX and epGX emulsions made with hexadecane and MCT oils.

Emulsifier	Oil	TSI_{max}	k (h-1)	D[3,2] (μm)		D[4,3] (μm)	
				t = 0 h	t = 96 h	t = 0 h	t = 96 h
sGX	Hexadecane	15.724 ± 1.242	0.020 ± 0.002	0.096 ± 0.001	0.106 ± 0.002	1.502 ± 0.140	1.630 ± 0.028
	MCT	14.687 ± 3.737	0.006 ± 0.002	0.122 ± 0.002	0.140 ± 0.002	1.453 ± 0.133	3.033 ± 0.279
epGX	Hexadecane	15.720 ± 3.902	0.014 ± 0.005	0.084 ± 0.001	0.088 ± 0.002	0.375 ± 0.003	0.420 ± 0.012
	MCT	18.307 ± 1.100	0.003 ± 0.0004	0.094 ± 0.001	0.112 ± 0.001	0.550 ± 0.009	1.695 ± 0.106

6 Discussions

In this section, experimental results that are presented in Chapter 5 are further discussed. This chapter starts (Section 6.1) by discussing the formation of interfacial layer by GX based on the results where the adsorption process of GX to the oil-water interface was described. Next, the results from the evaluation of GXs as emulsifiers for emulsion-based carrier of hydrophobic compound are discussed, particularly the implications of the results in the interfacial properties of GX (Section 6.2). Finally, the mechanism by which GXs stabilize emulsions is discussed, especially in terms of their nature as complex mixtures (Section 6.3).

6.1 Formation of interfacial layer by GX

As discussed in Section 2.2.1, the adsorption of emulsifiers onto the oil-water interface is an integral part of the emulsification process, which starts the formation of an interfacial layer. DIFT, QCM-D, AFM, DLS, and NR were used to understand the role of the polysaccharide and lignin fractions of GX towards the formation of interfacial layer at the oil-water interface.

Results from the DIFT experiments (Section 5.1.1) showed a general idea on the adsorption dynamics of GX to the oil-water interface. As shown in Figure 10, the onset of the rapid fall phase of the interfacial tension values became earlier in the order of esGX > sGX > epGX > CMGX, which correlated to the amount of lignin in the GX extracts. Lignin was also shown to not only accelerate the adsorption process, but it enabled the adsorption process to occur in the first place. This was proven by comparing the adsorption of CMGX to CMC. Both were negatively-charged polysaccharides, but CMGX contained a small amount of residual lignin, while CMC did not; Figure 10 indicated that CMGX was adsorbed to the interface (despite being the slowest among the GXs), while CMC was not. However, MC was also adsorbed despite not containing any lignin, even at a faster rate than the GXs (with the exception of esGX). This indicated the possibility that the adsorption might not have been merely due to the presence of lignin, but by the way it increased the overall hydrophobicity of the GX systems. It is well-known that hemicelluloses can be chemically modified to improve their hydrophobicity by grafting different hydrophobic moieties[247], including xylans[215, 216], although lignin has not been used synthetically to endow hydrophobicity to hemicellulose. The

hydrophobicity of lignin itself has been debated, as it is possible to produce both hydrophobic[248-250] and hydrophilic lignin[13, 251] only by virtue of extraction. Nevertheless, it was clear that in this current GX system, the residual lignin is relatively more hydrophobic compared to the polysaccharide fraction.

The apparent concentration dependence of the adsorption (Figure 11) also indicated that the adsorption process of GX to the interface is diffusion-controlled. The comparison between the DIFT profiles of the different GXs at 0.003% (w/v) in Figure 11 showed how the curves of sGX and esGX practically overlapped, which confirmed and strengthened the previous evidence[47] where BE-type LCC was preferentially adsorbed at the interface, which only occurred for sGX and esGX. Assuming that at such low concentration the adsorption was dominated by the most-easily adsorbed species, the adsorption shown in Figure 11 proved that the most easily adsorbed species of sGX was partitioned to the ethanol-soluble fraction during precipitation. Difference in adsorption between fractions within the same extract has also been previously observed for gum arabic, where the protein-rich fractions were found to be more adsorbed at the oil-water interface[191].

Charge-carrying amphiphilic polymers are known to be affected by the presence of dissolved ions, which alter the inter- and intrachain interactions, resulting in changes in their solubility, conformation, and interaction with water, which subsequently affects their adsorption to interfaces[252, 253]. This sensitivity to ionic strength has also been observed in charged polysaccharides[254]. As the GXs have the 4-*O*-methylglucuronic acid residues, GX could also be affected by the presence of salt in a similar way as polyelectrolytes. Based on Figure 12, it was evident that the effect of salt in the dispersions was more pronounced with an increasing amount of polysaccharide in the GX fraction. CMGX, which had additional carboxymethyl groups, was particularly affected, having the largest gap between the salt-free and with-salt adsorption. Interestingly, the shape of the curves appeared to remain the same with and without salt, indicating that the presence of salt did not affect the adsorption rate; the lower DIFT values might instead indicate that the packing of the GX at the interface was denser in the presence of salt than in absence, as illustrated in Figure 35, using epGX as a representative. A higher-density packing of adsorbed monolayer of amphiphilic polymers at the interface has previously been reported, although it was measured at a solid-liquid interface. The increased density was attributed mainly to the screening of the electrical double layer in-between the polymer particles, although it was also reported that the monolayers were more swollen in the presence of salt[255]. An enhanced adsorption was also shown for xylans on poly(ethylene terephthalate)[256]. Interestingly, the presence of salt reduced the hydrodynamic radius of charged polysaccharide chains in solutions[254]. A more complete study of the physical state of the adsorbed layer would be needed to confirm how GX is packed at the interface.

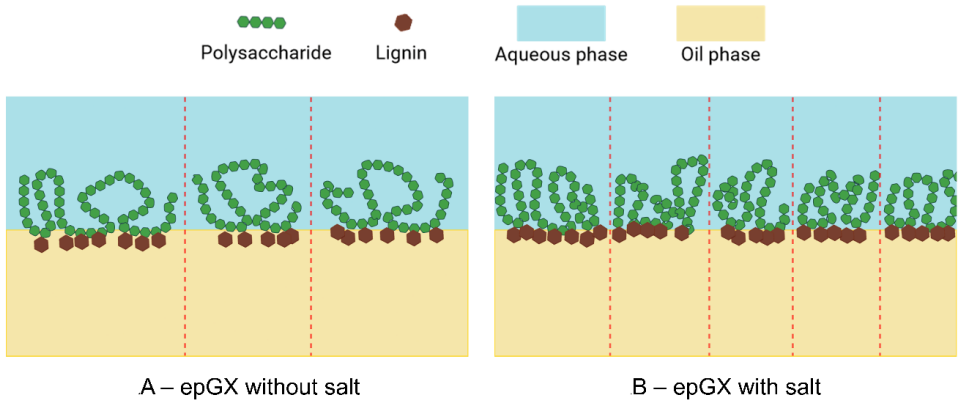

Figure 35. Illustration of the packing of epGX with (A) and without (B) the presence of salt. Created using BioRender.com.

The mismatch of esGX adsorption behavior between the DIFT and QCM-D results gave a major highlight about the nature of the interfacial layer. Despite the major role of lignin in the adsorption of GX to the oil-water interface (as deduced from the DIFT results), those results indicated that the interface was primarily built by the polysaccharide fraction instead of the lignin fraction. This agreed with the fact that esGX was composed primarily of species with lower molar mass than epGX[47]. Consequently, this means that for a given interface area occupied by esGX, the interfacial layer would be lighter compared to the same area occupied by epGX. Additionally, this also indicates that the lignin moiety in the different GXs might be small and light in size, at least those involved in the passive adsorption process. CMGX, on the other hand, might have been lightweight simply due to the lack of adsorption, as the QCM-D result was in agreement with the high DIFT values.

The D-f curves (Figure 15) from the QCM-D result also support this hypothesis of a polysaccharide-dominated interface. The slope of a D-f curve reflects the viscoelasticity of the adsorbed layer; a steeper slope indicates a more viscous character, and changes in the slope along an increasing oscillation frequency signify modifications to the adsorbed layer due to adsorption and possible rearrangement of the materials at the interface[257, 258]. Of the four GXs, only esGX experienced a steeper slope at a higher frequency; this may indicate that the adsorption first involved the lignin-rich, followed by an adsorption of species with more polysaccharide component, which are more hydrated and thus more viscous. The other GXs started out being steep, followed by a more gradual incline, which may be due to the rearrangement of the polysaccharide chains that caused the adsorbed layer to be stiffer. Other studies on the viscoelasticity of films of hemicelluloses adsorbed on other solid-liquid interfaces indeed showed similar viscoelasticity profiles[256, 259, 260], attributing the viscoelasticity to the relatively high

hydration level of the hemicellulose films[259]. The D-f curve for esGX, however, was unfamiliar; a study on the film formation of colloidal lignin particles showed a curve more similar to the hemicelluloses, starting with a viscous layer that matures into higher rigidity[261]. Such difference may be due to the fact that the GXs are combinations of both polysaccharide and lignin; additionally, the residual lignin in the GXs, especially esGX, may have a different conformation, causing it to behave differently physically. These findings, however, cannot be applied directly to represent the state of GXs at the oil-water interface. Instead, they must be proven by directly measuring the interfacial rheology of the adsorbed film, especially as the current QCM-D experiment was limited to a solid-liquid interface instead of a liquid-liquid interface.

AFM-based force spectroscopy has often been used to characterize the adsorption phenomena between various substrates, for example between proteins and polymer brush[262], between polymers and self-assembled monolayers[263], between oppositely-charged polyelectrolyte brushes[264], and between surfactant-polyelectrolyte complex and silica surface[265]. The force spectroscopy experiments in this study, while failing to characterize the adsorption of the tested emulsifiers through the adhesion force, showed the possibility that the adsorbed layer of GX, even when it was simply adsorbed passively, acted as a barrier between the beeswax film and the paraffin wax sphere. The origin of the little adhesion exhibited in the force-distance curve for sGX, which was absent for MC, was unclear, although there are two possible hypotheses. First, it could be a residual attraction from the beeswax layer underneath the adsorbed GX film, which may indicate that either the coverage was uneven or that the film was mobile enough that the pushing force of the paraffin wax sphere was enough to let some adhesion force be sensed – by extension, this adhesion was not observed in MC because the film formed by MC was stronger or less mobile. Proving this hypothesis might require the measurement of interfacial rheology of the adsorbed emulsifier films. The second hypothesis is that the small adhesion came from any exposed lignin contained in the sGX, which was not present in MC. This hypothesis might be more difficult to prove, however, as it requires testing the force measurements using lignin film. One problem with this method is that the hydrophobicity of lignin itself depends on the preparation method of the lignin-based material. For example, the residual lignin in the GX samples used in this thesis was evidently hydrophobic; however, many lignin-based nanoparticles that have been synthesized were hydrophilic in character[123, 261, 266].

The NR experiments were particularly difficult to execute, especially for the sapphire-matched contrast, where the experiment relied solely on the reflection of the neutron beams due to the adsorbed layers. The signal of the reflected beams was very weak, which made it difficult to align the neutron beams to the detector. Nevertheless, after subtraction of the background, it was still possible to obtain

some meaningful data from the results. Fitting results of the reflectivity profiles showed that the thickness of the interfacial layers formed by the different GXs were similar regardless of the type of GX and the chemical environment. At first, this finding was surprising, considering how the different GXs had different sizes in their dispersions (Figure 18, squares). However, GX are macromolecules; it is well-known that macromolecular emulsifiers, such as protein and amphiphilic polymers, can rearrange their conformations from the state in their dispersions into the state at the interface[267-269]. Therefore, it is possible that the GX molecules were able to rearrange as such to maximize the exposure of the hydrophobic domains towards the oil phase and the hydrophilic domains towards the aqueous phase, and in the equilibrium reaches a thickness that is less than their size in the dispersion. However, it has been previously reported in adsorbed multilayers on solid-liquid interfaces that heparin layers in a chitosan-heparin adsorbed multilayer became thicker with increasing ionic strength[270], while the opposite was exhibited in a chitosan-only adsorbed layer[271]. Similar sensitivity towards the aqueous environment has also been observed in oil-water interfaces, where the polyelectrolytes can also interact and penetrate the oil phase. The sensitivity depended on the type of the polyelectrolyte; the presence of salt reduced the thickness of adsorbed polystyrene-poly(dimethylaminoethylmethacrylate)[272], whereas for adsorbed bovine serum albumin[273, 274] and lysozyme the thickness and the volume fraction increased[274]; for both cases, changes in volume fraction of the adsorbed material at the oil and aqueous phases were observed. In this study, unfortunately, the depth of penetration of the GX at the interface could not be determined, which could have shown whether there was any effect of the different chemical environments to the conformation of both the polysaccharide and lignin fractions at the interface.

Additionally, it is worth noting that it is possible that GXs also exist as aggregates. The tendency of hemicelluloses to exist as aggregates in aqueous dispersion has been well documented[275, 276], even for GGM that was extracted by the PHWE method[44, 277], similar to the GXs used in this thesis. The fact that the particle size of the dispersions were several times the thickness of the interfacial layers could serve as an indication that the GXs indeed existed as aggregates in their dispersion, which dissociated during the adsorption process. The dimensions and shape of these aggregates are unclear; preliminary small-angle X-ray and neutron scattering (SAXS and SANS, respectively) (data not shown) indicated that there was no evidence of higher-order structure in the dispersions of GX, or in other words, any aggregates may exist as random coils. It is also unclear whether the insoluble lignin particles were incorporated within these aggregates. Nevertheless, observations on epGX suggest the existence of, at the very least, a “micellar” aggregate, possibly formed by LCC-carrying fractions. Micellar structures, while being more well-known for small-molecule surfactants, are quite commonly found in dispersions of polyelectrolytes, especially those composed of block copolymers[278]. In the

proposed case for GX, the “micellar” aggregates would have the lignin domains facing inwards while the polysaccharide domains facing outwards, which would dissociate and be rearranged as they are adsorbed at the interface, as illustrated in Figure 36. This proposal of a “micellar” aggregate was supported by observations made on epGX. Dispersions of epGX at pH 4.5 were not turbid and did not show significant amount of precipitation over time; and yet, the detected size of the dispersions (Figure 18, squares) was at least twenty- to thirty-times the thickness of the adsorbed layer. Had the lignin domains of the epGX molecules been exposed to the aqueous phase, stronger aggregation would have been more rampant due to the hydrophobic nature of the lignin domain in the GXs, leading to precipitation. A “micellar” structure, on the other hand, would have prevented the aggregation of the lignin domains by protecting them in the core of the “micellar” structure, supported by the electrostatic and steric repulsion from the polysaccharide fraction. Such structure has been previously proposed for gum arabic, where the three-dimensional aggregates were formed by the association of the protein chains that formed the core of the aggregates, surrounded by branched polysaccharide chains[279]. Nonetheless, a deeper study into the state of the GX dispersions is needed to confirm the presence of these “micellar” structures, including whether such types of aggregates also exist in sGX and esGX.

Combining the observations from DIFT, QCM-D, AFM, and NR results, a proposal on the state of the adsorbed interfacial layer formed by GX has been developed, as illustrated in Figure 37 (as viewed from the side); note that this model disregards non-adsorbed (i.e., chemical species that do not have any interfacial activity) and unadsorbed chemical species (i.e., those that are interfacially active, but were not adsorbed for lack of empty interface) in GX. The difference in the DIFT profiles may have arisen from the difference in how dense the interface is packed by the different GXs, with the density of the interfacial packing in the order of esGX > sGX > epGX > CMGX. However, despite having the densest packing, esGX was lightweight (ref. the QCM-D results, Section 5.1.2) as mostly short-chained polysaccharides were adsorbed, compared to sGX and epGX. The lignin domains are all pointed towards the oil phase, as they acted as the anchors for the polysaccharides. Finally, as indicated by the NR experiments, all types of GX formed films of similar thickness.

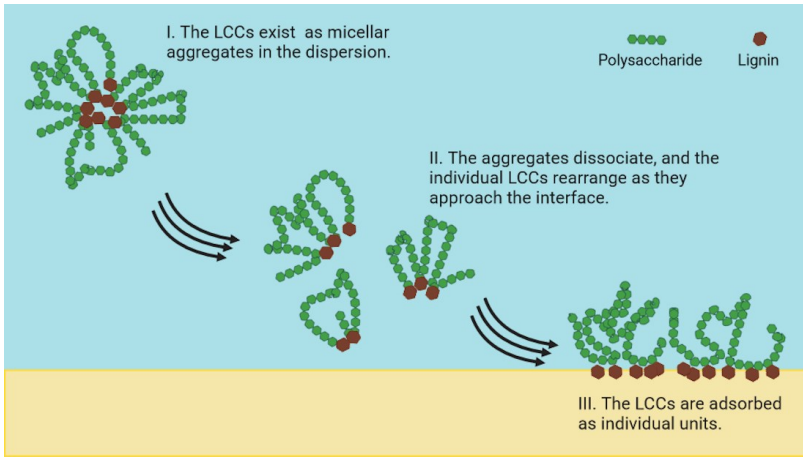

Figure 36. A hypothetical model of the existence of the 'micellar' aggregates of LCCs and their adsorption to the oil-water interface. Created using BioRender.com.

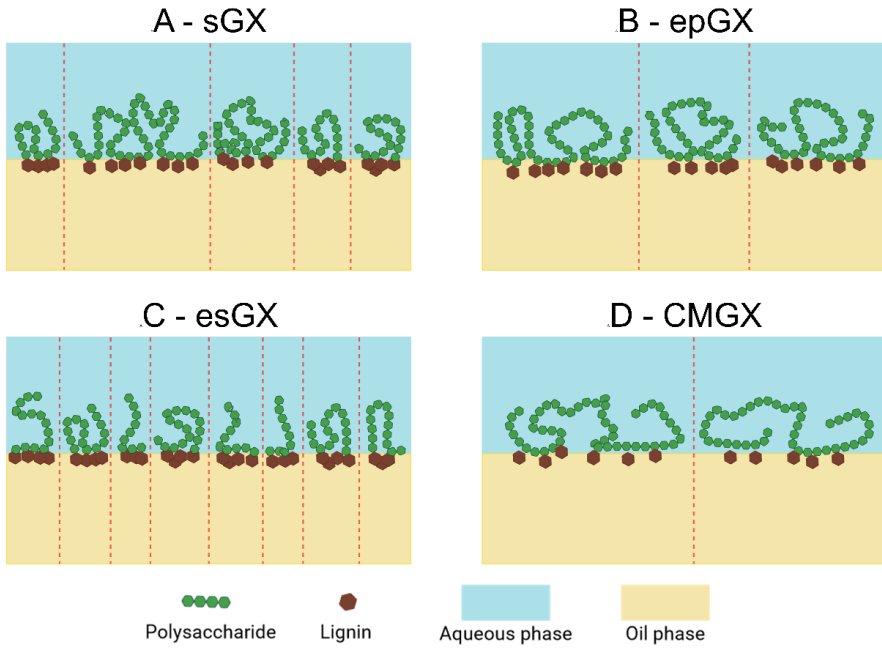

Figure 37. Illustration of the passively-adsorbed interfacial layer formed by sGX (A), epGX (B), esGX (C), and CMGX (D), showing the different amount of GX occupying the same area of interface. Created using BioRender.com.

However, one large shortcoming in the proposed model above is that it did not take into account the participation of the insoluble lignin particles. Both the DIFT and

NR experiments showed that the insoluble particles did not participate in the passive adsorption process, while results from the emulsion centrifugation (Figure 24) clearly showed that the insoluble particles were adsorbed on the emulsion droplets. It is well-known that the adsorption of many Pickering emulsifiers is non-spontaneous, thus requiring high-energy inputs to overcome the energy barrier for adsorption to the oil-water interface to occur[280, 281]. As such, the insoluble lignin particles would only be present at the interface following a high-energy emulsification process, such as the microfluidization used in this thesis. However, the localization of these insoluble particles is unknown; are they buried underneath the adsorbed LCCs (Figure 38A), or do they occupy the interface side-by-side to the LCCs (Figure 38B)? It would be rather interesting to probe the interface of the emulsions directly to measure the thickness of the interface, for example by SANS, as the insoluble particles might alter the thickness of the interface should they be buried underneath the polysaccharide layer. The possibility of applying isotopic contrast matching using deuterated water and oil would allow the measurement of the adsorbed interface as a hollow sphere (where the oil phase gives no contribution to the scattered intensity as the scattering length density is matched to the aqueous phase)[168, 282].

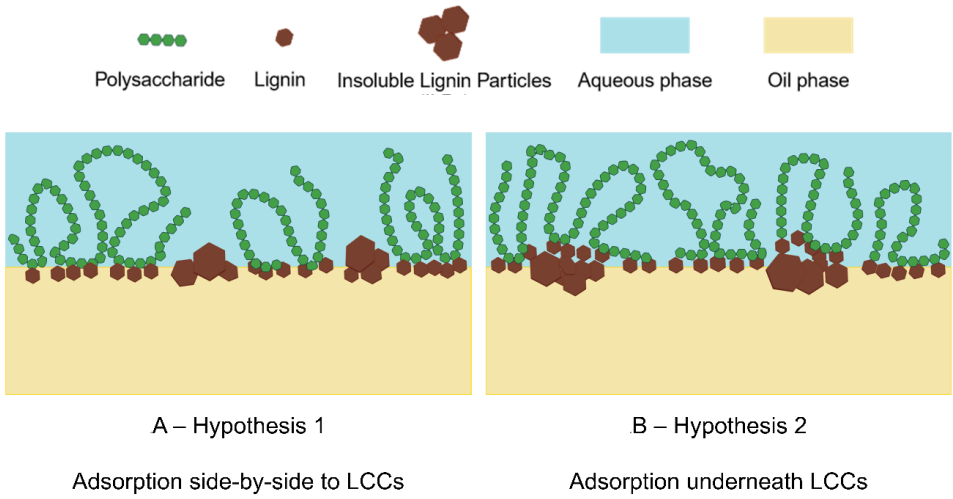

Figure 38. Illustration of the two hypotheses on the adsorption of insoluble lignin particles in sGX emulsions. Created using BioRender.com.

6.2 GX as a delivery system of hydrophobic compound

As detailed in Section 2.4, a suitable emulsifier for a delivery system of hydrophobic compound would be able to limit its degradation during storage as well as release it at the right place. In the case of vitamin D3, it is a light- and heat-sensitive vitamin which is unstable in the aqueous environment[283-285]. Additionally, it is

absorbed by the body through its incorporation into the mixed micelles formed by the digestion of triglycerides; this process occurs primarily in the intestinal phase of digestion [51, 229, 243]. The results of the storage stability test (Section 5.2.1) and the *in-vitro* digestion experiments (Sections 5.2.2 to 5.2.4) demonstrated the viability of both sGX and epGX as emulsifiers for vitamin D3-carrying emulsions, as they were able to protect the vitamin D3 cargo during five weeks of storage, and they also allowed the release of the vitamin D3 primarily during the intestinal phase of the *in-vitro* digestion. Meanwhile, esGX and CMGX were not included in the *in-vitro* digestion study as emulsions made with the former was highly unstable, while the latter involved chemical derivatization, which rendered both GXs unattractive for further commercial applications.

The results of the storage stability test, where there was no difference between the protective performance of sGX and epGX at either storage temperature, were rather surprising. Previous research on the antioxidative performance of PHWE GGM and GX showed a correlation between the amount of lignin and their antioxidative performance, for which a higher lignin content was associated with a lower formation of oil oxidation markers[31, 32, 220]. Therefore, the initial hypothesis was that the presence of lignin in the GXs would have allowed a superior protective performance by the GXs compared to lignin-free MC and casein, and also that the higher amount of lignin in sGX would have imparted better protection compared to epGX. Instead, the results may have highlighted that at least for emulsions carrying vitamin D3, a polysaccharide-based interfacial layer played a more important part. The suboptimal performance of casein at 40 ^{o}C storage could be attributed to the fact that vitamin D3 was able to partition itself into the casein matrix, particularly the β-casein subtype[287]; subsequently, the vitamin D3 could then partition into the aqueous phase, in which it was degraded faster. It is possible that the polysaccharide-based interfacial layers of GX and MC were able to prevent the diffusion of vitamin D3 out into the aqueous phase, contributing to the better stability performance. This observation also supported the remarks in Section 6.1, confirming a larger role of the polysaccharide fraction in the interfacial layer compared to previous studies, which largely highlighted the role of lignin.

As elaborated in Section 2.4, the lipolysis process is an inherently interfacial process, for which, in emulsion systems, can be controlled by choosing the correct emulsifier[228, 241, 286]. As shown in Figure 21A in Section 5.2.3, all the polysaccharide-based emulsifiers performed similarly, and all had a similar fatty acid release profile to each other. The large extent of lipolysis in the gastric phase was firstly attributed to the submicron droplet size, which translated to a large interfacial area, upon which the lipase molecules can act[288, 289]. Secondly, it was due to the fact that MCT oil was composed primarily of short, saturated fatty acids, which are more easily hydrolyzable compared to long-chain unsaturated fatty acids[288]. Casein, on the other hand, suffered a much larger amount of fatty acid

compared to the other emulsions even in the gastric phase; this was not surprising, as proteolysis already begins in the stomach[290], which would allow the weakening of the interfacial layer, giving more space for the lipases to attach. Remarkably, sGX did not show any difference to epGX despite the higher amount of lignin and the presence of the insoluble lignin particles. Lignin is known to increase the activity of pancreatic lipase, although the extent is dependent on the molar mass of the lignin[291]. It was therefore reasonable to expect that sGX should have suffered a more extensive lipolysis compared to epGX. The lack of observable impact of lignin content towards lipolysis might indicate that the lignin moiety is buried within the polysaccharide layer at the interface, as exposed lignin could have interacted with the lipase molecules and altered their activity. This explanation would have been more in-line with the model in Figure 38B. Another possible explanation is that the lignin moiety in both sGX and epGX consist of species with low molar mass that are too small to exert any impact on the activity of the lipases. However, to date it has not been possible to determine the molar mass or even the particle size of lignin within wood hemicelluloses separately from the polysaccharide fraction in wood hemicelluloses.

While the storage stability test and lipolysis profiles did not show any difference between sGX and epGX as emulsifiers, the opposite was seen for the vitamin D3 release profile. The release of cargo compound from a lipid-based delivery system usually goes hand-in-hand with the extent of lipolysis, especially considering that the compound is to be incorporated into the mixed micelle system[292, 293]. This was certainly not the case in the tested emulsifiers, as the lipolysis progression was similar between the polysaccharide emulsifiers. Therefore, the difference in release profile might have been caused by the interaction between vitamin D3 and lignin. Lignin-based materials are known to be able to hold hydrophobic drugs, which gave them the potential as an alternative carrier for those compounds[294-296]. Hence, it is possible that the vitamin D3 was first partitioned into the insoluble lignin particles of sGX before diffusing into the mixed micelles. The association of an emulsion's cargo compound with its emulsifier has previously been observed in various cyclodextrin-stabilized Pickering emulsions[297]. This hypothesis is also supported by the low partitioning coefficient of vitamin D3 (log P = 6.2[292]), which suggests that it may be localized within the oil droplets to be closer to the interfacial layer, which could facilitate its association to the lignin particles at the interface. This observation would also explain the release behavior exhibited by casein, which, as mentioned in the discussion of the stability test, was known to associate with vitamin D3[287]. Meanwhile, insoluble lignin particles were absent in epGX, and while it still contained some lignin, it may have been too small for the vitamin D3 molecules to associate with, and therefore was released immediately into the mixed micelles. The association between the lignin moiety and vitamin D3 is illustrated in Figure 39. These observations further strengthened the hypothesis that the interfacial layer built by GX has a more polysaccharide than lignin

character. Nevertheless, the aforementioned hypothesis must be further verified and proven by follow-up experiments. For example, other cargo compounds could be tested, in particular those with higher log P values, such as carotenoids, to verify whether the association occurred already within the emulsion or whether the cargo only associated with the interfacial materials after the lipolysis have occurred[292]. Additionally, while esGX would probably not be used in commercial emulsion formulations, it could showcase whether it was necessary to have insoluble lignin particles in the system to delay the release of the cargo compounds.

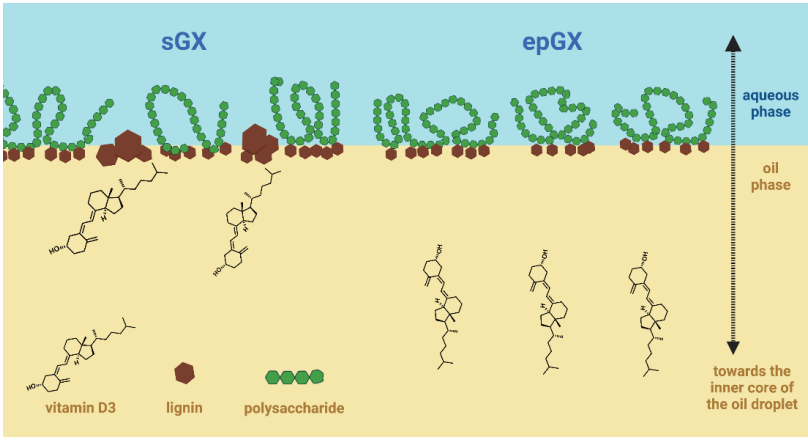

Figure 39. Illustration of the association of vitamin D3 to sGX and epGX. Created using BioRender.com.

6.3 Stabilization of emulsions by GX

Comparing the stabilization performance of the four GXs in different chemical environments showed how the properties of GX affected the stability of their emulsions, even though the resulting emulsions may not have been the most ideally-stable emulsions. Eventually, as elaborated in the Introduction, the results of this thesis would serve as a basis towards the industrial exploitation of GX and other hemicelluloses from lignocellulosic materials. A comparison between sGX and epGX is an important aspect in the future industrial application of GX, considering the trade-offs between the two. The sGX, being the crude extract obtained by directly spray-drying the extracted GX, is the prime candidate for application, considering the simplicity of production and superior stabilizing property; however, the higher amount of lignin can be detrimental for purposes where color and flavor are considered important[38]. On the other hand, epGX exhibited a much less pronounced sensorial effect than sGX[38], but it has so far shown inferior stability performance[31, 45]. From a mechanistic point of view,

fractionating sGX into epGX and esGX would indicate how much of the polysaccharide-rich and lignin-rich fractions contribute towards the stabilization mechanism of sGX, as well as explain the contribution of the polysaccharide and insoluble lignin fractions. The derivatization of epGX into CMGX added additional negative charge-carrying moieties into the GX, for which contribution of the electrostatic charges towards the stabilization mechanism was probed. The contribution of electrostatic repulsion towards the stabilization was also probed by the addition of salt into the continuous phase. The comparison of two pH values dug into the electrostatic contributions as well, considering that both the polysaccharide and lignin fractions of GX contain carboxylic and phenolic groups, respectively. However, it also examined the role of solubility, as an alkali environment solubilizes lignin[298, 299] while deacetylates the polysaccharide fraction[83, 84].

The results of the Turbiscan experiments (Figure 31) in this thesis showed that epGX emulsions were actually as stable, if not better, than sGX at all the tested environments, which did not correspond to previous stability studies conducted on either of them. Meanwhile, both CMGX and esGX were considerably less stable than both sGX and epGX as was found in previous tests, with the exception at pH 10 without salt, where all emulsions were similarly stable. The main destabilization mechanism of the GX emulsions appeared to be phase separation, in particular creaming, as evident from the visual assessment of the emulsions (Section 5.3.1); additionally, the improvement of stability simply by switching into an oil with higher density (from hexadecane to MCT) despite the larger droplet size also confirmed that gravitational separation was indeed one of the most critical points in stabilizing GX emulsions. This was contradictory to the main point of creating submicron-sized emulsion droplets, which should have experienced less buoyancy force due to the small droplet size[131]. One of the main factors in promoting the creaming process is the low viscosity of the GX emulsions. This has been shown in the comparison between GX-stabilized emulsions and those stabilized by MC and CMC (Supporting Publication A)[45]. Both MC and CMC created emulsions with higher viscosity than the GXs, and they experienced a much slower destabilization compared to the GXs, despite having a similar submicron droplet distribution to sGX and epGX. In absence of the droplet-arresting viscosity, the GX-stabilized oil droplets appeared to rely on electrostatic repulsion to avoid droplet-droplet collision, considering how the addition of salt imparted poorer stability to the emulsions. The stability of emulsions in the presence of salt in their aqueous phase varies according to the type of ions, the concentration of the ions, and the type of emulsifier. For example, emulsions stabilized by polysaccharides from the green algae *Ulva fasciata* were insensitive towards sodium ion between 0.01-0.05 M, while calcium ions between 0.02-0.05 M destabilized the emulsions[300]. Similar results were observed in emulsions stabilized by tomato seed proteins, although different pH levels imparted several differences in the salt sensitivity[301].

Emulsions stabilized by native soy protein isolate, on the other hand, experienced destabilization by 0.3 M NaCl[302]. In complex emulsifiers containing several different interfacially-active species, one component may be more sensitive to salt than the other, as was the case with α- and β-caseins[303]. In this study, both the polysaccharide and lignin fractions appeared to be sensitive against salt, although in different ways. The polysaccharide fraction's sensitivity to salt was more pronounced in the interfacial tension measurements (Sections 5.1.1 and 6.1). On the other hand, in emulsified systems the lignin fraction appeared to be more sensitive towards salt, to the effect of destabilizing the emulsions.

However, another major factor in the destabilization of GX-stabilized emulsions was the size distribution profiles of the oil droplets. As exhibited in Section 5.3.3, all GXs produced emulsions with multimodal size distribution, with the most unstable ones (esGX and CMGX) had a higher proportion of droplets sized more than 1 μm in diameter, while the more stable ones (sGX and epGX) had higher proportions of submicron droplets. This was also clear from the initial droplet size results; esGX, in particular, had exceptionally large D[4,3] values, in line with the rapid flocculation that occurred immediately after microfluidization. The droplets sized above 1 μm were initially suggested to be flocculates based on a previous study, which indeed existed, as shown in the micrographs of the emulsions (Supporting Publication A)[45]. Nonetheless, size measurements using added SDS showed that the larger droplet population was not flocculates, but instead truly a second population of droplets that is larger in diameter. The formation of this larger population of droplet is currently unclear; it is possible that each population was made by the adsorption of different species in GX, which might have been adsorbed at a different rate, or was unable to resist coalescence post-droplet-formation. A similar bimodal droplet distribution was observed in flaxseed press cake extract-stabilized emulsions, which disappeared following fractionation of the extract [304]. However, it was not observed in gum arabic-stabilized emulsions[191]. Bimodal droplet distribution was also observed in emulsions stabilized by soy protein and lecithin mixture, which changed based on the severity of ultrasonic processing of the emulsions. Therefore, it is possible that the nature of GX as a mixture of different species was not by itself a reason for the bimodality, but instead it may be related to the interfacial structure or to the difference in adsorption rate. Unfortunately, it is currently not possible to separate the emulsions based on their size and analyze the composition and structure of the interfaces associated with the different size populations.

All the GX-stabilized emulsions seemed to suffer from droplet growth in one mode or another. Both coalescence and Ostwald ripening appeared to have occurred, although those did not seem to be the major cause of droplet growth, especially not for sGX and epGX. Signs of Ostwald ripening, namely narrowing of the distribution peak of the smaller droplets and the enlargement of the peak of the larger ones [144,

145], was only apparent in emulsions made with MCT oil (Figure 33). Emulsions stabilized by CMGX appeared to be highly susceptible against coalescence; their droplet size distribution (Figures 27D, H, L, and P) clearly showed enlargement of the droplets into a larger population that was not accompanied by the formation of flocs, seen in their micrographs (Figure 25D, H, L, and P). The lack of flocculation in CMGX might have been caused by the strong negative charge of their emulsions even in the presence of salt (Figure 30); however, the interfacial layer might have not been strong enough or thick enough to resist coalescence when the droplet collision was able to counteract the electrostatic repulsion. Studies based on milk protein-stabilized emulsions have indeed shown the effect of interfacial viscoelasticity[148, 149] and thickness of the adsorbed layers[305] in preventing coalescence. It would therefore be beneficial to study the rheological properties of adsorbed GXs to see whether any correlation could be made with their emulsion stabilization performance.

Flocculation, on the other hand, was rampant for esGX-stabilized emulsions, especially at acidic pH. This coincided with the low solubility of lignin at acidic pH, for which esGX is rich in. Micrographs of esGX emulsions at pH 4.5 (Figure 25C) clearly showed the accumulation of insoluble lignin particles at the inter-droplet junctions, indicating that these insoluble lignin particles were primarily responsible for the formation of flocs by acting as bridges between the droplets. The presence of salt worsened the destabilization, as exhibited by the Turbiscan results (Figure 31); the initial D[3,2] of esGX at pH 4.5 (Table 4) was significantly higher in the presence of salt, suggesting that even the submicron droplets were prone to flocculation; and the micrograph (Figure 25G) also showed a heavier clumping of the lignin particles at the inter-droplet junction. Aggregation of colloidal particles due to the presence of salt has been well-documented, even in lignocellulosic materials[306-310]. The aggregation was induced as attractive forces, such as hydrophobic interactions[309], van der Waals forces[306, 310], or ionic binding[307, 308] were able to overcome the remaining repulsion once the electrostatic contribution was screened. As multivalent salts were not used in this study to evaluate ion binding, the driving force behind the lignin-driven aggregation may have either been van der Waals forces or hydrophobic interactions. While it is not possible with the current data to conclude which forces were more dominant, the apparent hydrophobic nature of the lignin moiety in GX may suggest the contribution of hydrophobic interactions. The lignin-driven aggregation was not only present in esGX emulsions, but also in sGX emulsions, as shown by how the droplet size distribution of sGX and esGX were similarly changed by the addition of SDS, while polysaccharide-rich epGX and CMGX were largely unaffected (Figure 28); nevertheless, the droplets of sGX were probably too small for the lignin-driven aggregates to be visible under the optical microscope. The lignin-driven aggregation would have also been responsible for the heavy flocculation experienced by sGX emulsions in the gastric phase during *in-vitro* digestion, where the drop of pH

triggered some of the lignin to become insoluble and drive the aggregation[298, 306].

As discussed in Section 6.1, it was clear that the insoluble particles participated in building the interface, although it was unclear whether they were completely buried under the LCCs or were adsorbed in the same plane (Figure 35). The observation that the insoluble lignin particle was responsible in bridging flocculation of the emulsion droplets pointed in favor of them occupying the same plane (similar to Figure 35A), considering that if they had been buried completely, then they would not have acted as bridges in the flocculation process. On the other hand, the discussion on the lipolysis result (Section 6.2) seemed to be in favor of the hypothesis that the particles were buried under (Figure 35B). However, since sGX also included the longer-chain polysaccharide fractions which may have been adsorbed, if they were adsorbed in close enough proximity to the insoluble lignin particles and the chains were flexible enough, it could be that the polysaccharide chains shielded the insoluble particles from the lipase molecules when they attacked the oil droplets. Nevertheless, as esGX emulsions were not subjected to lipolysis trials, there is no evidence that might have supported one hypothesis over the other. If the esGX emulsions, with shorter polysaccharide chains and larger insoluble lignin particles, showed an altered lipolysis activity compared to sGX, then the hypothesis might be viable; otherwise, other experimental methods would be needed to verify this claim.

The aforementioned results are the first report of the negative contribution of the lignin fraction of GX towards emulsion stabilization; previous studies have primarily reported the positive effects of the higher lignin content, which boosted both physical and chemical stability of the emulsions[31, 32, 220]. Another study with GGM from spruce even suggested that the insoluble lignin particles were contributing positively towards the stabilization of emulsions through Pickering stabilization[33]. As already discussed in Section 6.1, the nature of hydrophobicity or hydrophilicity of lignin itself has been unclear, with different preparation methods yielding different characters[13, 248-251]. These discrepancies suggested that the molecular arrangement of the lignin molecules derived by its preparation method might be the key towards understanding the hydrophobic or hydrophilic nature of lignin.

Surprisingly, all GXs appeared to make excellently stable emulsions at pH 10, as shown in the Turbiscan results (Figure 31), even for esGX, which was highly unstable in the acidic condition. The emulsions were primarily stabilized by electrostatic repulsion, as demonstrated by their highly negative zeta potential (Figure 30) as well as the fact that the addition of salt destabilized the emulsions. Minor flocs were still observed in esGX emulsions, although to a much less extent than at pH 4.5; there was also a large variation in the change of D[4,3] for esGX at

pH 10 without salt under SDS, which may signify a susceptibility towards coalescence regardless of the apparent stability. This result may indicate that the GXs would perform better when more of it is solubilized[83], which has been one of the main motivations in derivatizing hemicelluloses[83, 216]. The specific reason for this enhanced stability at pH 10 is outside of the scope of this study. Nevertheless, the fact that lignin is both more soluble and more negatively-charged at pH 10[299, 306] may lead to a hypothesis that the contribution of the lignin's charge towards the overall electrostatic potential of the oil droplets is bigger at pH 10 than at pH 4.5. Such hypothesis was, nonetheless, taken under the assumption that the alkali condition did not alter the conformation of the GX at the interface. This enhanced stability at pH 10, while might not be useful for food applications, may open the potential to use GX in enhanced oil recovery applications, where alkali solutions of surfactants are often used to improve the extraction of crude oils[141].

Interestingly, epGX emulsions at pH 10 showed a white precipitate, both after centrifugation (Figure 24J and N) and after storage (not shown). The white color suggested a lack of lignin, if not the complete absence, while its insolubility may have been caused by a complete deacetylation of the polysaccharide chain; this deacetylation was surprising, given that deacetylation has only been reported under the use of stronger alkali such as hydroxides[84], not by a weakly-deprotonizing species like a carbonate. The fact that it precipitated may indicate that a non-lignin-carrying polysaccharide fraction existed in the dispersion[83] which did not participate in the interfacial layer.

7 Conclusions

This doctoral thesis was conducted to establish the roles and interplay between the polysaccharide and the lignin fractions of PHWE GX in forming an interfacial layer at the oil-water interface in relation to their functionalities as emulsifiers. The compositional complexity of GX was addressed by evaluating different types of GX obtainable by antisolvent fractionation and chemical derivatization. Analyses of the acquired results produced the following conclusions.

Firstly, GX formed an adsorbed layer by the diffusion of the GX molecules from the continuous phase to the oil-water interface, in which the lignin moiety provided hydrophobicity as a driving force to attach and anchor the GX molecules. As the molecules arrived at the interface, they underwent rearrangement and, when existing as aggregates, they dissociated, to align the polysaccharide moieties towards the aqueous phase, forming the bulk of the interfacial layer. Meanwhile, the lignin moieties were pointed towards the oil phase.

Secondly, insoluble lignin particles were proven to be adsorbed at the oil-water interface of the oil droplets, although only with the assistance of a high-energy input. These insoluble lignin particles acted as a two-sided blade in the functionality of the emulsions. On one hand, they may slow down the release of hydrophobic bioactive compounds loaded in the emulsions, bestowing a controlled-release profile that could be beneficial for drug- and nutraceutical-delivery systems. On the other hand, when present excessively and in the absence of long-chain polysaccharides, they destabilize the emulsions by facilitating bridging flocculation; this also proved the protective role of the polysaccharide fraction in the interfacial layer. However, the localization of these insoluble lignin particles still needs to be verified through further experiments.

Thirdly, varying the chemical environment of the emulsions affected the emulsion stability in several different ways. Due to its low viscosity, GX-stabilized emulsions were heavily reliant on electrostatic repulsion for stability, as shown by how the presence of salt destabilized the emulsions regardless of GX type and the improved stability in alkali conditions. Both the polysaccharide and lignin fractions contributed to the electrostatic repulsion, but the lignin fraction's contribution was more apparent at an alkali condition, when the polyphenols in the lignin fraction were deprotonated and they became more soluble. The lignin fraction was also

more sensitive towards the ionic environment, as it was GXs with a higher amount of lignin aggregated more heavily in the presence of salt. On the contrary, the stability of emulsions stabilized by the polysaccharide-rich epGX was less affected by pH and salt content despite the deacetylation of the polysaccharide chain that led to some loss of solubility.

Lastly, GX emulsions were proven to be a potential candidate as a carrier of hydrophobic bioactive compounds, as it successfully protected vitamin D3 from degradation during storage and allowed the release of vitamin D3 during the intestinal digestion phase without excessive discharge in the gastric phase. The presence of insoluble lignin particles potentially held the vitamin D3 from partitioning into the aqueous phase too fast, leading to a controlled-release profile. Nevertheless, further studies are needed using a variation of other hydrophobic compounds to verify the mechanism of this prolonged retention.

To summarize the conclusions and to answer the aim of this thesis, the polysaccharide and the lignin fractions of PHWE GX worked together to endow stability to an emulsion system, where the polysaccharide fraction built the overall structure of the interfacial layer while the lignin fraction drove the adsorption and anchored GX to the interface. Both components contributed to the emulsion stabilization by providing electrostatic repulsion. Excess lignin in the form of insoluble lignin particles endowed an additional functionality by allowing longer retention of a hydrophobic cargo compound, while at the same time promoted bridging flocculation; the presence of a long-chain polysaccharide was able to attenuate this effect, possibly by providing a physical barrier to prevent the lignin moieties in different droplets from contacting each other.

8 Outlook

The results discussed in this thesis have highlighted the potential of wood hemicelluloses, in particular PHWE GX, as tunable emulsifiers that can be customized according to their composition. This thesis has principally exhibited that adjusting the ratio of polysaccharide to lignin, and to some extent the state of lignin in the material (i.e., LCC or insoluble particle), could be the key in adjusting their emulsifying and stabilizing capabilities. Nevertheless, there are still several unaddressed questions that would complete the building blocks of a full roadmap of hemicellulose customization. First, this thesis did not address the impact of acetylation towards the emulsifying properties. As overviewed in Section 2.1, the acetylation of hemicelluloses affects its solubility; the level of acetylation of spruce GGMs were found to affect its rheological properties, and even low-acetyl GGMs are known to form gels following a high-energy treatment. Thus, it is reasonable to assume that the level of acetylation would influence their capabilities as emulsifiers. Second, as discussed in Section 6.3, the fate of the insoluble lignin particles left several important questions about its role in the emulsion stabilization, in particular its localization at the interface. Other methods may be explored to investigate this potential, such as SANS and interfacial rheology. Third, while the conclusion of this thesis (particularly the one obtained in Publication III) implied the existence of a particular ratio of polysaccharide-to-lignin that is ideal for emulsion stabilization, it was not yet possible to determine the actual ratio. This was especially due to the fact that varying the lignin amount in the hemicelluloses is not as simple as adding externally-produced lignin, as the physical and chemical state of said lignin may not be the same as those originally present in the extract. Fourth, this thesis specifically studied GX from birch wood extracted by PHWE; therefore, the relationship or conclusions obtained here may not apply directly on other hemicelluloses from different lignocellulosic feedstocks, for example PHWE GGM from spruce or xylans from wheat and oat. Addressing those four knowledge gaps would allow the construction of a generalized model to predict how a given hemicellulose with different properties would behave as emulsifiers.

As stated in the introduction, the long-term vision of this thesis is for wood hemicelluloses to become a sustainable alternative emulsifier for the food industry. While this thesis was not aimed to provide the specifications for an optimal emulsion-based products, the results can still be relevant for product formulators who are interested in applying wood hemicelluloses into their emulsion-based

products, upon which they can base their optimization strategies. Firstly, this thesis provides a rationale of which GX grade should be used in a particular application. For example, for products where appearance and flavor are essential, formulators may want to use epGX instead of sGX; on the contrary, formulators who want to maximize the antioxidant or cargo release profile should instead use sGX for their product. Optimization of the emulsification properties by combining sGX and epGX together has also not been explored, and it could further tailor the emulsion to suit the intended products. Additionally, while the low viscosity of GX emulsions may be desirable in fortifying beverages, obtaining thicker emulsion products may require the addition of texture modifiers. Interactions between GX and these texture modifiers, if present, may influence the stability of the emulsions, and must thus be optimized, both in terms of the choice of texture modifier and its concentration. Lastly, while this thesis demonstrated the protection and release properties of vitamin D3, the behavior may differ when other hydrophobic cargo compounds are used, which should also be investigated.

Regardless of the remaining knowledge gaps, the work presented in this thesis has contributed to the methodology for analyzing the interfacial properties of natural materials, that are often difficult to purify or are highly disperse. For example, *in-vitro* digestion experiments have primarily been used to assess how different emulsifiers with known interfacial properties, pulling conclusions on how interfacial features affect digestibility. This study was, to the author's best knowledge, the first instance of using *in-vitro* digestion as a method to deduce the interfacial property of a given emulsifier. Meanwhile, the other methods used in this thesis, while they have been often used for well-defined emulsifier systems such as surfactants and synthetic amphiphilic polymers, have rarely been used to describe natural materials, often due to the limitations on how far conclusions can be taken from the results. For instance, the DIFT measurements have mostly been applied to small-molecule surfactants and well-defined proteins, and for those systems their respective adsorption isotherms could be declared, as their molar masses were more definite. On the other hand, the molar mass values of GXs are highly disperse, and thus its adsorption isotherm was more difficult to define. Thus, this study compared different fractions and concentrations of GXs to understand their adsorption behavior relative to each other. The approaches used in this thesis were built upon the years of work performed by multiple scientists on gum arabic, and hopefully other complex, naturally-derived materials could be characterized more deeply using the array of tools utilized here.

Finally, the findings in this thesis would hopefully contribute towards a more widespread usage of hemicelluloses isolated from lignocellulosic feedstocks, especially in systems that involve emulsions, be it in food, drugs, cosmetics, or other technical emulsions. Concrete applications of these hemicelluloses would create a demand for them, which would incentivize the exploitation of lignocellulosic

materials. Lignocellulosic materials are relatively more environmentally compatible compared to synthetic counterparts, and many lignocellulosic feedstocks already exist as waste or byproducts of current agriculture and forestry industries. Subsequently, it would contribute to a more circular and sustainable use of natural resources.

References

[1] S. Jørgensen, L.J.T. Pedersen, The Circular Rather than the Linear Economy, RESTART Sustainable Business Model Innovation, Springer International Publishing, Cham, 2018, pp. 103-120.
[2] R. Merli, M. Preziosi, A. Acampora, How do scholars approach the circular economy? A systematic literature review, Journal of Cleaner Production 178 (2018) 703-722.
[3] M. Weiss, J. Haufe, M. Carus, M. Brandão, S. Bringezu, B. Hermann, M.K. Patel, A Review of the Environmental Impacts of Biobased Materials, Journal of Industrial Ecology 16(s1) (2012) S169-S181.
[4] G. Fiorentino, A. Zucaro, S. Ulgiati, Towards an energy efficient chemistry. Switching from fossil to bio-based products in a life cycle perspective, Energy 170 (2019) 720-729.
[5] L. Yang, X.-C. Wang, M. Dai, B. Chen, Y. Qiao, H. Deng, D. Zhang, Y. Zhang, C.M. Villas Bôas de Almeida, A.S.F. Chiu, J.J. Klemeš, Y. Wang, Shifting from fossil-based economy to bio-based economy: Status quo, challenges, and prospects, Energy 228 (2021) 120533.
[6] L. Jiménez, A. Rodríguez, A. Pérez, A. Moral, L. Serrano, Alternative raw materials and pulping process using clean technologies, Industrial Crops and Products 28(1) (2008) 11-16.
[7] M.D. Smith, An Abbreviated Historical and Structural Introduction to Lignocellulose, Understanding Lignocellulose: Synergistic Computational and Analytic Methods, American Chemical Society2019, pp. 1-15.
[8] A.J. Ragauskas, G.T. Beckham, M.J. Biddy, R. Chandra, F. Chen, M.F. Davis, B.H. Davison, R.A. Dixon, P. Gilna, M. Keller, P. Langan, A.K. Naskar, J.N. Saddler, T.J. Tschaplinski, G.A. Tuskan, C.E. Wyman, Lignin Valorization: Improving Lignin Processing in the Biorefinery, Science 344(6185) (2014) 1246843.
[9] R. Abejón, A Bibliometric Study of Scientific Publications regarding Hemicellulose Valorization during the 2000–2016 Period: Identification of Alternatives and Hot Topics, ChemEngineering 2(1) (2018) 7.
[10] S. Sethupathy, G. Murillo Morales, L. Gao, H. Wang, B. Yang, J. Jiang, J. Sun, D. Zhu, Lignin valorization: Status, challenges and opportunities, Bioresource Technology 347 (2022) 126696.
[11] R. Abejón, H. Pérez-Acebo, L. Clavijo, Alternatives for Chemical and Biochemical Lignin Valorization: Hot Topics from a Bibliometric Analysis of the Research Published During the 2000–2016 Period, Processes 6(8) (2018) 98.

[12] F. Abik, C. Palasingh, M. Bhattarai, S. Leivers, A. Ström, B. Westereng, K.S. Mikkonen, T. Nypelö, Potential of Wood Hemicelluloses and Their Derivates as Food Ingredients, Journal of Agricultural and Food Chemistry 71(6) (2023) 2667-2683.
[13] A. Tribot, G. Amer, M. Abdou Alio, H. de Baynast, C. Delattre, A. Pons, J.-D. Mathias, J.-M. Callois, C. Vial, P. Michaud, C.-G. Dussap, Wood-lignin: Supply, extraction processes and use as bio-based material, European Polymer Journal 112 (2019) 228-240.
[14] M.F. Qaseem, H. Shaheen, A.-M. Wu, Cell wall hemicellulose for sustainable industrial utilization, Renewable and Sustainable Energy Reviews 144 (2021) 110996.
[15] S. Qiu, M.P. Yadav, L. Yin, Characterization and functionalities study of hemicellulose and cellulose components isolated from sorghum bran, bagasse and biomass, Food Chemistry 230 (2017) 225-233.
[16] Y. Zhao, H. Sun, B. Yang, Y. Weng, Hemicellulose-Based Film: Potential Green Films for Food Packaging, Polymers 12(8) (2020) 1775.
[17] K.S. Mikkonen, M. Tenkanen, Sustainable food-packaging materials based on future biorefinery products: Xylans and mannans, Trends in Food Science & Technology 28(2) (2012) 90-102.
[18] P. Kilpeläinen, K. Leppänen, P. Spetz, V. Kitunen, H. Ilvesniemi, A. Pranovich, S. Willför, BIOREFINERY. Pressurised hot water extraction of acetylated xylan from birch sawdust, Nordic Pulp & Paper Research Journal 27(4) (2012) 680-688.
[19] P.O. Kilpeläinen, S.S. Hautala, O.O. Byman, L.J. Tanner, R.I. Korpinen, M.K.J. Lillandt, A.V. Pranovich, V.H. Kitunen, S.M. Willför, H.S. Ilvesniemi, Pressurized hot water flow-through extraction system scale up from the laboratory to the pilot scale, Green Chemistry 16(6) (2014) 3186-3194.
[20] K. Leppänen, P. Spetz, A. Pranovich, K. Hartonen, V. Kitunen, H. Ilvesniemi, Pressurized hot water extraction of Norway spruce hemicelluloses using a flow-through system, Wood Science and Technology 45(2) (2011) 223-236.
[21] T. Song, A. Pranovich, I. Sumerskiy, B. Holmbom, Extraction of galactoglucomannan from spruce wood with pressurised hot water, Holzforschung 62(6) (2008) 659-666.
[22] L. Pitkänen, M. Heinonen, K.S. Mikkonen, Safety considerations of plant polysaccharides for food use: a case study on phenolic-rich softwood galactoglucomannan extract, Food & Function 9(4) (2018) 1931-1943.
[23] J.V. Rissanen, H. Grénman, C. Xu, S. Willför, D.Y. Murzin, T. Salmi, Obtaining Spruce Hemicelluloses of Desired Molar Mass by using Pressurized Hot Water Extraction, ChemSusChem 7(10) (2014) 2947-2953.
[24] A. Halahlah, F. Abik, M.H. Lahtinen, A. Kemppinen, K. Kaipanen, P.O. Kilpeläinen, D. Granato, T.M. Ho, K.S. Mikkonen, Effects of pH and temperature of ultrafiltration on the composition and physicochemical properties of hot-water-extracted softwood galactoglucomannans, Industrial Crops and Products 198 (2023) 116656.
[25] R. Korpinen, M. Kallioinen, J. Hemming, A. Pranovich, M. Mänttäri, S. Willför, Comparative evaluation of various lignin determination methods on hemicellulose-rich fractions of spruce and birch obtained by pressurized hot-water extraction (PHWE) and subsequent ultrafiltration (UF), Holzforschung 68(8) (2014) 971-979.
[26] C. Howell, A.C.S. Hastrup, R. Jara, F.H. Larsen, B. Goodell, J. Jellison, Effects of hot water extraction and fungal decay on wood crystalline cellulose structure, Cellulose 18(5) (2011) 1179-1190.

[27] P.A. Penttilä, P. Kilpeläinen, L. Tolonen, J.-P. Suuronen, H. Sixta, S. Willför, R. Serimaa, Effects of pressurized hot water extraction on the nanoscale structure of birch sawdust, Cellulose 20(5) (2013) 2335-2347.
[28] H. Kumar, L.P. Christopher, Recent trends and developments in dissolving pulp production and application, Cellulose 24(6) (2017) 2347-2365.
[29] K.S. Mikkonen, S. Kirjoranta, C. Xu, J. Hemming, A. Pranovich, M. Bhattarai, L. Peltonen, P. Kilpeläinen, N. Maina, M. Tenkanen, M. Lehtonen, S. Willför, Environmentally-compatible alkyd paints stabilized by wood hemicelluloses, Industrial Crops and Products 133 (2019) 212-220.
[30] M. Bhattarai, L. Pitkänen, V. Kitunen, R. Korpinen, H. Ilvesniemi, P.O. Kilpeläinen, M. Lehtonen, K.S. Mikkonen, Functionality of spruce galactoglucomannans in oil-in-water emulsions, Food Hydrocolloids 86 (2019) 154-161.
[31] M.H. Lahtinen, F. Valoppi, V. Juntti, S. Heikkinen, P.O. Kilpeläinen, N.H. Maina, K.S. Mikkonen, Lignin-Rich PHWE Hemicellulose Extracts Responsible for Extended Emulsion Stabilization, Frontiers in Chemistry 7 (2019).
[32] M. Lehtonen, M. Merinen, P.O. Kilpeläinen, C. Xu, S.M. Willför, K.S. Mikkonen, Phenolic residues in spruce galactoglucomannans improve stabilization of oil-in-water emulsions, Journal of Colloid and Interface Science 512 (2018) 536-547.
[33] F. Valoppi, M.H. Lahtinen, M. Bhattarai, S.J. Kirjoranta, V.K. Juntti, L.J. Peltonen, P.O. Kilpeläinen, K.S. Mikkonen, Centrifugal fractionation of softwood extracts improves the biorefinery workflow and yields functional emulsifiers, Green Chemistry 21(17) (2019) 4691-4705.
[34] D. Granato, D. Reshamwala, R. Korpinen, L. Azevedo, M.A. Vieira do Carmo, T.M. Cruz, M.B. Marques, M. Wen, L. Zhang, V. Marjomäki, P. Kilpeläinen, From the forest to the plate – Hemicelluloses, galactoglucomannan, glucuronoxylan, and phenolic-rich extracts from unconventional sources as functional food ingredients, Food Chemistry 381 (2022) 132284.
[35] E. Kynkäänniemi, M.H. Lahtinen, C. Jian, A. Salonen, T. Hatanpää, K.S. Mikkonen, A.-M. Pajari, Gut microbiota can utilize prebiotic birch glucuronoxylan in production of short-chain fatty acids in rats, Food & Function 13(6) (2022) 3746-3759.
[36] E. Kynkäänniemi, J. Lindén, S. Ngambundit, L.A. Saarimäki, D. Greco, H. Slaba, M.H. Lahtinen, K.S. Mikkonen, A.-M. Pajari, Polyphenol- and Glucuronoxylan-Rich Fiber Extract from Birch (Betula sp.) Wood Regulates Colonic Barrier Function and Cell Proliferation in Healthy Rats, Journal of Agricultural and Food Chemistry 72(7) (2024) 3495-3505.
[37] M.H. Lahtinen, E. Kynkäänniemi, C. Jian, A. Salonen, A.-M. Pajari, K.S. Mikkonen, Metabolic Fate of Lignin in Birch Glucuronoxylan Extracts as Dietary Fiber Studied in a Rat Model, Molecular Nutrition & Food Research 67(20) (2023) 2300201.
[38] S. Kirjoranta, A. Knaapila, P. Kilpeläinen, K.S. Mikkonen, Sensory profile of hemicellulose-rich wood extracts in yogurt models, Cellulose 27(13) (2020) 7607-7620.
[39] D.J. McClements, Food emulsions: principles, practices, and techniques, CRC press2015.
[40] V. Norn, Emulsifiers in Food Technology, John Wiley & Sons, Incorporated, Newark, UNITED KINGDOM, 2015.

[41] C. Berton-Carabin, K. Schroën, Towards new food emulsions: designing the interface and beyond, Current Opinion in Food Science 27 (2019) 74-81.
[42] D.J. McClements, L. Bai, C. Chung, Recent Advances in the Utilization of Natural Emulsifiers to Form and Stabilize Emulsions, Annual Review of Food Science and Technology 8(Volume 8, 2017) (2017) 205-236.
[43] K.S. Mikkonen, D. Merger, P. Kilpeläinen, L. Murtomäki, U.S. Schmidt, M. Wilhelm, Determination of physical emulsion stabilization mechanisms of wood hemicelluloses via rheological and interfacial characterization, Soft Matter 12(42) (2016) 8690-8700.
[44] M. Bhattarai, Associative behavior of spruce galactoglucomannans in aqueous solutions and emulsions, (2020).
[45] T.M. Ho, F. Abik, S. Hietala, E. Isaza Ferro, L. Pitkänen, D.W. Juhl, T. Vosegaard, P.O. Kilpeläinen, K.S. Mikkonen, Wood lignocellulosic stabilizers: effect of their characteristics on stability and rheological properties of emulsions, Cellulose 30(2) (2023) 753-773.
[46] V.K. Maurya, A. Shakya, K. Bashir, K. Jan, D.J. McClements, Fortification by design: A rational approach to designing vitamin D delivery systems for foods and beverages, Comprehensive Reviews in Food Science and Food Safety 22(1) (2023) 135-186.
[47] D.M.d. Carvalho, M.H. Lahtinen, M. Bhattarai, M. Lawoko, K.S. Mikkonen, Active role of lignin in anchoring wood-based stabilizers to the emulsion interface, Green Chemistry 23(22) (2021) 9084-9098.
[48] J. Gerard, S. Paradis, B. Thibaut, Survey on the chemical composition of several tropical wood species
Suivi de la composition chimique de plusieurs espèces de bois tropicaux, Bois et Forêts des Tropiques 342 (2019).
[49] L. Liu, X.P. Ye, A.R. Womac, S. Sokhansanj, Variability of biomass chemical composition and rapid analysis using FT-NIR techniques, Carbohydrate Polymers 81(4) (2010) 820-829.
[50] Y. Yang, R.D. Yanai, F.R. Fatemi, C.R. Levine, P.J. Lilly, R.D. Briggs, Sources of variability in tissue chemistry in northern hardwood species, Canadian Journal of Forest Research 46(3) (2016) 285-296.
[51] B. Öztürk, Nanoemulsions for food fortification with lipophilic vitamins: Production challenges, stability, and bioavailability, European Journal of Lipid Science and Technology 119(7) (2017) 1500539.
[52] H. Dubois, E. Verkasalo, H. Claessens, Potential of Birch (Betula pendula Roth and B. pubescens Ehrh.) for Forestry and Forest-Based Industry Sector within the Changing Climatic and Socio-Economic Context of Western Europe, Forests 11(3) (2020) 336.
[53] J. Hynynen, P. Niemistö, A. Viherä-Aarnio, A. Brunner, S. Hein, P. Velling, Silviculture of birch (Betula pendula Roth and Betula pubescens Ehrh.) in northern Europe, Forestry: An International Journal of Forest Research 83(1) (2009) 103-119.
[54] E. Sjöström, Wood Chemistry : Fundamentals and Applications, Academic Press, San Diego, 1993.
[55] L. Salmén, On the organization of hemicelluloses in the wood cell wall, Cellulose 29(3) (2022) 1349-1355.
[56] O.M. Terrett, J.J. Lyczakowski, L. Yu, D. Iuga, W.T. Franks, S.P. Brown, R. Dupree, P. Dupree, Molecular architecture of softwood revealed by solid-state NMR, Nature Communications 10(1) (2019) 4978.

[57] J. Berglund, D. Mikkelsen, B.M. Flanagan, S. Dhital, S. Gaunitz, G. Henriksson, M.E. Lindström, G.E. Yakubov, M.J. Gidley, F. Vilaplana, Wood hemicelluloses exert distinct biomechanical contributions to cellulose fibrillar networks, Nature Communications 11(1) (2020) 4692.
[58] A. Kirui, W. Zhao, F. Deligey, H. Yang, X. Kang, F. Mentink-Vigier, T. Wang, Carbohydrate-aromatic interface and molecular architecture of lignocellulose, Nature Communications 13(1) (2022) 538.
[59] D. Fengel, G. Wegener, Wood: Chemistry, Ultrastructure, Reactions, De Gruyter, Berlin, New York, 1983.
[60] A. Ebringerová, Z. Hromádková, T. Heinze, Hemicellulose, in: T. Heinze (Ed.), Polysaccharides I: Structure, Characterization and Use, Springer Berlin Heidelberg, Berlin, Heidelberg, 2005, pp. 1-67.
[61] A. Duval, M. Lawoko, A review on lignin-based polymeric, micro- and nano-structured materials, Reactive and Functional Polymers 85 (2014) 78-96.
[62] R.-C. Sun, Lignin Source and Structural Characterization, ChemSusChem 13(17) (2020) 4385-4393.
[63] E.M. Anderson, M.L. Stone, R. Katahira, M. Reed, W. Muchero, K.J. Ramirez, G.T. Beckham, Y. Román-Leshkov, Differences in S/G ratio in natural poplar variants do not predict catalytic depolymerization monomer yields, Nature Communications 10(1) (2019) 2033.
[64] G. Zinovyev, I. Sulaeva, S. Podzimek, D. Rössner, I. Kilpeläinen, I. Sumerskii, T. Rosenau, A. Potthast, Getting Closer to Absolute Molar Masses of Technical Lignins, ChemSusChem 11(18) (2018) 3259-3268.
[65] C. Nitsos, R. Stoklosa, A. Karnaouri, D. Vörös, H. Lange, D. Hodge, C. Crestini, U. Rova, P. Christakopoulos, Isolation and Characterization of Organosolv and Alkaline Lignins from Hardwood and Softwood Biomass, ACS Sustainable Chemistry & Engineering 4(10) (2016) 5181-5193.
[66] S.M. Braaten, B.E. Christensen, G.E. Fredheim, Comparison of Molecular Weight and Molecular Weight Distributions of Softwood and Hardwood Lignosulfonates, Journal of Wood Chemistry and Technology 23(2) (2003) 197-215.
[67] D. Tarasov, M. Leitch, P. Fatehi, Lignin–carbohydrate complexes: properties, applications, analyses, and methods of extraction: a review, Biotechnology for Biofuels 11(1) (2018) 269.
[68] Y. Pu, F. Hu, F. Huang, B.H. Davison, A.J. Ragauskas, Assessing the molecular structure basis for biomass recalcitrance during dilute acid and hydrothermal pretreatments, Biotechnology for Biofuels 6(1) (2013) 15.
[69] G. Bali, X. Meng, J.I. Deneff, Q. Sun, A.J. Ragauskas, The Effect of Alkaline Pretreatment Methods on Cellulose Structure and Accessibility, ChemSusChem 8(2) (2015) 275-279.
[70] T. Heinze, Cellulose: Structure and Properties, in: O.J. Rojas (Ed.), Cellulose Chemistry and Properties: Fibers, Nanocelluloses and Advanced Materials, Springer International Publishing, Cham, 2016, pp. 1-52.
[71] P. Sannigrahi, S.J. Miller, A.J. Ragauskas, Effects of organosolv pretreatment and enzymatic hydrolysis on cellulose structure and crystallinity in Loblolly pine, Carbohydrate Research 345(7) (2010) 965-970.
[72] R.L. Silveira, S.R. Stoyanov, A. Kovalenko, M.S. Skaf, Cellulose Aggregation under Hydrothermal Pretreatment Conditions, Biomacromolecules 17(8) (2016) 2582-2590.

[73] H. Chen, Y. Yu, T. Zhong, Y. Wu, Y. Li, Z. Wu, B. Fei, Effect of alkali treatment on microstructure and mechanical properties of individual bamboo fibers, Cellulose 24(1) (2017) 333-347.
[74] Y. Lu, Q. He, G. Fan, Q. Cheng, G. Song, Extraction and modification of hemicellulose from lignocellulosic biomass: A review, Green Processing and Synthesis 10(1) (2021) 779-804.
[75] X. Chen, M. Lawoko, A.v. Heiningen, Kinetics and mechanism of autohydrolysis of hardwoods, Bioresource Technology 101(20) (2010) 7812-7819.
[76] J.S. Gütsch, T. Nousiainen, H. Sixta, Comparative evaluation of autohydrolysis and acid-catalyzed hydrolysis of Eucalyptus globulus wood, Bioresource Technology 109 (2012) 77-85.
[77] G. Garrote, M.A. Kabel, H.A. Schols, E. Falqué, H. Domínguez, J.c. Parajó, Effects of Eucalyptus globulus Wood Autohydrolysis Conditions on the Reaction Products, Journal of Agricultural and Food Chemistry 55(22) (2007) 9006-9013.
[78] D. Nabarlatz, X. Farriol, D. Montané, Kinetic Modeling of the Autohydrolysis of Lignocellulosic Biomass for the Production of Hemicellulose-Derived Oligosaccharides, Industrial & Engineering Chemistry Research 43(15) (2004) 4124-4131.
[79] F. Delbecq, Y. Wang, A. Muralidhara, K. El Ouardi, G. Marlair, C. Len, Hydrolysis of Hemicellulose and Derivatives—A Review of Recent Advances in the Production of Furfural, Frontiers in Chemistry 6 (2018).
[80] Y. Luo, Z. Li, X. Li, X. Liu, J. Fan, J.H. Clark, C. Hu, The production of furfural directly from hemicellulose in lignocellulosic biomass: A review, Catalysis Today 319 (2019) 14-24.
[81] C. Laine, K. Kemppainen, L. Kuutti, A. Varhimo, S. Asikainen, A. Grönroos, M. Määttänen, J. Buchert, A. Harlin, Extraction of xylan from wood pulp and brewer's spent grain, Industrial Crops and Products 70 (2015) 231-237.
[82] W. Geng, R. Narron, X. Jiang, J.J. Pawlak, H.-m. Chang, S. Park, H. Jameel, R.A. Venditti, The influence of lignin content and structure on hemicellulose alkaline extraction for non-wood and hardwood lignocellulosic biomass, Cellulose 26(5) (2019) 3219-3230.
[83] K.S. Mikkonen, Strategies for structuring diverse emulsion systems by using wood lignocellulose-derived stabilizers, Green Chemistry 22(4) (2020) 1019-1037.
[84] L. Santibáñez, C. Henríquez, R. Corro-Tejeda, S. Bernal, B. Armijo, O. Salazar, Xylooligosaccharides from lignocellulosic biomass: A comprehensive review, Carbohydrate Polymers 251 (2021) 117118.
[85] Anonymous, Xylan (Beechwood), 2024. https://www.megazyme.com/xylan-beechwood-purified. (Accessed 17 July 2024 2024).
[86] Anonymous, CH-Bioforce - Hemicellulose, 2024. https://www.ch-bioforce.com/hemicellulose/. (Accessed 17 July 2024 2024).
[87] Anonymous, Solutions for Industry, 2024. https://www.borealbioproducts.com/products-for-industry. (Accessed 17 July 2024 2024).
[88] B. Saake, T. Kruse, J. Puls, Investigation on molar mass, solubility and enzymatic fragmentation of xylans by multi-detected SEC chromatography, Bioresource Technology 80(3) (2001) 195-204.
[89] D.M.d. Carvalho, M.H. Lahtinen, M. Lawoko, K.S. Mikkonen, Enrichment and Identification of Lignin–Carbohydrate Complexes in Softwood Extract, ACS Sustainable Chemistry & Engineering 8(31) (2020) 11795-11804.

[90] M. Bhattarai, I. Sulaeva, L. Pitkänen, I. Kontro, M. Tenkanen, A. Potthast, K.S. Mikkonen, Colloidal features of softwood galactoglucomannans-rich extract, Carbohydrate Polymers 241 (2020) 116368.
[91] M.T. Maloney, T.W. Chapman, A.J. Baker, An Engineering Analysis of the Production of Xylose by Dilute Acid Hydrolysis of Hardwood Hemicellulose, Biotechnology Progress 2(4) (1986) 192-202.
[92] F.M. Gírio, C. Fonseca, F. Carvalheiro, L.C. Duarte, S. Marques, R. Bogel-Łukasik, Hemicelluloses for fuel ethanol: A review, Bioresource Technology 101(13) (2010) 4775-4800.
[93] B.C. Saha, Hemicellulose bioconversion, Journal of Industrial Microbiology and Biotechnology 30(5) (2003) 279-291.
[94] Y. Delgado Arcaño, O.D. Valmaña García, D. Mandelli, W.A. Carvalho, L.A. Magalhães Pontes, Xylitol: A review on the progress and challenges of its production by chemical route, Catalysis Today 344 (2020) 2-14.
[95] E. Winkelhausen, S. Kuzmanova, Microbial conversion of d-xylose to xylitol, Journal of Fermentation and Bioengineering 86(1) (1998) 1-14.
[96] A. Gasmi Benahmed, A. Gasmi, M. Arshad, M. Shanaida, R. Lysiuk, M. Peana, I. Pshyk-Titko, S. Adamiv, Y. Shanaida, G. Bjørklund, Health benefits of xylitol, Applied Microbiology and Biotechnology 104(17) (2020) 7225-7237.
[97] Anonymous, P2X Solutions and Danisco Sweeteners signed a contract on the delivery of green hydrogen, P2X Solutions Oy, 2023.
[98] Anonymous, Fazer's xylitol factory in Lahti has started its operations – the plant is the only one in the world to make xylitol from oat hulls, Oy Karl Fazer Ab, 2022.
[99] S. Rivas, B. Gullón, P. Gullón, J.L. Alonso, J.C. Parajó, Manufacture and Properties of Bifidogenic Saccharides Derived from Wood Mannan, Journal of Agricultural and Food Chemistry 60(17) (2012) 4296-4305.
[100] K. Shimizu, M. Ishihara, Isolation and Characterization of Oligosaccharides from the Hydrolyzate of Larch Wood Glucomannan with Endo-β-d-Mannanase, Agricultural and Biological Chemistry 47(5) (1983) 949-955.
[101] L. Bhatia, A. Sharma, R.K. Bachheti, A.K. Chandel, Lignocellulose derived functional oligosaccharides: production, properties, and health benefits, Preparative Biochemistry & Biotechnology 49(8) (2019) 744-758.
[102] V. Narisetty, P. Parhi, B. Mohan, S. Hakkim Hazeena, A. Naresh Kumar, B. Gullón, A. Srivastava, L.M. Nair, M. Paul Alphy, R. Sindhu, V. Kumar, E. Castro, M. Kumar Awasthi, P. Binod, Valorization of renewable resources to functional oligosaccharides: Recent trends and future prospective, Bioresource Technology 346 (2022) 126590.
[103] R. Chelliah, N.H. Kim, S. Park, Y. Park, S.-J. Yeon, K. Barathikannan, S. Vijayalakshmi, D.-H. Oh, Revolutionizing Renewable Resources: Cutting-Edge Trends and Future Prospects in the Valorization of Oligosaccharides, Fermentation 10(4) (2024) 195.
[104] I. Ratcliffe, P.A. Williams, C. Viebke, J. Meadows, Physicochemical Characterization of Konjac Glucomannan, Biomacromolecules 6(4) (2005) 1977-1986.
[105] S. Singh, G. Singh, S.K. Arya, Mannans: An overview of properties and application in food products, International Journal of Biological Macromolecules 119 (2018) 79-95.

[106] J.J. Liao, N.H.A. Latif, D. Trache, N. Brosse, M.H. Hussin, Current advancement on the isolation, characterization and application of lignin, International Journal of Biological Macromolecules 162 (2020) 985-1024.
[107] D.R. Lobato-Peralta, E. Duque-Brito, H.I. Villafán-Vidales, A. Longoria, P.J. Sebastian, A.K. Cuentas-Gallegos, C.A. Arancibia-Bulnes, P.U. Okoye, A review on trends in lignin extraction and valorization of lignocellulosic biomass for energy applications, Journal of Cleaner Production 293 (2021) 126123.
[108] T. Persson, A.S. Jönsson, Isolation of hemicelluloses by ultrafiltration of thermomechanical pulp mill process water—Influence of operating conditions, Chemical Engineering Research and Design 88(12) (2010) 1548-1554.
[109] Anonymous, Lignin production with LignoBoost®, 2024. https://www.valmet.com/pulp/other-value-adding-processes/lignin-extraction/. (Accessed 17 July 2024 2024).
[110] Anonymous, LigninClub Ecosystem - Who we are, 2024. https://ligninclub.fi/who-we-are/. (Accessed 17 July 2024 2024).
[111] J. Saari, E. Sermyagina, J. Kaikko, M. Haider, M. Hamaguchi, E. Vakkilainen, Evaluation of the Energy Efficiency Improvement Potential through Back-End Heat Recovery in the Kraft Recovery Boiler, Energies 14(6) (2021) 1550.
[112] R. Morya, M. Kumar, I. Tyagi, A. Kumar Pandey, J. Park, T. Raj, R. Sirohi, V. Kumar, S.-H. Kim, Recent advances in black liquor valorization, Bioresource Technology 350 (2022) 126916.
[113] M. Naqvi, J. Yan, E. Dahlquist, Black liquor gasification integrated in pulp and paper mills: A critical review, Bioresource Technology 101(21) (2010) 8001-8015.
[114] Anonymous, RenFuel has been awarded a grant of SEK 1.8 million for the project "One Lignin Oil from many Lignins", RenFuel, Sweden, 2023.
[115] Z. Peng, X. Jiang, C. Si, A. Joao Cárdenas-Oscanoa, C. Huang, Advances of Modified Lignin as Substitute to Develop Lignin-Based Phenol-Formaldehyde Resin Adhesives, ChemSusChem 16(15) (2023) e202300174.
[116] Y. Guo, D. Tian, F. Shen, G. Yang, L. Long, J. He, C. Song, J. Zhang, Y. Zhu, C. Huang, S. Deng, Transparent Cellulose/Technical Lignin Composite Films for Advanced Packaging, Polymers 11(9) (2019) 1455.
[117] A. Khan, J.C. Colmenares, R. Gläser, Lignin-Based Composite Materials for Photocatalysis and Photovoltaics, in: L. Serrano, R. Luque, B.F. Sels (Eds.), Lignin Chemistry, Springer International Publishing, Cham, 2020, pp. 1-31.
[118] W. Thielemans, E. Can, S.S. Morye, R.P. Wool, Novel applications of lignin in composite materials, Journal of Applied Polymer Science 83(2) (2002) 323-331.
[119] H.-M. Wang, T.-Q. Yuan, G.-Y. Song, R.-C. Sun, Advanced and versatile lignin-derived biodegradable composite film materials toward a sustainable world, Green Chemistry 23(11) (2021) 3790-3817.
[120] Anonymous, Prisma Composites - Our Technology, 2024. https://prismacomposites.com/our-technology/#material. (Accessed 17 July 2024 2024).
[121] Y. Meng, J. Lu, Y. Cheng, Q. Li, H. Wang, Lignin-based hydrogels: A review of preparation, properties, and application, International Journal of Biological Macromolecules 135 (2019) 1006-1019.
[122] D. Rico-García, L. Ruiz-Rubio, L. Pérez-Alvarez, S.L. Hernández-Olmos, G.L. Guerrero-Ramírez, J.L. Vilas-Vilela, Lignin-Based Hydrogels: Synthesis and Applications, Polymers 12(1) (2020) 81.

[123] M. Österberg, M.H. Sipponen, B.D. Mattos, O.J. Rojas, Spherical lignin particles: a review on their sustainability and applications, Green Chemistry 22(9) (2020) 2712-2733.
[124] M.H. Sipponen, H. Lange, C. Crestini, A. Henn, M. Österberg, Lignin for Nano- and Microscaled Carrier Systems: Applications, Trends, and Challenges, ChemSusChem 12(10) (2019) 2039-2054.
[125] S. Beisl, A. Friedl, A. Miltner, Lignin from Micro- to Nanosize: Applications, International Journal of Molecular Sciences 18(11) (2017) 2367.
[126] Anonymous, Lignovations - Technology: Lignovations develop high-performance ingredients from biomass., 2024. https://lignovations.com/technology/. (Accessed 17 July 2024 2024).
[127] T.F. Tadros, Interfacial Phenomena and Colloid Stability : Basic Principles, De Gruyter, Inc., Berlin/Boston, GERMANY, 2015.
[128] T.F. Tadros, Emulsion Formation and Stability, John Wiley & Sons, Incorporated, Newark, GERMANY, 2013.
[129] D.C. Clark, M. Coke, P.J. Wilde, D.R. Wilson, Molecular Diffusion at Interfaces and its Relationship to Disperse Phase Stability, in: E. Dickinson (Ed.), Food Polymers, Gels and Colloids, Woodhead Publishing1991, pp. 272-276.
[130] F. Ravera, K. Dziza, E. Santini, L. Cristofolini, L. Liggieri, Emulsification and emulsion stability: The role of the interfacial properties, Advances in Colloid and Interface Science 288 (2021) 102344.
[131] D.J. McClements, Edible nanoemulsions: fabrication, properties, and functional performance, Soft Matter 7(6) (2011) 2297-2316.
[132] A. Anonymous, Food and Feed Information Portal Database Version 5.1. https://ec.europa.eu/food/food-feed-portal/screen/food-additives/search. (Accessed 16 July 2024 2024).
[133] J.E. Marine, S.R. Menon, S.J. Rumbelow, Chapter 3 - Surfactants (polysorbate and poloxamer): synthesis, characterization, and degradation, in: A.V. Koulov, S.K. Singh (Eds.), Surfactants in Biopharmaceutical Development, Academic Press2023, pp. 23-57.
[134] A. Corma, S. Iborra, S. Miquel, J. Primo, Catalysts for the Production of Fine Chemicals: Production of Food Emulsifiers, Monoglycerides, by Glycerolysis of Fats with Solid Base Catalysts, Journal of Catalysis 173(2) (1998) 315-321.
[135] G.O. Phillips, P.A. Williams, G.O. Phillips, P.A. Williams, Handbook of Hydrocolloids, Elsevier Science & Technology, Cambridge, UNITED KINGDOM, 2009.
[136] V. Patel, R. Lalani, D. Bardoliwala, S. Ghosh, A. Misra, Lipid-Based Oral Formulation Strategies for Lipophilic Drugs, AAPS PharmSciTech 19(8) (2018) 3609-3630.
[137] C.J.H. Porter, N.L. Trevaskis, W.N. Charman, Lipids and lipid-based formulations: optimizing the oral delivery of lipophilic drugs, Nature Reviews Drug Discovery 6(3) (2007) 231-248.
[138] B.J. Boyd, T.-H. Nguyen, A. Müllertz, Lipids in Oral Controlled Release Drug Delivery, in: C.G. Wilson, P.J. Crowley (Eds.), Controlled Release in Oral Drug Delivery, Springer US, Boston, MA, 2011, pp. 299-327.
[139] W. Faisal, F. Almomani, A critical review of the development and demulsification processes applied for oil recovery from oil in water emulsions, Chemosphere 291 (2022) 133099.

[140] E. Yonguep, K.F. Kapiamba, K.J. Kabamba, M. Chowdhury, Formation, stabilization and chemical demulsification of crude oil-in-water emulsions: A review, Petroleum Research 7(4) (2022) 459-472.
[141] Y. Zhou, D. Yin, W. Chen, B. Liu, X. Zhang, A comprehensive review of emulsion and its field application for enhanced oil recovery, Energy Science & Engineering 7(4) (2019) 1046-1058.
[142] S.S. Lim, M.Y. Baik, E.A. Decker, L. Henson, L. Michael Popplewell, D.J. McClements, S.J. Choi, Stabilization of orange oil-in-water emulsions: A new role for ester gum as an Ostwald ripening inhibitor, Food Chemistry 128(4) (2011) 1023-1028.
[143] L.A. Trujillo-Cayado, J. Santos, N. Calero, M.-C. Alfaro-Rodríguez, J. Muñoz, Strategies for reducing Ostwald ripening phenomenon in nanoemulsions based on thyme essential oil, Journal of the Science of Food and Agriculture 100(4) (2020) 1671-1677.
[144] J. Santos, N. Calero, L.A. Trujillo-Cayado, M.C. Garcia, J. Muñoz, Assessing differences between Ostwald ripening and coalescence by rheology, laser diffraction and multiple light scattering, Colloids and Surfaces B: Biointerfaces 159 (2017) 405-411.
[145] T.J. Wooster, M. Golding, P. Sanguansri, Impact of Oil Type on Nanoemulsion Formation and Ostwald Ripening Stability, Langmuir 24(22) (2008) 12758-12765.
[146] B. Zeeb, M. Gibis, L. Fischer, J. Weiss, Influence of interfacial properties on Ostwald ripening in crosslinked multilayered oil-in-water emulsions, Journal of Colloid and Interface Science 387(1) (2012) 65-73.
[147] S.H. Park, C.R. Hong, S.J. Choi, Prevention of Ostwald ripening in orange oil emulsions: Impact of surfactant type and Ostwald ripening inhibitor type, LWT 134 (2020) 110180.
[148] H.W. Yarranton, P. Urrutia, D.M. Sztukowski, Effect of interfacial rheology on model emulsion coalescence: II. Emulsion coalescence, Journal of Colloid and Interface Science 310(1) (2007) 253-259.
[149] E. Dickinson, B.S. Murray, G. Stainsby, Coalescence stability of emulsion-sized droplets at a planar oil–water interface and the relationship to protein film surface rheology, Journal of the Chemical Society, Faraday Transactions 1: Physical Chemistry in Condensed Phases 84(3) (1988) 871-883.
[150] R. Chanamai, D.J. McClements, Depletion Flocculation of Beverage Emulsions by Gum Arabic and Modified Starch, Journal of Food Science 66(3) (2001) 457-463.
[151] E. Dickinson, M. Golding, Depletion flocculation of emulsions containing unadsorbed sodium caseinate, Food Hydrocolloids 11(1) (1997) 13-18.
[152] D.J. French, P. Taylor, J. Fowler, P.S. Clegg, Making and breaking bridges in a Pickering emulsion, Journal of Colloid and Interface Science 441 (2015) 30-38.
[153] E. Dickinson, Flocculation of protein-stabilized oil-in-water emulsions, Colloids and Surfaces B: Biointerfaces 81(1) (2010) 130-140.
[154] E. Dickinson, K. Pawlowsky, Effect of ι-Carrageenan on Flocculation, Creaming, and Rheology of a Protein-Stabilized Emulsion, Journal of Agricultural and Food Chemistry 45(10) (1997) 3799-3806.
[155] E. Dickinson, Hydrocolloids as emulsifiers and emulsion stabilizers, Food Hydrocolloids 23(6) (2009) 1473-1482.
[156] Y. Matsuda, Y. Biyajima, T. Sato, Thermal Denaturation, Renaturation, and Aggregation of a Double-Helical Polysaccharide Xanthan in Aqueous Solution, Polymer Journal 41(7) (2009) 526-532.

[157] C.G. Lopez, S.E. Rogers, R.H. Colby, P. Graham, J.T. Cabral, Structure of sodium carboxymethyl cellulose aqueous solutions: A SANS and rheology study, Journal of Polymer Science Part B: Polymer Physics 53(7) (2015) 492-501.
[158] B. Nyström, A.-L. Kjøniksen, N. Beheshti, K. Zhu, K.D. Knudsen, Rheological and structural aspects on association of hydrophobically modified polysaccharides, Soft Matter 5(7) (2009) 1328-1339.
[159] L. Bai, F. Liu, X. Xu, S. Huan, J. Gu, D.J. McClements, Impact of polysaccharide molecular characteristics on viscosity enhancement and depletion flocculation, Journal of Food Engineering 207 (2017) 35-45.
[160] C. Chung, B. Degner, D.J. McClements, Designing reduced-fat food emulsions: Locust bean gum–fat droplet interactions, Food Hydrocolloids 32(2) (2013) 263-270.
[161] M. HENNOCK, R.R. RAHALKAR, P. RICHMOND, Effect of Xanthan Gum Upon the Rheology and Stability of Oil-Water Emulsions, Journal of Food Science 49(5) (1984) 1271-1274.
[162] A.G. Gaonkar, Surface and interfacial activities and emulsion characteristics of some food hydrocolloids, Food Hydrocolloids 5(4) (1991) 329-337.
[163] C. Arancibia, S. Bayarri, E. Costell, Comparing Carboxymethyl Cellulose and Starch as Thickeners in Oil/Water Emulsions. Implications on Rheological and Structural Properties, Food Biophysics 8(2) (2013) 122-136.
[164] P. Shao, J. Feng, P. Sun, N. Xiang, B. Lu, D. Qiu, Recent advances in improving stability of food emulsion by plant polysaccharides, Food Research International 137 (2020) 109376.
[165] Y. Cao, E. Dickinson, D.J. Wedlock, Creaming and flocculation in emulsions containing polysaccharide, Food Hydrocolloids 4(3) (1990) 185-195.
[166] E. Dickinson, V.B. Galazka, Bridging Flocculation in Emulsions Made with a Mixture of Protein + Polysaccharide, in: E. Dickinson (Ed.), Food Polymers, Gels and Colloids, Woodhead Publishing1991, pp. 494-497.
[167] S. Aidarova, A. Sharipova, J. Krägel, R. Miller, Polyelectrolyte/surfactant mixtures in the bulk and at water/oil interfaces, Advances in Colloid and Interface Science 205 (2014) 87-93.
[168] M. Atgié, A. Chennevière, O. Masbernat, K. Roger, Emulsions Stabilized by Gum Arabic: How Diversity and Interfacial Networking Lead to Metastability, Langmuir 35(45) (2019) 14553-14565.
[169] J. Floury, A. Desrumaux, M.A.V. Axelos, J. Legrand, Effect of high pressure homogenisation on methylcellulose as food emulsifier, Journal of Food Engineering 58(3) (2003) 227-238.
[170] P.L. Nasatto, F. Pignon, J.L.M. Silveira, M.E.R. Duarte, M.D. Noseda, M. Rinaudo, Methylcellulose, a Cellulose Derivative with Original Physical Properties and Extended Applications, Polymers 7(5) (2015) 777-803.
[171] C. Wollenweber, A.V. Makievski, R. Miller, R. Daniels, Adsorption of hydroxypropyl methylcellulose at the liquid/liquid interface and the effect on emulsion stability, Colloids and Surfaces A: Physicochemical and Engineering Aspects 172(1) (2000) 91-101.
[172] R. Bodvik, A. Dedinaite, L. Karlson, M. Bergström, P. Bäverbäck, J.S. Pedersen, K. Edwards, G. Karlsson, I. Varga, P.M. Claesson, Aggregation and network formation of aqueous methylcellulose and hydroxypropylmethylcellulose solutions, Colloids and Surfaces A: Physicochemical and Engineering Aspects 354(1) (2010) 162-171.

[173] C. Li, Y. Li, P. Sun, C. Yang, Pickering emulsions stabilized by native starch granules, Colloids and Surfaces A: Physicochemical and Engineering Aspects 431 (2013) 142-149.
[174] M. Matos, A. Marefati, R. Bordes, G. Gutiérrez, M. Rayner, Combined emulsifying capacity of polysaccharide particles of different size and shape, Carbohydrate Polymers 169 (2017) 127-138.
[175] B.S. Murray, Pickering emulsions for food and drinks, Current Opinion in Food Science 27 (2019) 57-63.
[176] M.R. Barkhordari, M. Fathi, Production and characterization of chitin nanocrystals from prawn shell and their application for stabilization of Pickering emulsions, Food Hydrocolloids 82 (2018) 338-345.
[177] S. Ge, L. Xiong, M. Li, J. Liu, J. Yang, R. Chang, C. Liang, Q. Sun, Characterizations of Pickering emulsions stabilized by starch nanoparticles: Influence of starch variety and particle size, Food Chemistry 234 (2017) 339-347.
[178] D.C. Malaspina, J. Faraudo, Molecular insight into the wetting behavior and amphiphilic character of cellulose nanocrystals, Advances in Colloid and Interface Science 267 (2019) 15-25.
[179] I. Kalashnikova, H. Bizot, B. Cathala, I. Capron, Modulation of Cellulose Nanocrystals Amphiphilic Properties to Stabilize Oil/Water Interface, Biomacromolecules 13(1) (2012) 267-275.
[180] H. Du Le, S.M. Loveday, H. Singh, A. Sarkar, Pickering emulsions stabilised by hydrophobically modified cellulose nanocrystals: Responsiveness to pH and ionic strength, Food Hydrocolloids 99 (2020) 105344.
[181] X. Song, Y. Pei, M. Qiao, F. Ma, H. Ren, Q. Zhao, Preparation and characterizations of Pickering emulsions stabilized by hydrophobic starch particles, Food Hydrocolloids 45 (2015) 256-263.
[182] C. Tang, S. Spinney, Z. Shi, J. Tang, B. Peng, J. Luo, K.C. Tam, Amphiphilic Cellulose Nanocrystals for Enhanced Pickering Emulsion Stabilization, Langmuir 34(43) (2018) 12897-12905.
[183] M.P. Yadav, R.A. Moreau, K.B. Hicks, Phenolic Acids, Lipids, and Proteins Associated with Purified Corn Fiber Arabinoxylans, Journal of Agricultural and Food Chemistry 55(3) (2007) 943-947.
[184] T. Wu, C. Liu, X. Hu, Enzymatic synthesis, characterization and properties of the protein-polysaccharide conjugate: A review, Food Chemistry 372 (2022) 131332.
[185] Q. Guo, X. Xiao, L. Lu, L. Ai, M. Xu, Y. Liu, H.D. Goff, Polyphenol–Polysaccharide Complex: Preparation, Characterization, and Potential Utilization in Food and Health, Annual Review of Food Science and Technology 13(Volume 13, 2022) (2022) 59-87.
[186] R. Jefferis, Glycosylation as a strategy to improve antibody-based therapeutics, Nature Reviews Drug Discovery 8(3) (2009) 226-234.
[187] M.P. Yadav, J. Manuel Igartuburu, Y. Yan, E.A. Nothnagel, Chemical investigation of the structural basis of the emulsifying activity of gum arabic, Food Hydrocolloids 21(2) (2007) 297-308.
[188] H. Niu, X. Chen, T. Luo, H. Chen, X. Fu, The interfacial behavior and long-term stability of emulsions stabilized by gum arabic and sugar beet pectin, Carbohydrate Polymers 291 (2022) 119623.
[189] C. Sanchez, D. Renard, P. Robert, C. Schmitt, J. Lefebvre, Structure and rheological properties of acacia gum dispersions, Food Hydrocolloids 16(3) (2002) 257-267.

[190] M.E. Osman, A.R. Menzies, P.A. Williams, G.O. Phillips, T.C. Baldwin, The molecular characterisation of the polysaccharide gum from Acacia senegal, Carbohydrate Research 246(1) (1993) 303-318.
[191] M. Atgié, O. Masbernat, K. Roger, Emulsions Stabilized by Gum Arabic: Composition and Packing within Interfacial Films, Langmuir 35(4) (2019) 962-972.
[192] F. Liu, C. Ma, Y. Gao, D.J. McClements, Food-Grade Covalent Complexes and Their Application as Nutraceutical Delivery Systems: A Review, Comprehensive Reviews in Food Science and Food Safety 16(1) (2017) 76-95.
[193] X. Chen, Y. Zhang, Y. Han, Q. Li, L. Wu, J. Zhang, X. Zhong, J. Xie, S. Shao, Y. Zhang, Z. Wu, Emulsifying Properties of Polysaccharide Conjugates Prepared from Chin-Brick Tea, Journal of Agricultural and Food Chemistry 67(36) (2019) 10165-10173.
[194] N.G. Diftis, T.A. Pirzas, V.D. Kiosseoglou, Emulsifying properties of gelatin conjugated to pectin under alkaline conditions, Journal of the Science of Food and Agriculture 85(5) (2005) 804-808.
[195] G. Cirillo, M. Curcio, O. Vittorio, F. Iemma, D. Restuccia, U.G. Spizzirri, F. Puoci, N. Picci, Polyphenol Conjugates and Human Health: A Perspective Review, Critical Reviews in Food Science and Nutrition 56(2) (2016) 326-337.
[196] H. Chen, M. Zhang, B. Xie, Components and antioxidant activity of polysaccharide conjugate from green tea, Food Chemistry 90(1) (2005) 17-21.
[197] J. Kolodziejczyk-Czepas, M. Bijak, J. Saluk, M.B. Ponczek, H.M. Zbikowska, P. Nowak, M. Tsirigotis-Maniecka, I. Pawlaczyk, Radical scavenging and antioxidant effects of Matricaria chamomilla polyphenolic–polysaccharide conjugates, International Journal of Biological Macromolecules 72 (2015) 1152-1158.
[198] M. Tsirigotis-Maniecka, I. Pawlaczyk-Graja, R. Ziewiecki, S. Balicki, M. Matulová, P. Capek, F. Czechowski, R. Gancarz, The polyphenolic-polysaccharide complex of Agrimonia eupatoria L. as an indirect thrombin inhibitor - isolation and chemical characterization, International Journal of Biological Macromolecules 125 (2019) 124-132.
[199] S. Yan, J.M. Regenstein, B. Qi, Y. Li, Construction of protein-, polysaccharide- and polyphenol-based conjugates as delivery systems, Critical Reviews in Food Science and Nutrition (2023) 1-19.
[200] F. Lei, F. Liu, F. Yuan, Y. Gao, Impact of chitosan–EGCG conjugates on physicochemical stability of β-carotene emulsion, Food Hydrocolloids 39 (2014) 163-170.
[201] S. Beck, P. Choi, S.H. Mushrif, Origins of covalent linkages within the lignin–carbohydrate network of biomass, Physical Chemistry Chemical Physics 24(34) (2022) 20480-20490.
[202] M. Lawoko, G. Henriksson, G. Gellerstedt, Structural Differences between the Lignin–Carbohydrate Complexes Present in Wood and in Chemical Pulps, Biomacromolecules 6(6) (2005) 3467-3473.
[203] M.Y. Balakshin, E.A. Capanema, H.-m. Chang, MWL fraction with a high concentration of lignin-carbohydrate linkages: Isolation and 2D NMR spectroscopic analysis, Holzforschung 61(1) (2007) 1-7.
[204] T.-Q. Yuan, S.-N. Sun, F. Xu, R.-C. Sun, Characterization of Lignin Structures and Lignin–Carbohydrate Complex (LCC) Linkages by Quantitative 13C and 2D HSQC NMR Spectroscopy, Journal of Agricultural and Food Chemistry 59(19) (2011) 10604-10614.

[205] S. Herrera, Wood-based ethanol advances on international front... Cellulosic fuel from trees gets a closer look, Industrial Biotechnology 2(2) (2006) 101-107.
[206] M. Asgher, S.A. Qamar, M. Bilal, H.M.N. Iqbal, Bio-based active food packaging materials: Sustainable alternative to conventional petrochemical-based packaging materials, Food Research International 137 (2020) 109625.
[207] L. Maleki, U. Edlund, A.-C. Albertsson, Synthesis of full interpenetrating hemicellulose hydrogel networks, Carbohydrate Polymers 170 (2017) 254-263.
[208] S. Vodo, N. Taarji, M. Bouhoute, L.d.O. Felipe, M.A. Neves, I. Kobayashi, K. Uemura, M. Nakajima, Potential of bagasse obtained using hydrothermal liquefaction pre-treatment as a natural emulsifier, International Journal of Food Science & Technology 55(4) (2020) 1485-1496.
[209] Y.-F. Li, P.-P. Yue, X. Hao, J. Bian, J.-L. Ren, F. Peng, R.-C. Sun, Comparison of emulsifying capacity of two hemicelluloses from moso bamboo in soy oil-in-water emulsions, RSC Advances 10(8) (2020) 4657-4663.
[210] S. Wang, W. Gao, Y. Wang, T. Song, H. Qi, Z. Xiang, Emulsifying properties of naturally acetylated xylans and their application in lutein delivery emulsion, Carbohydrate Polymers 296 (2022) 119927.
[211] S. Wang, Z. Xiang, Highly Stable Pickering Emulsions with Xylan Hydrate Nanocrystals, Nanomaterials 11(10) (2021) 2558.
[212] S. Yu, G. Peng, D. Wu, Rod-like xylan nanocrystals as stabilizer towards fabricating oil-in-water pickering emulsions, Colloids and Surfaces A: Physicochemical and Engineering Aspects 675 (2023) 132129.
[213] K.S. Mikkonen, M. Tenkanen, P. Cooke, C. Xu, H. Rita, S. Willför, B. Holmbom, K.B. Hicks, M.P. Yadav, Mannans as stabilizers of oil-in-water beverage emulsions, LWT - Food Science and Technology 42(4) (2009) 849-855.
[214] K.S. Mikkonen, C. Xu, C. Berton-Carabin, K. Schroën, Spruce galactoglucomannans in rapeseed oil-in-water emulsions: Efficient stabilization performance and structural partitioning, Food Hydrocolloids 52 (2016) 615-624.
[215] A. Ebringerová, I. Sroková, P. Talába, M. Kačuráková, Z. Hromádková, Amphiphilic beechwood glucuronoxylan derivatives, Journal of Applied Polymer Science 67(9) (1998) 1523-1530.
[216] T. Nypelö, C. Laine, M. Aoki, T. Tammelin, U. Henniges, Etherification of Wood-Based Hemicelluloses for Interfacial Activity, Biomacromolecules 17(5) (2016) 1894-1901.
[217] C. Xu, C. Eckerman, A. Smeds, M. Reunanen, P.C. Eklund, R. Sjöholm, S. Willför, Carboxymethylated spruce galactoglucomannans: preparation, characterisation, dispersion stability, water-in-oil emulsion stability, and sorption on cellulose surface, Nordic Pulp & Paper Research Journal 26(2) (2011) 1-12.
[218] D. Dax, P. Eklund, J. Hemming, J. Sarfraz, P. Backman, C. Xu, S. Willför, Amphiphilic spruce galactoglucomannan derivatives based on naturally-occurring fatty acids, BioResources 8(3) (2013) 3771-3790.
[219] H.N. Cheng, A. Biswas, S. Kim, C.R. Alves, R.F. Furtado, Synthesis and Characterization of Hydrophobically Modified Xylans, Polymers 13(2) (2021) 291.
[220] M. Lehtonen, S. Teräslahti, C. Xu, M.P. Yadav, A.-M. Lampi, K.S. Mikkonen, Spruce galactoglucomannans inhibit lipid oxidation in rapeseed oil-in-water emulsions, Food Hydrocolloids 58 (2016) 255-266.
[221] N. Feng, J. Hu, S. Liang, X. Yang, X. Zhu, Y. Feng, X. Zhao, F. Tang, J. Yang, Q. Wu, Physical and oxidative stability of flaxseed oil-in-water emulsions prepared by natural lignin-carbohydrate complex, International Journal of Biological Macromolecules 270 (2024) 132154.

[222] F. Valoppi, N. Maina, M. Allén, R. Miglioli, P.O. Kilpeläinen, K.S. Mikkonen, Spruce galactoglucomannan-stabilized emulsions as essential fatty acid delivery systems for functionalized drinkable yogurt and oat-based beverage, European Food Research and Technology 245(7) (2019) 1387-1398.
[223] V. Dubois, S. Breton, M. Linder, J. Fanni, M. Parmentier, Fatty acid profiles of 80 vegetable oils with regard to their nutritional potential, European Journal of Lipid Science and Technology 109(7) (2007) 710-732.
[224] M. GROOTVELD, C.J.L. SILWOOD, P. ADDIS, A. CLAXSON, B.B. SERRA, M. VIANA, HEALTH EFFECTS OF OXIDIZED HEATED OILS1, Foodservice Research International 13(1) (2001) 41-55.
[225] T.H. Liao, P. Hamosh, M. Hamosh, Fat Digestion by Lingual Lipase: Mechanism of Lipolysis in the Stomach and Upper Small Intestine, Pediatric Research 18(5) (1984) 402-409.
[226] M. Mukherjee, Human digestive and metabolic lipases—a brief review, Journal of Molecular Catalysis B: Enzymatic 22(5) (2003) 369-376.
[227] D.J. McClements, The biophysics of digestion: lipids, Current Opinion in Food Science 21 (2018) 1-6.
[228] P.J. Wilde, B.S. Chu, Interfacial & colloidal aspects of lipid digestion, Advances in Colloid and Interface Science 165(1) (2011) 14-22.
[229] J. Iqbal, M.M. Hussain, Intestinal lipid absorption, American Journal of Physiology-Endocrinology and Metabolism 296(6) (2009) E1183-E1194.
[230] M. Golding, T.J. Wooster, The influence of emulsion structure and stability on lipid digestion, Current Opinion in Colloid & Interface Science 15(1) (2010) 90-101.
[231] H. Singh, A. Ye, D. Horne, Structuring food emulsions in the gastrointestinal tract to modify lipid digestion, Progress in Lipid Research 48(2) (2009) 92-100.
[232] D.J. McClements, Food hydrocolloids: Application as functional ingredients to control lipid digestion and bioavailability, Food Hydrocolloids 111 (2021) 106404.
[233] L. Mao, S. Miao, Structuring Food Emulsions to Improve Nutrient Delivery During Digestion, Food Engineering Reviews 7(4) (2015) 439-451.
[234] M.R. Infantes-Garcia, S.H.E. Verkempinck, T. Del Castillo-Santaella, J. Maldonado-Valderrama, M.E. Hendrickx, T. Grauwet, In vitro gastric lipid digestion of emulsions with mixed emulsifiers: Correlation between lipolysis kinetics and interfacial characteristics, Food Hydrocolloids 128 (2022) 107576.
[235] L. Marciani, R. Faulks, M.S.J. Wickham, D. Bush, B. Pick, J. Wright, E.F. Cox, A. Fillery-Travis, P.A. Gowland, R.C. Spiller, Effect of intragastric acid stability of fat emulsions on gastric emptying, plasma lipid profile and postprandial satiety, British Journal of Nutrition 101(6) (2008) 919-928.
[236] D. Liu, H.L. Parker, J. Curcic, S. Kozerke, A. Steingoetter, Emulsion Stability Modulates Gastric Secretion and Its Mixing with Emulsified Fat in Healthy Adults in a Randomized Magnetic Resonance Imaging Study123, The Journal of Nutrition 146(10) (2016) 2158-2164.
[237] M. Golding, Chapter 5 - Exploring the Relationship between Fat Surface Area and Lipid Digestibility, in: M. Boland, M. Golding, H. Singh (Eds.), Food Structures, Digestion and Health, Academic Press, San Diego, 2014, pp. 145-167.
[238] S. Lee, K. Jo, S.-K.-C. Jeong, Y.-S. Choi, S. Jung, Strategies for modulating the lipid digestion of emulsions in the gastrointestinal tract, Critical Reviews in Food Science and Nutrition (2023) 1-16.

[239] M. Beysseriat, E.A. Decker, D.J. McClements, Preliminary study of the influence of dietary fiber on the properties of oil-in-water emulsions passing through an in vitro human digestion model, Food Hydrocolloids 20(6) (2006) 800-809.
[240] H.D. Williams, N.L. Trevaskis, S.A. Charman, R.M. Shanker, W.N. Charman, C.W. Pouton, C.J.H. Porter, Strategies to Address Low Drug Solubility in Discovery and Development, Pharmacological Reviews 65(1) (2013) 315-499.
[241] X. Chen, Y. Chen, Y. Liu, L. Zou, D.J. McClements, W. Liu, A review of recent progress in improving the bioavailability of nutraceutical-loaded emulsions after oral intake, Comprehensive Reviews in Food Science and Food Safety 21(5) (2022) 3963-4001.
[242] R.F.S. Gonçalves, J.T. Martins, L. Abrunhosa, A.A. Vicente, A.C. Pinheiro, Nanoemulsions for Enhancement of Curcumin Bioavailability and Their Safety Evaluation: Effect of Emulsifier Type, Nanomaterials 11(3) (2021) 815.
[243] H.D. Williams, N.L. Trevaskis, Y.Y. Yeap, M.U. Anby, C.W. Pouton, C.J.H. Porter, Lipid-Based Formulations and Drug Supersaturation: Harnessing the Unique Benefits of the Lipid Digestion/Absorption Pathway, Pharmaceutical Research 30(12) (2013) 2976-2992.
[244] I.F. McClements, D.J. McClements, Designing healthier plant-based foods: Fortification, digestion, and bioavailability, Food Research International 169 (2023) 112853.
[245] D.J. McClements, Development of Next-Generation Nutritionally Fortified Plant-Based Milk Substitutes: Structural Design Principles, Foods 9(4) (2020) 421.
[246] S. Sethi, S.K. Tyagi, R.K. Anurag, Plant-based milk alternatives an emerging segment of functional beverages: a review, Journal of Food Science and Technology 53(9) (2016) 3408-3423.
[247] A.G. Cunha, A. Gandini, Turning polysaccharides into hydrophobic materials: a critical review. Part 2. Hemicelluloses, chitin/chitosan, starch, pectin and alginates, Cellulose 17(6) (2010) 1045-1065.
[248] E. Korotkova, A. Pranovich, J. Wärnå, T. Salmi, D.Y. Murzin, S. Willför, Lignin isolation from spruce wood with low concentration aqueous alkali at high temperature and pressure: influence of hot-water pre-extraction, Green Chemistry 17(11) (2015) 5058-5068.
[249] W. Lin, J. Yang, Y. Zheng, C. Huang, Q. Yong, Understanding the effects of different residual lignin fractions in acid-pretreated bamboo residues on its enzymatic digestibility, Biotechnology for Biofuels 14(1) (2021) 143.
[250] A. Lisý, A. Ház, R. Nadányi, M. Jablonský, I. Šurina, About Hydrophobicity of Lignin: A Review of Selected Chemical Methods for Lignin Valorisation in Biopolymer Production, Energies 15(17) (2022) 6213.
[251] H. Sadeghifar, A. Ragauskas, Perspective on technical lignin fractionation, ACS sustainable chemistry & engineering 8(22) (2020) 8086-8101.
[252] E.J. Robertson, G.L. Richmond, Molecular Insights in the Structure and Layered Assembly of Polyelectrolytes at the Oil/Water Interface, The Journal of Physical Chemistry C 118(49) (2014) 28331-28343.
[253] S. Dodoo, R. Steitz, A. Laschewsky, R. von Klitzing, Effect of ionic strength and type of ions on the structure of water swollen polyelectrolyte multilayers, Physical Chemistry Chemical Physics 13(21) (2011) 10318-10325.
[254] M.G. Carneiro-da-Cunha, M.A. Cerqueira, B.W.S. Souza, J.A. Teixeira, A.A. Vicente, Influence of concentration, ionic strength and pH on zeta potential and

mean hydrodynamic diameter of edible polysaccharide solutions envisaged for multinanolayered films production, Carbohydrate Polymers 85(3) (2011) 522-528.
[255] P. Maroni, F.J. Montes Ruiz-Cabello, C. Cardoso, A. Tiraferri, Adsorbed mass of polymers on self-assembled monolayers: effect of surface chemistry and polymer charge, Langmuir 31(22) (2015) 6045-6054.
[256] N. Dimitrušev, L. Fras Zemljič, B. Saake, S. Strnad, Study of xylan adsorption onto poly(ethylene terephthalate) using QCM-D, Cellulose 25(8) (2018) 4357-4374.
[257] T. Saarinen, M. Österberg, J. Laine, Adsorption of polyelectrolyte multilayers and complexes on silica and cellulose surfaces studied by QCM-D, Colloids and Surfaces A: Physicochemical and Engineering Aspects 330(2) (2008) 134-142.
[258] T. Saarinen, M. Österberg, J. Laine, Properties of Cationic Polyelectrolyte Layers Adsorbed on Silica and Cellulose Surfaces Studied by QCM-D—Effect of Polyelectrolyte Charge Density and Molecular Weight, Journal of Dispersion Science and Technology 30(6) (2009) 969-979.
[259] P. Naidjonoka, M.A. Hernandez, G.K. Pálsson, F. Heinrich, H. Stålbrand, T. Nylander, On the interaction of softwood hemicellulose with cellulose surfaces in relation to molecular structure and physicochemical properties of hemicellulose, Soft Matter 16(30) (2020) 7063-7076.
[260] J. Lucenius, J.J. Valle-Delgado, K. Parikka, M. Österberg, Understanding hemicellulose-cellulose interactions in cellulose nanofibril-based composites, Journal of Colloid and Interface Science 555 (2019) 104-114.
[261] M. Farooq, T. Zou, J.J. Valle-Delgado, M.H. Sipponen, M. Morits, M. Österberg, Well-defined lignin model films from colloidal lignin particles, Langmuir 36(51) (2020) 15592-15602.
[262] C. Hentschel, H. Wagner, J. Smiatek, A. Heuer, H. Fuchs, X. Zhang, A. Studer, L. Chi, AFM-based force spectroscopy on polystyrene brushes: effect of brush thickness on protein adsorption, Langmuir 29(6) (2013) 1850-1856.
[263] C. Friedsam, A. Del Campo Bécares, U. Jonas, M. Seitz, H.E. Gaub, Adsorption of polyacrylic acid on self-assembled monolayers investigated by single-molecule force spectroscopy, New Journal of Physics 6(1) (2004) 9.
[264] E. Spruijt, M.A. Cohen Stuart, J. van der Gucht, Dynamic force spectroscopy of oppositely charged polyelectrolyte brushes, Macromolecules 43(3) (2010) 1543-1550.
[265] G. Maurdev, M.L. Gee, L. Meagher, Controlling the adsorbed conformation and desorption of polyelectrolyte with added surfactant via the adsorption mechanism: a direct force measurement study, Langmuir 18(24) (2002) 9401-9408.
[266] W. Zhao, B. Simmons, S. Singh, A. Ragauskas, G. Cheng, From lignin association to nano-/micro-particle preparation: extracting higher value of lignin, Green Chemistry 18(21) (2016) 5693-5700.
[267] C.J. Beverung, C.J. Radke, H.W. Blanch, Protein adsorption at the oil/water interface: characterization of adsorption kinetics by dynamic interfacial tension measurements, Biophysical Chemistry 81(1) (1999) 59-80.
[268] M. Miriani, M. Keerati-u-rai, M. Corredig, S. Iametti, F. Bonomi, Denaturation of soy proteins in solution and at the oil–water interface: A fluorescence study, Food Hydrocolloids 25(4) (2011) 620-626.
[269] V.J. Verruto, R.K. Le, P.K. Kilpatrick, Adsorption and molecular rearrangement of amphoteric species at oil– water interfaces, The Journal of Physical Chemistry B 113(42) (2009) 13788-13799.

[270] S. Boddohi, C.E. Killingsworth, M.J. Kipper, Polyelectrolyte multilayer assembly as a function of pH and ionic strength using the polysaccharides chitosan and heparin, Biomacromolecules 9(7) (2008) 2021-2028.
[271] A. Tiraferri, P. Maroni, D. Caro Rodríguez, M. Borkovec, Mechanism of chitosan adsorption on silica from aqueous solutions, Langmuir 30(17) (2014) 4980-4988.
[272] M. Protat, N. Bodin-Thomazo, F. Malloggi, J. Daillant, R.A. Campbell, G. Fragneto, E.B. Watkins, P. Perrin, N. Pantoustier, P. Guenoun, Neutron reflectivity measurements at the oil/water interface for the study of stimuli-responsive emulsions, The European Physical Journal E 41(7) (2018) 85.
[273] M. Campana, S. Hosking, J. Petkov, I. Tucker, J. Webster, A. Zarbakhsh, J. Lu, Adsorption of bovine serum albumin (BSA) at the oil/water interface: a neutron reflection study, Langmuir 31(20) (2015) 5614-5622.
[274] A. Theodoratou, L.-T. Lee, J. Oberdisse, A. Aubert-Pouëssel, Equilibrium protein adsorption on nanometric vegetable oil hybrid film/water interface using neutron reflectometry, Langmuir 35(20) (2019) 6620-6629.
[275] R. Schlesinger, T. Röder, G. Götzinger, H. Sixta, M. Harasek, A. Friedl, Influence of hemicellulose aggregate and gel layer formation on flux and retention during nanofiltration of alkaline solutions, Desalination 175(1) (2005) 121-134.
[276] I.C.M. Dea, D.A. Rees, R.J. Beveridge, G.N. Richards, Aggregation with change of conformation in solutions of hemicellulose xylans, Carbohydrate Research 29(2) (1973) 363-372.
[277] M. Bhattarai, F. Valoppi, S.-P. Hirvonen, S. Hietala, P. Kilpeläinen, V. Aseyev, K.S. Mikkonen, Time-dependent self-association of spruce galactoglucomannans depends on pH and mechanical shearing, Food Hydrocolloids 102 (2020) 105607.
[278] S. Förster, V. Abetz, A.H.E. Müller, Polyelectrolyte Block Copolymer Micelles, in: M. Schmidt (Ed.), Polyelectrolytes with Defined Molecular Architecture II, Springer Berlin Heidelberg, Berlin, Heidelberg, 2004, pp. 173-210.
[279] M. Atgié, J.C. Garrigues, A. Chennevière, O. Masbernat, K. Roger, Gum Arabic in solution: Composition and multi-scale structures, Food Hydrocolloids 91 (2019) 319-330.
[280] A. Schröder, J. Sprakel, K. Schroën, J.N. Spaen, C.C. Berton-Carabin, Coalescence stability of Pickering emulsions produced with lipid particles: A microfluidic study, Journal of Food Engineering 234 (2018) 63-72.
[281] J. Wu, G.-H. Ma, Recent Studies of Pickering Emulsions: Particles Make the Difference, Small 12(34) (2016) 4633-4648.
[282] B.l. Yesiltas, M. Torkkeli, L.s. Almásy, Z.n. Dudás, P.J. García-Moreno, A.-D.M. Sørensen, C. Jacobsen, M. Knaapila, Small-angle neutron scattering study of high fat fish oil-in-water emulsion stabilized with sodium caseinate and phosphatidylcholine, Langmuir 36(9) (2020) 2300-2306.
[283] Ž. Temova Rakuša, M. Pišlar, A. Kristl, R. Roškar, Comprehensive Stability Study of Vitamin D3 in Aqueous Solutions and Liquid Commercial Products, Pharmaceutics 13(5) (2021) 617.
[284] F. Mahmoodani, C.O. Perera, G. Abernethy, B. Fedrizzi, H. Chen, Lipid oxidation and vitamin D3 degradation in simulated whole milk powder as influenced by processing and storage, Food Chemistry 261 (2018) 149-156.
[285] M. Zareie, A. Abbasi, S. Faghih, Influence of Storage Conditions on the Stability of Vitamin D₃ and Kinetic Study of the Vitamin Degradation in Fortified Canola Oil during the Storage, Journal of Food Quality 2021 (2021) 5599140.

[286] Y. Tan, Z. Zhang, J. Muriel Mundo, D.J. McClements, Factors impacting lipid digestion and nutraceutical bioaccessibility assessed by standardized gastrointestinal model (INFOGEST): Emulsifier type, Food Research International 137 (2020) 109739.
[287] S.A. Forrest, R.Y. Yada, D. Rousseau, Interactions of Vitamin D3 with Bovine β-Lactoglobulin A and β-Casein, Journal of Agricultural and Food Chemistry 53(20) (2005) 8003-8009.
[288] M. Armand, P. Borel, P. Ythier, G. Dutot, C. Melin, M. Senft, H. Lafont, D. Lairon, Effects of droplet size, triacylglycerol composition, and calcium on the hydrolysis of complex emulsions by pancreatic lipase: an in vitro study, The Journal of Nutritional Biochemistry 3(7) (1992) 333-341.
[289] M.J. Dille, T. Baydin, K.A. Kristiansen, K.I. Draget, The impact of emulsion droplet size on in vitro lipolysis rate and in vivo plasma uptake kinetics of triglycerides and vitamin D3 in rats, Food & Function 12(7) (2021) 3219-3232.
[290] S.M. Loveday, Protein digestion and absorption: the influence of food processing, Nutrition Research Reviews 36(2) (2023) 544-559.
[291] J. Zhang, L. Xiao, Y. Yang, Z. Wang, G. Li, Lignin binding to pancreatic lipase and its influence on enzymatic activity, Food Chemistry 149 (2014) 99-106.
[292] A.M. Nik, M. Corredig, A.J. Wright, Release of lipophilic molecules during in vitro digestion of soy protein-stabilized emulsions, Molecular Nutrition & Food Research 55(S2) (2011) S278-S289.
[293] L. Yonekura, A. Nagao, Intestinal absorption of dietary carotenoids, Molecular Nutrition & Food Research 51(1) (2007) 107-115.
[294] P. Figueiredo, K. Lintinen, A. Kiriazis, V. Hynninen, Z. Liu, T. Bauleth-Ramos, A. Rahikkala, A. Correia, T. Kohout, B. Sarmento, In vitro evaluation of biodegradable lignin-based nanoparticles for drug delivery and enhanced antiproliferation effect in cancer cells, Biomaterials 121 (2017) 97-108.
[295] J.H. Lee, J.S. Im, X. Jin, T.M. Kim, J.W. Choi, In vitro and in vivo Evaluation of drug-encapsulated lignin nanoparticles for release control, ACS Sustainable Chemistry & Engineering 10(18) (2022) 5792-5802.
[296] M. Witzler, A. Alzagameem, M. Bergs, B.E. Khaldi-Hansen, S.E. Klein, D. Hielscher, B. Kamm, J. Kreyenschmidt, E. Tobiasch, M. Schulze, Lignin-Derived Biomaterials for Drug Release and Tissue Engineering, Molecules 23(8) (2018) 1885.
[297] M. Jug, B.K. Yoon, J.A. Jackman, Cyclodextrin-based Pickering emulsions: functional properties and drug delivery applications, Journal of Inclusion Phenomena and Macrocyclic Chemistry 101(1) (2021) 31-50.
[298] E. Melro, L. Alves, F.E. Antunes, B. Medronho, A brief overview on lignin dissolution, Journal of Molecular Liquids 265 (2018) 578-584.
[299] E. Melro, A. Filipe, D. Sousa, A.J.M. Valente, A. Romano, F.E. Antunes, B. Medronho, Dissolution of kraft lignin in alkaline solutions, International Journal of Biological Macromolecules 148 (2020) 688-695.
[300] P. Shao, H. Ma, J. Zhu, Q. Qiu, Impact of ionic strength on physicochemical stability of o/w emulsions stabilized by Ulva fasciata polysaccharide, Food Hydrocolloids 69 (2017) 202-209.
[301] A. Sarkar, H. Kamaruddin, A. Bentley, S. Wang, Emulsion stabilization by tomato seed protein isolate: Influence of pH, ionic strength and thermal treatment, Food Hydrocolloids 57 (2016) 160-168.

[302] Y. Shao, C.-H. Tang, Characteristics and oxidative stability of soy protein-stabilized oil-in-water emulsions: Influence of ionic strength and heat pretreatment, Food Hydrocolloids 37 (2014) 149-158.
[303] E. Dickinson, M.G. Semenova, A.S. Antipova, Salt stability of casein emulsions, Food Hydrocolloids 12(2) (1998) 227-235.
[304] E. Drozłowska, A. Bartkowiak, Ł. Łopusiewicz, Characterization of Flaxseed Oil Bimodal Emulsions Prepared with Flaxseed Oil Cake Extract Applied as a Natural Emulsifying Agent, Polymers 12(10) (2020) 2207.
[305] S. Tcholakova, N.D. Denkov, I.B. Ivanov, B. Campbell, Coalescence stability of emulsions containing globular milk proteins, Advances in Colloid and Interface Science 123-126 (2006) 259-293.
[306] M. Lievonen, J.J. Valle-Delgado, M.-L. Mattinen, E.-L. Hult, K. Lintinen, M.A. Kostiainen, A. Paananen, G.R. Szilvay, H. Setälä, M. Österberg, A simple process for lignin nanoparticle preparation, Green Chemistry 18(5) (2016) 1416-1422.
[307] M. Norgren, H. Edlund, L. Wågberg, B. Lindström, G. Annergren, Aggregation of kraft lignin derivatives under conditions relevant to the process, part I: phase behaviour, Colloids and Surfaces A: Physicochemical and Engineering Aspects 194(1) (2001) 85-96.
[308] T. Cao, M. Elimelech, Colloidal stability of cellulose nanocrystals in aqueous solutions containing monovalent, divalent, and trivalent inorganic salts, Journal of Colloid and Interface Science 584 (2021) 456-463.
[309] N. Bizmark, M.A. Ioannidis, Effects of ionic strength on the colloidal stability and interfacial assembly of hydrophobic ethyl cellulose nanoparticles, Langmuir 31(34) (2015) 9282-9289.
[310] A.B. Fall, S.B. Lindstrom, O. Sundman, L. Ödberg, L. Wågberg, Colloidal stability of aqueous nanofibrillated cellulose dispersions, Langmuir 27(18) (2011) 11332-11338.